Desulfurization of Hydrocarbon Fuels at Ambient Conditions Using Supported Silver Oxide-Titania Sorbents

by

Sachin Appukuttan Nair

A dissertation submitted to the Graduate Faculty of
Auburn University
in partial fulfillment of the
requirements for the Degree of
Doctor of Philosophy

Auburn, Alabama
December 13, 2010

Keywords: Desulfurization, Silver, Titanium Oxide, Hydrocarbon Fuels, Adsorption, Dispersion

Approved by

Bruce J Tatarchuk, Chair, Professor Director of Chemical Engineering
Yoon Y Lee, Alumni Professor of Chemical Engineering
William Ashurst, Assistant Professor of Chemical Engineering
Dong-Joo (Daniel) Kim, Associate Professor of Materials Engineering

Report Documentation Page

Form Approved
OMB No. 0704-0188

1. REPORT DATE	2. REPORT TYPE	3. DATES COVERED
2010		**00-00-2010 to 00-00-2010**

4. TITLE AND SUBTITLE	5a. CONTRACT NUMBER
Desulfurization of Hydrocarbon Fuels at Ambient Conditions Using Supported Silver Oxide-Titania Sorbents	5b. GRANT NUMBER
	5c. PROGRAM ELEMENT NUMBER
6. AUTHOR(S)	5d. PROJECT NUMBER
	5e. TASK NUMBER
	5f. WORK UNIT NUMBER
7. PERFORMING ORGANIZATION NAME(S) AND ADDRESS(ES) **Auburn University ,Auburn,AL,36849**	8. PERFORMING ORGANIZATION REPORT NUMBER
9. SPONSORING/MONITORING AGENCY NAME(S) AND ADDRESS(ES)	10. SPONSOR/MONITOR'S ACRONYM(S)
	11. SPONSOR/MONITOR'S REPORT NUMBER(S)

12. DISTRIBUTION/AVAILABILITY STATEMENT
Approved for public release; distribution unlimited

13. SUPPLEMENTARY NOTES

14. ABSTRACT

Sulfur in refined fuels is considered a significant cause for atmospheric pollution such as acid rain and smog. Sulfur is also a poison for electrocatalysts in fuel cells and catalysts in hydrocarbon refining and reformation processes. Thus sulfur removal is essential for large scale production of transportation fuels as well as in smaller scales for mobile and stationary fuel cell and reforming applications. Hydro desulfurization (HDS) is the most prevalent desulfurization technology used currently. Several alternative technologies have been reported to be effective in sulfur removal from liquids such as catalytic oxidation, biological sulfur removal and membrane separation. The presented work focuses on the formulation, optimization and mechanistic investigations of adsorptive desulfurization adsorbents for liquid fuels at ambient conditions. Dispersed silver oxides on supports such as TiO2, γ-Al2O3 and SiO2 were observed to be effective desulfurizing agents for refined fuels at ambient conditions. Among the supports, TiO2 was found to be the most stable. Using titanium oxide of varying surface characteristics, it was determined that sulfur capacity corresponded to the specific surface area. Increasing the Ag loading on the support was observed to decrease dispersion and simultaneously decrease the sulfur capacity. At 4 Wt.% Ag loading, the sulfur capacity of the sorbent was 6.3 mgS/g for JP5 fuel containing 1172 ppmw sulfur. The sorbent composition was thermally regenerated (450:C) to 10 cycles using air as a stripping medium. Variation in desulfurization efficiency between JP5, JP8 and a lighter fraction of JP5 was established and correlated to the variation in sulfur speciation of the fuels. Lower concentration of trimethyl benzothiophenes in the lighter fraction JP5 resulted in the highest sulfur capacity demonstrated by Ag/TiO2. These studies on performance, effects of composition, fuel chemistry and regeneration procedures are presented in Chapter III. With the composition and performance of the sorbent established, synthesis procedures were optimized considering impregnation, drying and calcination stages. The effect of synthesis conditions on the sulfur capacity was correlated to the resulting pore structure and dispersion of Ag (Chapter IV). Incipient wetness among the various impregnation techniques resulted in the highest sulfur capacity. Calcination temperatures above 500 :C were observed to degrade the pore structure and thus lower the sulfur capacity of the sorbent. Characterization techniques such as BET surface area measurements, oxygen chemisorption, temperature programmed reduction (TPR), ultraviolet spectroscopy were used to study the adsorbent composition. The variation in the oxidation state of Ag with weight loading was determined using TPR and thermogravimetry. At 4% Ag

15. SUBJECT TERMS

16. SECURITY CLASSIFICATION OF:			17. LIMITATION OF ABSTRACT	18. NUMBER OF PAGES	19a. NAME OF RESPONSIBLE PERSON
a. REPORT	b. ABSTRACT	c. THIS PAGE			
unclassified	**unclassified**	**unclassified**	**Same as Report (SAR)**	**161**	

Abstract

Sulfur in refined fuels is considered a significant cause for atmospheric pollution such as acid rain and smog. Sulfur is also a poison for electrocatalysts in fuel cells and catalysts in hydrocarbon refining and reformation processes. Thus sulfur removal is essential for large scale production of transportation fuels as well as in smaller scales for mobile and stationary fuel cell and reforming applications. Hydro desulfurization (HDS) is the most prevalent desulfurization technology used currently. Several alternative technologies have been reported to be effective in sulfur removal from liquids such as catalytic oxidation, biological sulfur removal and membrane separation. The presented work focuses on the formulation, optimization and mechanistic investigations of adsorptive desulfurization adsorbents for liquid fuels at ambient conditions.

Dispersed silver oxides on supports such as TiO_2, γ-Al_2O_3 and SiO_2 were observed to be effective desulfurizing agents for refined fuels at ambient conditions. Among the supports, TiO_2 was found to be the most stable. Using titanium oxide of varying surface characteristics, it was determined that sulfur capacity corresponded to the specific surface area. Increasing the Ag loading on the support was observed to decrease dispersion and simultaneously decrease the sulfur capacity. At 4 Wt.% Ag loading, the sulfur capacity of the sorbent was 6.3 mgS/g for JP5 fuel containing 1172 ppmw sulfur. The sorbent composition was thermally regenerated (450^oC) to 10 cycles using air as a

stripping medium. Variation in desulfurization efficiency between JP5, JP8 and a lighter fraction of JP5 was established and correlated to the variation in sulfur speciation of the fuels. Lower concentration of trimethyl benzothiophenes in the lighter fraction JP5 resulted in the highest sulfur capacity demonstrated by Ag/TiO_2. These studies on performance, effects of composition, fuel chemistry and regeneration procedures are presented in Chapter III.

With the composition and performance of the sorbent established, synthesis procedures were optimized considering impregnation, drying and calcination stages. The effect of synthesis conditions on the sulfur capacity was correlated to the resulting pore structure and dispersion of Ag (Chapter IV). Incipient wetness among the various impregnation techniques resulted in the highest sulfur capacity. Calcination temperatures above 500 ^{o}C were observed to degrade the pore structure and thus lower the sulfur capacity of the sorbent. Characterization techniques such as BET surface area measurements, oxygen chemisorption, temperature programmed reduction (TPR), ultraviolet spectroscopy were used to study the adsorbent composition. The variation in the oxidation state of Ag with weight loading was determined using TPR and thermogravimetry. At 4% Ag loading approximately 28% of the deposited Ag was found to exist as the oxide. Lowering the metal loading significantly increased the dispersion. These dispersed Ag oxides were observed to be stable to temperatures of 550^{o}C. UV spectroscopy showed absorption bands representing oxides of Ag while bands representing metallic Ag were absent. It was therefore concluded that a majority of the Ag at the adsorption interface existed in the

oxide phase. This indicated an alternative mechanism of sulfur removal compared to other transition metal based sorbents where the active material is considered to be the metal ion. Several aspects to be considered during the scale-up of adsorption units such as bed configuration, liquid face velocity and bed temperature and the effect on sulfur capacity was addressed as well.

Having established the composition of the sorbent with respect to the oxidation state of Ag present, the dispersion of Ag and pore structure, several studies were carried out to determine the mechanism of sulfur removal in these materials (Chapter V & VI). Variation in desulfurization efficiency between sulfur aromatics varying in structure aspects such as aromaticity and presence of side chains were linked to the chemistry of the active center. These studies established that the active centers were acidic in nature. Probe molecules were used to poison the active centers and subjected to desulfurization studies. Surface complexes formed from the probe molecules were also identified using IR spectroscopy. These experiments indicated that the surface group responsible for the sulfur capacity was single or geminal hydroxyl groups. Equilibrium isotherms were also established for thiophene, benzothiophene, dibenzothiophene and 46 dimethyl dibenzothiophene at 22, 40 and 60^{o}C and fitted to Langmuir, Freundlich and Fritz-Schlunder models (Chapter VII). The adsorption data followed the Langmuir model indicating that sulfur removal was effected by associative physical adsorption.

Acknowledgments

This dissertation is a result of collaboration and unbound support of a lot of people. I would like to acknowledge the guidance and encouragement of my advisor Dr. Bruce Tatarchuk. I would like to express my sincere gratitude to Dr. Yoon Lee, Dr. Robert Ashurst and Dr. Daniel Kim for serving on my committee. This work would not have been possible without the cooperation and support of my colleagues at the Center for Microfibrous Materials Manufacturing, especially Dwight Cahela, Dr. Don Cahela, Dr. Alexander Samokhvalov, Dr. Wenhua Zhu, Megan Schumacher, Kimberly Dennis, Shirish Punde, Ranjeeth kalluri, Priyanka Dhage, A. H. M Hussain, Amogh Karwa, Abhijeeth Phalle, Ryan Sothen among many others. I am very thankful for being associated with Hongyun Yang and Tory Barron at Intramicron Inc. for their advice and guidance on various aspects of this work. I am also grateful to Sue Allen Abner and Karen Cochran for their administrative support throughout my tenure at Auburn. I would also like to acknowledge financial support from the Office of Naval Research for this work.

Most importantly, my time in graduate school would not have been possible without the unwavering support of my parents and their trust in my abilities. I also appreciate the guidance of my brother Manoj throughout my life. My sincere gratitude to my life-long friends Sriram and Nishad for their motivation, support and advice.

Table of Contents

List of Tables

List of Figures

I. Introduction and Literature Review

I.1 Motivation

Atmospheric sulfur emission is a significant environmental issue and has been dealt with through regulation of sulfur in transportation fuels. Sulfur does not hamper the performance of internal combustion engines. However, the use of sulfur containing fuels in catalytic systems severely degrades their performance. Sulfur tolerance of PEM fuel cells is less than 1 ppmw. Most fuel reformer catalysts are also not sulfur tolerant. This necessitates desulfurization of fuels prior to their use for these applications.

Sulfur is generally removed during refining processes. Sulfur regulations for commercial transportation fuels are tighter than for logistic fuels. Jet fuels in general have much higher sulfur content than commercial transportation fuels. Fuel clean-up thus is an inevitable part of fuel cell operations for military operations. These systems need to be portable, have a small foot-print, require minimal utilities for operation, low maintenance, and have good sulfur removal efficiency.

Adsorptive sulfur removal is the simplest technology available for such applications. However, there are some issues with adsorptive sulfur removal. Most adsorbents demonstrate low sulfur capacity and are generally not regenerable. One of

the goals of this research was to develop a sulfur adsorbent with high sulfur capacity. Regenerability of the composition was mandatory. Following formulation, optimization and scale-up operations, physiochemical characterization was carried out. Knowledge of the chemical composition and surface structure will provide information on optimization of adsorption performance. A study of the mechanism of sulfur removal would suffice in development of more effective sorbents.

I.2 Introduction

Anthropogenic sulfur emissions cause environmental pollution in the form of acid rain, smog and dry deposition. Reduction of sulfur emissions is considered a primary means of improving air quality. Sulfur removal is thus an important process in the clean-up of transportation fuels. Besides being an environmental pollutant, sulfur is a poison to reformer catalysts as well as fuel cell electro-catalysts. The EPA mandates sulfur levels for gasoline to be 30-80 ppmw and highway diesel levels to be lowered to 15 ppmw by 2010 [1]. Standards developed by the European Committee for Standardization mandates a maximum sulfur content of 10 ppmw by 2009. Sulfur emissions world over have been on the decline as a result of regulation [2]. Military logistic fuels such as JP5, JP8 are not bound by these regulations. It is thus not feasible to use reformate gases derived from these fuels in fuel cell systems without some kind of sulfur abatement technology.

I.3 Engineering a sorbent for desulfurization of liquid fuels

Liquid phase sorbents have sulfur capacities an order of magnitude lower compared to ZnO based sorbents used for gas phase (H_2S removal) applications. Therefore the most important characteristic of a desulfurization sorbent is its sulfur capacity. Since sulfur capacities are low for these sorbents, reuse of the sorbent bed over multiple cycles is a prerequisite for any practical sorbent.

Several parameters need to be considered during the development of a regenerable sorbent. The sorbent is required to retain its sulfur capacity over multiple adsorption-regeneration cycles. The sulfur capacity over multiple cycles maybe affected by several factors; chemical/morphological changes to the active species or collapse of the support pore structure due to thermal cycling. Several operational requirements need to be considered during regeneration. Thermal regeneration is the simplest regeneration technique. Thermal regeneration may be carried out in oxidizing (air), inert or reducing atmospheres depending on the composition of the sorbent; air being ideal. The thermal requirement for regeneration is a critical parameter as well as the time required for regeneration. Ideally regeneration temperature would be close to operating temperature to minimize heat exchange requirements. Regeneration has also been demonstrated using organic solvents to strip adsorbed sulfur at ambient temperatures. This approach has limitations pertaining to storage and disposal of the solvent.

Bed operating conditions such as fuel flow rate, bed dimensions and pressure drop also influences adsorbent performance. Low face velocities are required for liquid phase desulfurization compared to gas phase systems. Thus pressure drop during the adsorption phase is not a significant issue. However, a large amount of purge gas is required during regeneration; initially to vaporize and transport hydrocarbons in the pores of the sorbent and subsequently to strip the captured sulfur. Pressure drop in the bed thus becomes a significant factor during the thermal regeneration.

Another important factor to be considered during the design of liquid phase sulfur sorbents is the bed liquid hold-up. The amount of fuel trapped in the bed following an adsorption cycle needs to be removed during regeneration. The liquid held up maybe removed by draining the bed, air blow-down and vaporization. The amount of fuel entrapped in the bed depends on the packing density of the particles and the pore volume.

The method of preparation and its scalability is also a significant issue in the adoption of a desulfurization sorbent. Large amounts of sorbents are likely to be needed for practical desulfurization units due to their low sulfur capacity and thus raw material availability is a challenge. Several methods have been used in the manufacture of these sorbents. Impregnation, ion-exchange and comulling and pelletizing are common methods for synthesis. The cost is also an important factor in development of a sorbent composition.

I.4 Literature Review

I.4.1 Existing Technologies

Hydrodesulfurization (HDS) has been the most widely used and effective sulfur abatement technology in refining. Even though majority of low-sulfur hydrocarbon fuels are derived through HDS, there are limitations. Production of ultra low-sulfur fuels require catalyst volumes many times that is presently employed using the known reaction pathways for hydrotreating [3]. Adsorptive desulfurizing units can provide low sulfur fuel for sulfur intolerant systems such as fuel cells and catalyst beds. Operability of a desulfurizer at ambient conditions without the requirement for hydrogen provides many advantages over conventional systems. Several emergent technologies have diverged from HDS to provide low sulfur products. Sorption, catalytic oxidation, pervaporation are among the most promising.

Oxidative desulfurization (ODS) is being pursued as an alternative to sorptive sulfur removal. Typically an oxidative reagent such as hydrogen peroxide is used in conjunction with a catalyst to oxidize the sulfur in the fuel to sulfoxides or sulfones. Catalysts in aqueous state such as organic acids, polyoxometallic acids or their salt solutions as well as supported transition metal catalysts such as Mo/Al_2O_3 have been used. The oxidation products are generally removed through an extraction process using solvents such as acetonitrile. This technology has been reported to reduce sulfur concentration from hundreds of ppmw to tens of ppmw [4-8]. The use of molecular oxygen in conjunction with a catalytic component such as Fe(III) nitrate or bromide

followed by an adsorption step has been tried as a ODS variation. This method has some advantages over the bi-phasic oxidant-catalyst systems offering better mass transfer[9]. Solid oxidizing agents such as a peoxycarboxylic-acid-functionalized hexagonal mesoporous silica (HMS) have also been employed for ODS[10].

Bio catalytic sulfur removal has also been demonstrated using several varieties of microorganisms [11-15]. Strains of both aerobic and anaerobic microorganisms have been demonstrated to be effective desulfurization agents while preserving aliphatic and aromatic content of the fuel. Desulfurisation has been achieved under mesophilic (25 to 40°C) conditions with Rhodococcus erythropolis, R. sphaericus, R. rhodochrous, and Arthrobacter sp. and under thermophilic (above 50°C) conditions with a Paenibacillus sp. The main bottleneck in the biodesulfurization processes is the low biocatalytic activity followed by the low stability of the biocatalysts. The highest conversion was reported by Rhizodium meliloti at 1200 mg DBT/g of dry biocatalyst/h. Development of better biocatalysts are now pursued through genetic engineering.

Treatises that detail various deep desulfurization technology is dealt with elsewhere[16, 17]. Pervaporation techniques have achieved significant prominence in the recent years with the advancement in membrane technology [18-21]. Since the development of the S-Brane process by Grace Davison in 2002, several manufacturers have taken this path to desulfurization.

I.4.2 Compositions for adsorptive desulfurization

Several adsorbents have been reported to have an excellent capacity for sulfur removal. A majority of these adsorbents have transition metal components. Transition metal oxides have been reported to be effective desulfurization agents [22-29]. Nickel has been shown to be effective in its reduced metallic form [30-32]. Supported chloride salts of copper and palladium have also been used [33, 34]. Selective desulfurization agents have been developed through ion exchange of Cu, Ag, Ce, Ni and other metal ions into zeolite structures [33, 35-40]. Active metals have been supported on SiO_2, Al_2O_3 [30, 41, 42] and activated carbon [30, 42]. ZnO based sorbents were initially commercialized in the ZSorb process developed by Philips petroleum corporation [43] followed by improvements from several researchers [29, 44].

Comparison of sulfur capacities of reported sorbents is a difficult task due to the variation in sorbent structure, testing conditions and the composition of the challenge fuels used. Table I.1 lists performance data for sulfur sorbents that have been reported in literature and the corresponding test conditions. Most of the performance data was obtained using challenge fuels with sulfur concentration less than 500 ppmw of sulfur. The highest breakthrough sulfur capacity was reported for $CuCl_2$ /Al_2O_3 sorbent at 6.38 mg/g followed by the Cu-Y zeolite at 5.44 mg/g. Challenge sulfur concentration was below 400 ppmw in both the cases. Saturation sulfur capacities were 11.16 and 12.16 mg/g respectively. In comparison the Ni based sorbent had much lower sulfur capacity demonstrating a breakthrough capacity of 0.3 mg/g and saturation capacity of 1.7 mg/g. The lower capacity maybe attributed to higher LHSV used in the desulfurization tests.

The listed sorbent compositions are active only in their reduced state. This poses a significant disadvantage in practical applications. Either the sorbent needs to be transported in an oxygen-free atmosphere or it requires in-situ activation in a reducing gas. Limited studies have been carried out on the regeneration of these sorbents. Some have been regenerated using organic solvents, others thermally in inert atmospheres. The sorbents needed to be reactivated in a reducing atmosphere following any regeneration procedure. These conditions required for operation are disadvantageous to practical application of such sorbents.

Sorbent	Surf. area [m^2/g]	Part. size [µm]	Bed Dim. l/d [mm]	Challenge Sulfur Conc. [ppmw]	Flow conditions LHSV FR	Sulfur Capacity Saturation [mgS/g]	Sulfur capacity Breakthrough ≤1ppmw [mgS/g]
Ni adsorbent [32]	80	40	150/4.6	220	$24h^{-1}$	1.7	0.3
Cu-Y[34]	NR	NR	NR	297.2	0.5cc/min	12.16	5.44
CuCl/ Al_2O_3 [45]	NR	NR	NR	364.1	NR	11.16	6.38
$PdCl_2/Al_2O_3$ [34]	174	100-150	NR	1172	0.05cc/min SV=$2.3h^{-1}$		2.08

Table I.1. A comparison of performance of reported sulfur adsorbents and test conditions

I.5 Merits of adsorptive desulfurization

Adsorptive desulfurization processes addresses some of the inadequacies associated with the HDS process. Sorptive sulfur units operating at ambient conditions in the absence of hydrogen provide a cost effective and scalable alternative. Sorbents maybe developed to selectively capture sulfur heterocycles with alkyl side chains that have been shown to be resistant to hydrodesulfurization [46-48]. Thus the process is most suited for fuel cell applications where reformation is required at the point of use.

Adsorptive desulfurization may also be considered to be an alternative to process intensification of hydrotreating processes to cope with tightening sulfur regulations which calls for higher operating temperatures and pressures, increase in the consumption of hydrogen and development of more active catalysts. Sorbents that selectively remove the sulfur species that represent the hardest species to hydrotreat may be operated in tandem to traditional hydrotreating units. Large scale application of sorptive desulfurization maybe realized with such units.

I.6 Silver sorbents

The affinity of silver for sulfur is evident from the fact that silver tarnishes due to the formation of silver sulfide at room temperature. Several other researchers and inventors have utilized this fact for applications including sulfur removal from liquid fuels [24, 49-52].

The affinity of silver for sulfur is evident from the fact that silver tarnishes due to the formation of multi-layer silver sulfide at room temperature. Several other researchers and inventors have utilized this fact for applications including sulfur removal from liquid fuels [24, 49-52]. Silver based catalysts have been widely employed for oxidation reactions such as ethylene oxidation, propene epoxidation and oxidative dehydrogenation [53-58]. These catalysts have been characterized in great detail.

Silver supported on TiO_2 is active in the oxidized state in contrast with the majority of reported adsorbents that are active reduced. This accounts for their regenerability in oxidative conditions. The absence of activation steps also makes the materials easier to handle and transport, simplifying regeneration procedures. Therefore the mechanism of sulfur adsorption would vary from that reported for a majority of adsorbents.

I.7 Mechanism of sulfur removal

Sulfur removal using Ag based adsorbents maybe possible through three mechanisms; the formation of a sulfide on the surface [59-62], strong chemisorption [63-65], physical adsorption or a combination thereof. These mechanisms differ by the strength of interaction between the sulfur heterocycle and the active center. Multi-layer sulfide formation is a possible mechanism as observed in the tarnishing of silver objects in air. High selectivity for trace amounts of sulfur in fuels also suggests strong chemisorption as a possible mechanism of sulfur removal. Sulfur removal may result from physical adsorption through Van der waal's interactions between sulfur

heterocycle and active center as a majority of industrial adsorption processes are designed based on physical adsorption.

Sulfur adsorption has been generally attributed to the interaction of transition metals with π electron cloud on sulfur aromatics. Variation in sulfur speciation of fuels has been noted to influence the performance of sulfur adsorbents. This was attributed to the variation in π electron density between sulfur heterocycles. Delocalization of π electrons is influenced by the number of aromatic rings on the aromatic. π complexation have been used to explain sulfur capacity of Cu-Y type zeolites. Variation in electron density of aromatic ring brought about by the sulfur atom has been attributed to higher adsorption selectivity. The lone pair of electrons on the sulfur atom conjugates with π electrons on the aromatic ring. The d orbitals on the Cu atom back donate electron density to anti-bonding π orbitals (π*) of the sulfur rings resulting in π bonding between the solute and Cu atoms [66]. Similarly, higher HDS activity of benzothiophene (BT) has been attributed to the non-uniform electron distribution compared to dibenzothiophene (DBT) [67]. Adsorptive desulfurization selectivity has been observed to increase with increasing electron density on the sulfur atom [47].

These mechanisms require the transition metal to be in the reduced state. In the case of Ag based sorbents developed in this work, the metal is in the oxide phase. Consequently, interactions at the adsorption interface would involve the oxide or associated species. This would indicate mechanisms distinct from those reported for earlier adsorbents. Acid functional groups are frequently associated with catalytic

activity of transition metal oxide surfaces. Hese groups might play a significant role in interactions at the adsorption interface.

I.8 Role of acidic centers on sulfur adsorption

The role of acidic centers has been established for a myriad of industrially relevant heterogeneous reactions. Acidity on solid surfaces is categorized into two types, Lewis and Bronsted. Lewis acid sites (LAS) are coordinatively unsaturated centers which are electron acceptors, whereas Bronsted acid sites (BAS) are proton donors. The breaking of a crystal lattice at the surface leads to the appearance of ions with a tendency for additional coordination. Bronsted acid centers are either hydroxyl groups (bridging or otherwise) with sufficiently mobile protons or coordinated water or H_3O^+ ions. The OH bond length, the vibrational frequencies and the charge on the hydrogen atom of the bridging OH group affect the acidic strength [68]. Catalytic activity and selectivity of metal oxides have been related to their acid-base properties which are a function of the nature of constituents, composition, preparation and pre-treatment procedures [69]. Previous research has dealt extensively with the relationship between strength and concentration of surface acid sites and their catalytic activity for various reactions [70]. Mixed metal oxides also generate surface acidity over their individual end members because of an increase in polarizability of surface hydroxyl (OH) groups [71, 72].

Surface acidity has been linked to the photocatalytic activity of TiO_2; influenced by surface area, crystal structure and density of surface OH groups [73]. Basic OH groups

has been identified on TiO_2 surfaces as well [74]. Basic functional groups on activated carbons have been reported to be involved in methane adsorption [75] and oxygen/carboxylic groups for water vapor adsorption [76]. Therefore the role of surface functional groups in sulfur removal by TiO_2 based adsorbents was assessed.

Measurement of surface acidity and the correlation with sulfur capacity was therefore studied for Ag based sorbents. NH_3 is a strong base and is readily adsorbed on strong as well as weak acid sites. It has been used as a probe molecule to test the acidic properties of metal oxide surfaces [77-79]. NH_3 interacts with acid sites resulting from anion vacancies, lewis and bronsted sites [80]. NH_3 chemisorption was thus used to obtain the overall (Lewis and Bronsted) acidity of the sorbents. Contribution of Bronsted acidity of Al_2O_3, TiO_2 and SiO_2 with and without Ag was established from acid-base titration method [81] using 2,6-Lutidine as a probe and Hammett indicators [82-84]. 2, 6-Lutidine was chosen as the basic probe molecules because the sterically hindered amine is preferentially adsorbed in proton acid sites even in presence of strong Lewis acid sites [85, 86].

I.9 Synopsis

The cycle of development work carried out in this research project is depicted in Figure I.1. Ag/TiO_2 adsorbent composition was identified as a promising candidate for desulfurization of logistic fuels. The synthesis parameters were established for maximum sulfur capacity. Procedures for scale-up of the sorbent were established to manufacture kilogram sized batches. Operational parameters such as face velocity, bed

temperature and configuration were established. Regeneration conditions were also established and demonstrated to 10 cycles.

Efforts were subsequently focused on understanding the mechanism of sulfur removal and molecular interactions at the adsorption interface. The primary step involved in this process was the physiochemical characterization of the surface. Among the details investigated was the pore structure of the adsorbent, the dispersion of Ag on the surface and their effect on sulfur capacity. The oxidation state of Ag at the adsorption interface was established using both spectroscopic and chemical techniques.

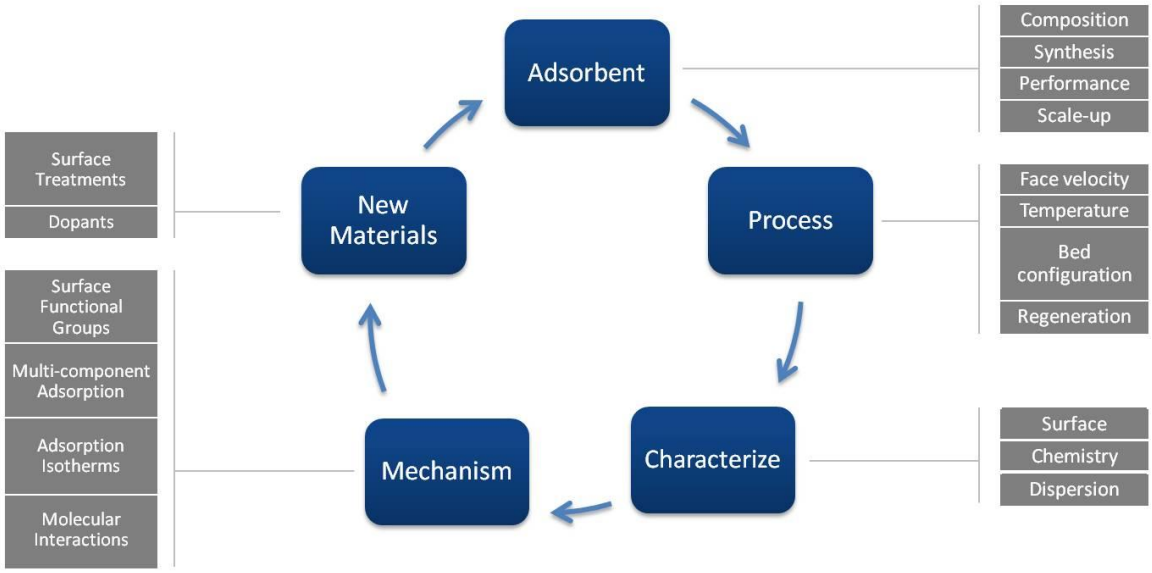

Figure I.1. The synopsis of breadth of research activities carried out on Ag based sorbents presented

From the information obtained from characterization data, a model for sulfur removal was built combined with other characteristics of the system such as multi-component adsorption, the contribution of surface functional groups and adsorption isotherms established for common sulfur aromatics found in natural fuels.

II. Experimental Details

II.1 Sorbent preparation

TiO_2 support was obtained from St. Gobain Norpro Grade ST61120 (Type 1) as 3.2 mm pellets. Grade 21 SiO_2 obtained from Grace Davison Co. and catalyst support Grade γ-Al_2O_3 obtained from Alfa Aesar were also used as supports (Table II.1). The pellets were crushed and sieved to size and dried in a convection oven for at least 6h at 110^{o}C prior to use. Incipient wetness impregnation was used to disperse silver on the support using $AgNO_3$ [99.9% purity from Alfa Aesar Co] solution in water. The concentration of the impregnating solution was adjusted to obtain the required Ag loading on the support. Typically the volume of impregnating solution was maintained at 90% of the pore volume of the support. The resulting particles were then dried at 110^{o}C for 6h followed by calcination in air at 400^{o}C for 2h. A maximum of 15% variation in sulfur capacity was observed between batches of sorbent of the same composition. Therefore, for every performance comparison presented in this work, the same batch of sorbent was used to provide a consistent basis for comparison.

Cu-Y zeolite was tested prepared using liquid phase ion exchange as reported previously [38, 87]. The adsorbent was pretreated in flowing (ultrapure) He at 450^{o}C for

2 hours *in situ* prior to desulfurization studies. $PdCl_2$ on γ-Al_2O_3 composition was prepared using thermal dispersion techniques [45, 88]. The adsorbent was pretreated in (ultrapure) He at 350^oC (ramped to temperature at 1 deg/min) and held at temperature for 2h prior to testing for sulfur capacity. Selexorb CDX (1.4mm spherical particles) was obtained from BASF Inc. and tested following pre-treatment in air at 250^oC for 2h.

Support	**Vendor**	**Grade**	**BET Surface area [m^2/g]**	**Pore volume [cc/g]**
TiO_2	St. Gobain Nor Pro	Type 1	153	0.46
SiO_2	Grace Davison	Grade 21	319	0.80
γ-Al_2O_3	Alfa Aesar	Catalyst support	256	1.2
Na Y	Strem Chemicals	Molecular sieve	472	0.37
Selexorb	BASF	CDX	411	0.39

Table II.1. Properties of various supports used for the preparation of sulfur adsorbents

II.2 Saturation sulfur capacity

Preliminary analysis of sulfur capacity was carried out through saturation tests wherein a known mass of the sorbent composition was agitated gently in a known weight of JP5 fuel for 48h. An estimation of the sulfur capacity was thus obtained from the sulfur content of the resulting fuel.

II.3 Sorbent breakthrough performance

The breakthrough characteristics of the sorbents were determined in a packed column configuration where the challenge fuel flowed from the bottom of the bed to

the top. It was observed that this configuration minimized channeling and wall-slip effects giving consistent breakthrough data. 10.0 g of the sorbent was used in all the breakthrough studies. The bed was contained in quartz tubing supported on both ends by quartz wool. The tube ID was 16 mm and the length varied depending on the sorbent composition as well as bed loading. The varied bed lengths employed in this work are mentioned at the appropriate instances. Dead spots in the bed were avoided by tapping the bed on the side prior to testing to ensure consistent packing. None of the sorbents were activated *in situ* nor was any step followed to wash the bed with a sulfur-free solvent to remove trapped air. The fuel flow rate was maintained by peristaltic pump. The bed output was sampled at regular intervals for analysis of sulfur content. The adsorption/regeneration system is shown schematically in Figure II.1. The concept of $t_{1/2}$ was used to estimate the saturation capacity for cases where sorption was not carried out to bed exhaustion. Here the symmetry of breakthrough curve was considered and sulfur capacity estimated from Equation II-1.

$$\int_0^{t_{sat}} q_t dt = t_{½} q_{t_{½}} \qquad \text{Equation II-1}$$

Here q represented the sulfur capacity (mg/g), t_{sat} the saturation time (min), $t_{½}$ the time for outlet sulfur concentration to reach half the inlet, $q_{t½}$ the sulfur capacity at $t_{½}$ point.

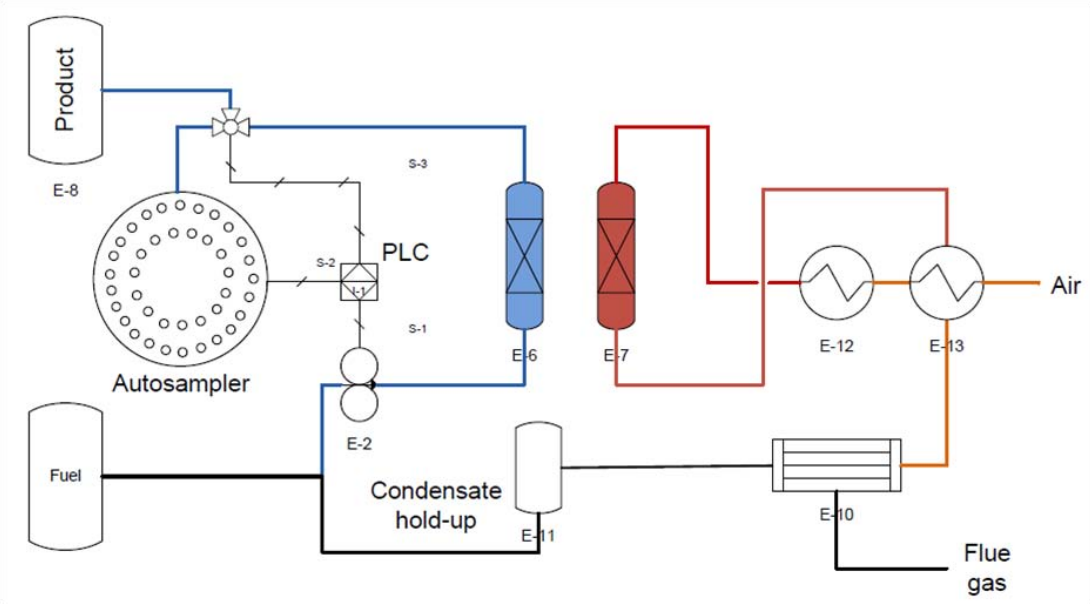

Figure II.1. Schematic of bench scale desulfurization unit used for adsorption-regeneration studies

II.4 Challenge fuels

Model fuels consisting of 3500±10 ppmw thiophene [T] (99.5% Arcos Organics), methyl thiophene [MT] (98% Alfa Aesar), benzothiophene [BT] (97% Arcos Organics), dibenzothiophene [DBT] (98% Alfa Aesar Co.), 4,6 dimethyl dibenzothiophene [4,6 DMDBT] (97% Sigma Aldrich.) in n-octane (97% Arcos Organics) were used for breakthrough tests to study the effect of structure of sulfur aromatics on adsorption. Model fuel with benzothiophene (3500+-10ppmw) and 15 ppmw of antioxidant 2,6 Di-tert-butyl-4-methylphenol (>99.0% Sigma-Aldrich), 15 ppmw of metal deactivator Alfa-alfa 1 methylethylenediimino-di-ortho-cresol (>99.0% Sigma-Aldrich), Ethanol 15.0 Vol% and 100 ppmw water representing fuel additives/ contaminants were also tested for the effect on sulfur capacity.

Sharper breakthroughs obtained using model fuels were useful in identifying the differences in breakthrough performance of sorbents compared to real fuels. Model fuels also reduced the effects of competitive adsorption posed by sulfur-free aromatics present in natural fuels. The major sulfur species in the fuels were identified using analytical standards obtained from Chiron AS.

II.5 Analysis of sulfur

A Varian CP3800GC equipped with a Pulsed Flame Photometric Detector (PFPD) containing a sulfur specific optical filter was used to determine the sulfur content of the sorbent bed outlet. The GC column employed was a Restek crossboard column of length 30m, inner diameter of 0.25mm and 0.25µm d_f (film thickness). The PFPD detector was calibrated using standards of subsequent dilutions of both real fuels as well as sulfur heterocycles in n-octane. The injector operated at split ratios between 0 and 80 using a 1 µl injection volume. The lower detection limit of the PFPD was observed to be 20 ppbw total sulfur with the injector in splitless mode. Sulfur content was also determined using an Antek 9000VS Total Sulfur Analyzer. The instrument was calibrated using sulfur standards as mentioned above. The lower detection limit of the instrument was observed to be 200 ppbw.

II.6 Sorbent characterization

II.6.1 Specific surface area

BET surface areas, pore volumes and pore size distributions were obtained using a Quantachrome AS1 surface area and pore size analyzer using nitrogen adsorption at 77K. This method of measuring surface area was developed by Brunauer, Emmett and Teller (BET) in 1938. Their model considered multi-layer adsorption compared to the Langmuir model which modeled mono-layer adsorption on surfaces.

II.6.2 Oxygen chemisorption

Dispersion of transition metal ions on supports are routinely characterized by chemisorption of gases, such as H_2, CO etc. This technique is challenging with Ag because H_2 and CO do not adsorb to provide complete and well defined monolayer coverage [89]. The Quantachrome AS1 surface analysis module was also used to carry out oxygen chemisorption on the sorbent. The instrument utilized the static chemisorption technique. Selective oxygen chemisorption was used to determine the morphology of the supported Ag sorbent. A clean Ag surface was obtained by following a series of *in situ* pretreatment steps (Table II.2). The primary step was an evacuation step followed by H_2 reduction to provide reproducible O_2 uptakes. All surface Ag species were assumed to be in the reduced metallic state prior to uptake measurements.

Pretreatment Step	Temperature [°C]	Time [min]	Conditions
Surface cleaning/moisture removal	150	30	Vacuum
Reduction	300	60	Hydrogen
Removal of physically adsorbed H_2	300	60	Vacuum

Table II.2. Surface pre-treatment steps for Ag/TiO_2 sorbents for oxygen chemisorption

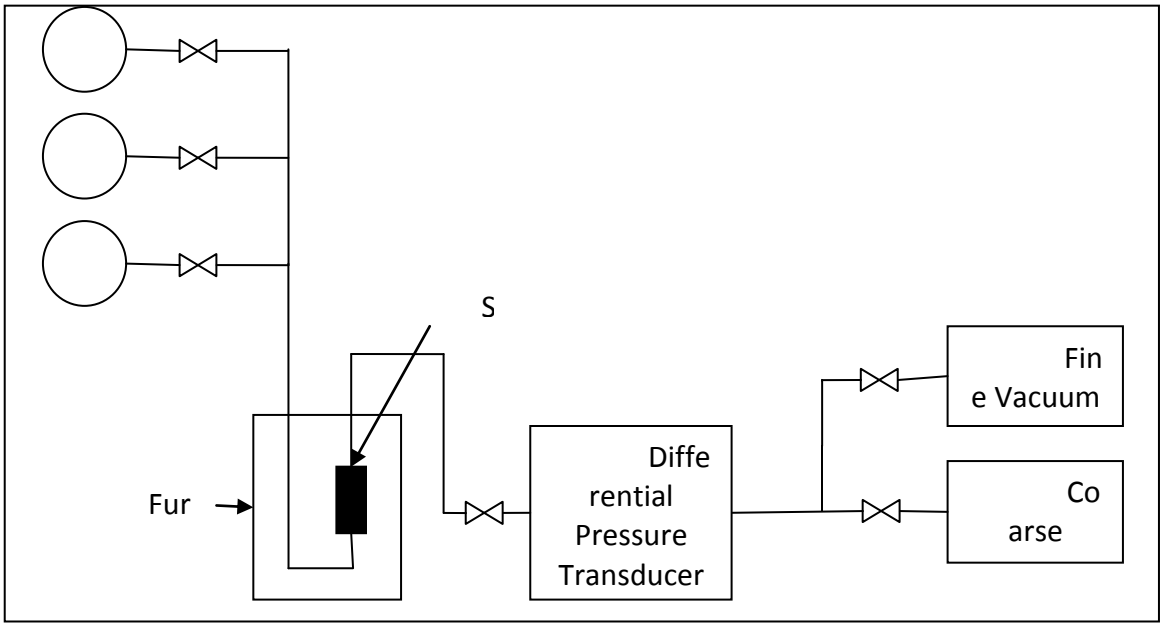

Figure II.2. Schematic representation of the Quantachrome AS-1 static volumetric chemisorption apparatus

The schematic of the Quantachrome AS-1 static volumetric apparatus used for determining oxygen uptake is shown in Figure II.2. Pretreatment as well as analysis gases were introduced into the manifold through microprocessor controlled solenoid valves. Sample pretreatment was programmed as macros wherein the gases, temperature and ramp soak profile are sequenced. Dosing sequences as well as pressure points was also programmed into the instrument.

The formation of a monolayer of oxygen required for accurate measurements on reduced Ag surfaces have been reported between 170 and 220°C with a stoichiometry of one oxygen atom to one silver atom [89-94]. Isotherms were therefore obtained at 170^{o}C. The equilibration time chosen was 10 min. The equilibration time ensures monolayer formation while minimizing bulk diffusion and spill-over to the support. Physical or weak adsorption was observed to be negligible at 170^{0}C. Therefore the combined oxygen uptake (physisorbed and chemisorbed) was considered for dispersion estimations. Dispersion (*D*) was estimated from Equation II-2.

$$D = \frac{N_m SM}{100L} \qquad \text{Equation II-2}$$

Here N_m represented the oxygen uptake (µmol/g), *S* the adsorption stoichiometry, *M* the molecular weight of metal and *L* the percentage metal loading. The active metal surface area (*s*) was estimated from Equation II-3.

$$s = \frac{N_m SA_m}{166} \qquad \text{Equation II-3}$$

A_m being the cross-sectional area occupied by each active surface atom (8.6960Å^{2}/Ag atom)

The average crystallite size was estimated from Equation II-4.

$$d = \frac{100Lf}{sZ} \qquad \text{Equation II-4}$$

Here *Z* represented density of Ag (10.5g/ml), *s* the active metal surface area and *f* the shape factor (6 for the assumed spherical shape)

II.6.3 Infrared spectroscopy

The samples were exposed to the probe molecules *exsitu* and pellets were prepared using KBr at a ratio of 1:100 by weight. Transmission of infrared beam through the sample was minimal due to the density of TiO_2 even at the high sample dilution rate. Consequently, intensities of representative bands were low for the samples analyzed. However, pertinent information on surface functional groups was obtained from the data.

II.6.4 X Ray diffraction

X-Ray diffraction has been used with limited success on supported silver catalysts. Diffraction patterns for Ag or silver oxides were not discernable at low loadings [57, 95, 96]. This has been attributed to the overlapping of the Ag peaks to that of the support materials [57, 96]. Ag crystals were however more discernable when prepared through precipitation methods [58] or by using more sensitive techniques such as XRDSR [97]. Powder XRD was carried out on the supported silver sorbents using a Rigaku miniflex with a Cu source at 30KV/15mA.

II.6.5 Temperature programmed reduction

Temperature programmed reduction involves the reduction of a solid by a gas while the temperature of the system is changed simultaneously in a predetermined way. Chemical information is derived from a record of the analysis of the gaseous

product. The reducing gas is generally hydrogen, whose concentration is monitored downstream of the reactor. The consumption of hydrogen is then recorded as a function of temperature. Metal support interactions as well as metal-metal interactions are discerned using the TPR technique. The technique is specifically applicable to systems of very small size that other spectroscopic techniques give minimal information because of lack of sensitivity.

TPR apparatus were custom assembled for the analysis of supported Ag sorbents as shown in Figure II.3. The instrument consisted of three parts:

- The gas manifold involved with gas pretreatment and handling
- The reactor and furnace with temperature control
- The gas analysis unit consisting of the TCD (Thermal Conductivity Detector) and the signal acquisition system.

The gas manifold consisted of 5 three way valves, 4 shutoff valves and two moisture traps and one oxygen trap. Four of the three way valves were used to switch the system between TPR analysis and sample pretreatment stages. While the sample pre-treatment is being carried out, the system will be in recycle loop where the reactor would be bypassed. This allows for a gas purge on the TCD detector preventing contamination and moisture condensation. Oxygen and moisture traps sufficed as the gas clean up for the reduction gas.

The reactor was a 1/8” ID quartz tube 18” in length. The sample for TPR was loaded into the reactor and supported on either end using quartz wool. The

temperature of the sample was monitored through a K-type thermocouple. The thermocouple also provided feed back to a temperature controller operating the furnace. Reducing gas employed was H_2 (4.95% in Ar).The samples were pre-heated in (moisture-free) air at 300°C for 1h prior to analysis. Approximately 0.4 g of sample was used in each experiment. The temperature was varied between 22 and 650°C at a heating rate of 10.5 deg/min. H_2 consumption was estimated from reduction profiles of Cu and Ni oxides (99.99% Alfa Aesar Co.) of known stoichiometry.

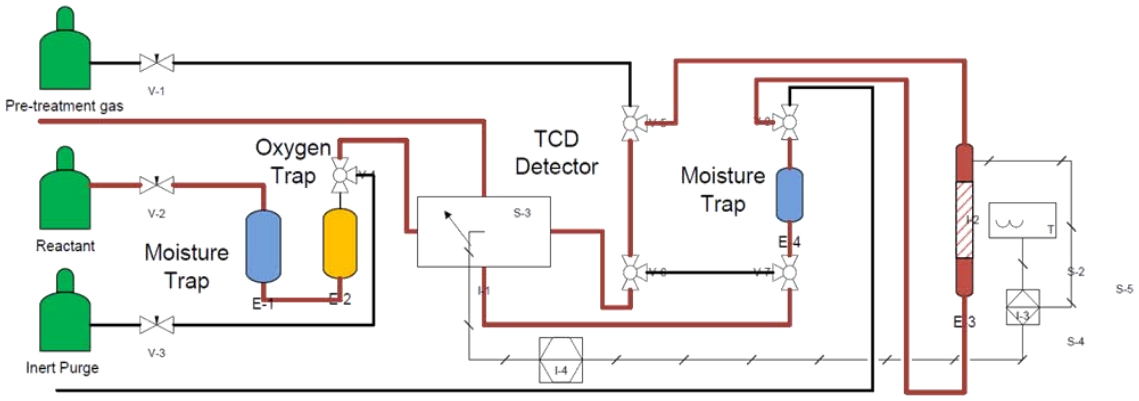

Figure II.3. Apparatus for temperature programmed reduction of Ag sorbents

II.6.6 Ultraviolet spectroscopy

Ultraviolet spectroscopy was carried out on Ag/TiO_2 varying Ag loading between 2 and 20 wt%. A Spectronic genesys 2 UV spectrometer was used to obtain the absorption spectra. Sorbent particles were dispersed in water (DIUF) (also used to obtain the baseline spectra) using an ultrasonic probe.

II.6.7 Thermogravimetric analysis

Thermogravimetric analysis was carried out using a TA Instruments Q50 TGA apparatus. 50-100mg samples were placed in a Pt sample holder and subjected to continuous heating from 25 to 650°C at a rate of 5 deg/min and then cooled to 25°C at the same rate. The analysis was carried out in air (breathing quality) that purged the sample chamber at 50 ml/min. Mass values (in % of the initial mass) pertaining to phase changes in the samples was obtained against sample temperature. Samples were analyzed in oxidizing (Air, zero grade, Airgas), reducing atmospheres (5% H_2/He, Airgas) and inert (N_2, UHP, Airgas) to identify phase changes in the Ag phase.

II.7 Sorbent pretreatment with probe molecules

Pretreatment with probe molecules was carried out *exsitu* either flowing the gas through a bed of the sorbent particles or exposure to vapor under vacuum. Pyridine (99% Alfa Aesar), Lutidine (99% Alfa Aesar), TMCS (99% Alfa Aesar) were placed in a beaker along with sorbent sample in a vacuum chamber. Chamber pressure was reduced to approximately 100mPa and held for 30 min. Breakthrough experiments for sulfur removal was carried out subsequently.

II.8 Ammonia chemisorption

Ammonia chemisorption was carried out in the Quantachrome AS1 surface analysis instrument. Acidity analysis included a pretreatment method consisting of ramping sample temperature to 400^{o}C at 10^{o}C/min in flowing air (zero grade, Airgas)

and then holding the sample at 400^{o}C for 2h. Following the air treatment, sample temperature was lowered to 175^{o}C and then evacuated for 30 min. Analysis was performed at 175^{o}C using a 10 combined point and 10 weak point titration method. Pretreatment and analysis conditions were reproduced from previous research [98]. The first isotherm collected after the sample preparation step represented the combined contribution of chemisorption (on strong sites) and physical adsorption on the sample. After obtaining the combined isotherm, the system was evacuated to remove all physically adsorbed NH_3. Chemisorbed gas is only removed from the surface when evacuation is carried out at a much higher temperature than the adsorption temperature. The weak isotherm was therefore obtained by admitting NH_3 following the evacuation step. The isotherm for the chemisorbed gas was obtained by subtracting the weak from the combined isotherm.

II.9 Potentiometric titration

0.2 g of the sorbent sample was added to a series of vials (around eight to ten vials) and 10 ml of dry Benzene (99%, Alfa Aesar) was added to each. 0.01 M solution of 2, 6-Lutidine (98+%, Alfa Aesar) was added to each of the samples and agitated mechanically for 4 hours. The equilibrated samples were subsequently tested with 0.1 Wt% solution of methyl yellow (98%, Alfa Aesar) indicator (pKa = +3.3). After shaking for 4 hours the color of the solid samples were observed. In presence of the indicator the solid samples turned red when acidic (pKa < +3.3) and yellow when basic (pKa > +3.3). For every sample, the volume of 2, 6-Lutidine solution was increased sequentially in

each vial so as to determine the amount of base required to neutralize the acid surface sites through titration. The preceding steps were repeated using smaller stepwise increases in volume of base between the ranges found in the previous trial and the amount of base was bracketed to even smaller intervals. For instance, the error range for TiO_2 samples was ±0.5 µmoles/g while that for Al_2O_3 samples was ±10 µmoles/g. The error range for the Ag loaded samples was ±25 µmoles/g. Thus the end points were determined from the colors of adsorbed Hammett indicators through a series of successive approximations. Details of the titration method are described elsewhere [99].

II.10 Equilibrium isotherms

Equilibrium studies were conducted at 22, 40 and 60±2^{o}C. Working solutions of concentrations between 1 and 3500 ppmw of the sulfur aromatic in n-octane were prepared from stock solutions. 10-50 ml of the working solution was then brought in contact with 0.1-0.2g of Ag/TiO_2 sorbent particles. Each sample was kept in a state of agitation (100rpm) for a period of 48h. The equilibrium solid phase concentration q (mg S/mg sorbent) was then determined from Equation II-5.

$$q = \frac{v}{m}(C_i - C_e) \qquad \text{Equation II-5}$$

Where C_i and C_e (mg/l) are the initial and equilibrium sulfur concentrations, v (ml) is the volume of solution and m (g) the mass of the sorbent.

III. Performance and Regenerability of Ag based Sorbents

III.1 Introduction

Supported silver oxides were tested as desulfurization compositions for high sulfur fuels and model fuel compositions. The effect of the variation in dispersion of Ag oxides on desulfurization performance was observed using TiO_2, γ-Al_2O_3 and SiO_2 as supports. Sorbents with varying support pore structure and Ag loading were tested. Facile regeneration was carried out in air for 10 cycles. Variation of sorbent performance with fuel chemistry was also examined. Preliminary characterization was also carried out to provide an understanding of the surface of the sorbents.

The surface morphology of silver catalysts similar in composition has been shown to vary extensively between the methods used for preparation, weight loading and the supports used. X-Ray diffraction has been used with limited success on supported silver catalysts. Diffraction patterns for silver metal or silver oxides were not discernable at low loadings [57, 95, 96]. This has been attributed to the overlapping of the Ag peaks to that of the support materials [57, 96]. Dispersion of transition metal ions on supports are routinely accomplished by chemisorption of gases, such as H_2, CO etc. This technique is difficult with Ag because H_2 and CO do not adsorb strongly and

reversibly to provide well defined monolayer coverages [89]. Oxygen has been successfully chemisorbed on Ag resulting in reproducible dispersion measurements. The formation of a monolayer of oxygen required for accurate measurements on reduced Ag surfaces have been reported between 170 and 220^{0}C with a stoichiometry of one oxygen atom to one silver atom [89-94].

III.2 Results and Discussion

III.2.1 Screening of active metals for sulfur adsorption

Preliminary data on sulfur removal performance with JP5 fuel was obtained from saturation tests carried out by contacting sorbent compositions with fuel for 48h to give sufficient time to determine equilibrium sulfur capacity. Cu, Ni, Mn, Co and Ag were the transition metals supported on Grade 21 SiO_2. Sorbents were prepared through incipient wetness method followed by drying (110^{0}C for 8h) and calcination (450^{0}C for 2h). Since thermal regeneration in air is ideal for multi-cycle operation, these compositions were tested for sulfur capacity in their oxidized form. 1.0g of sorbent was contacted with 5.0 g of JP5 (1172 ppmw sulfur) and agitated mechanically for 48h. Saturation sulfur capacity was estimated from sulfur content of the remaining fuel. The sulfur capacities of the compositions are shown in Figure III.1. It was observed that Ag demonstrated the highest sulfur capacity of 4.95 mgS/g. This observed higher sulfur capacity of supported silver warranted further research.

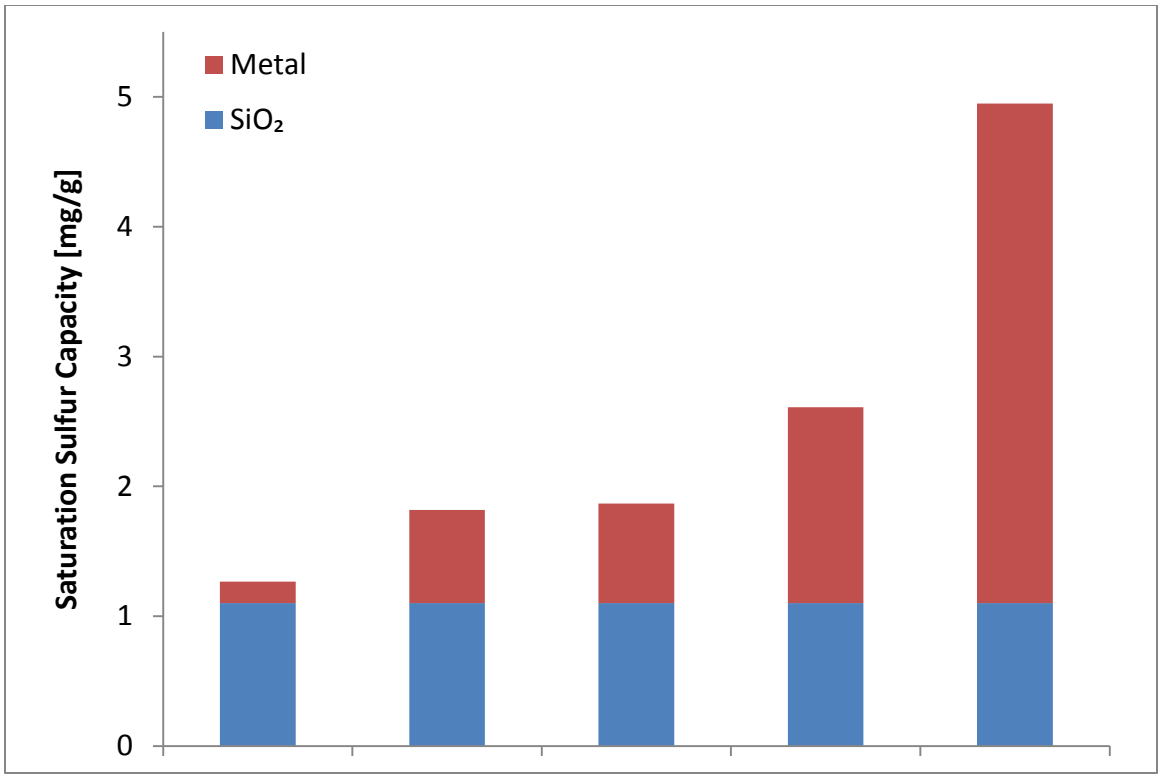

Figure III.1. Saturation sulfur capacities of 4.0 Wt.% transition metal ions supported on SiO_2 determined using JP5 fuel with 1172 ppmw sulfur

III.2.2 Sorbent Formulation

A sorbent composition consists of several critical constituents. A high surface area support is generally involved either to disperse an active component or itself provides exchange sites for adsorption. A second active component when involved is generally a transition metal and in rare cases a precious metal. The amount of the active component is important so is the dispersion achieved.

III.2.2.1 Effect of Support

Ag(4 Wt.%)/SiO_2 showed the highest affinity for sulfur among Mn, Co, Ni and Cu. Ag was further supported on TiO_2 and γ-Al_2O_3 in order to identify most effective support for desulfurization of liquid fuels. The nature of the support influences the dispersion of

silver besides being involved in strong interactions with Ag. They have also been reported to effect the activity of Ag based catalysts for ethylene as well as propylene oxidation [100]. Such metal support interactions are likely to influence the sulfur capacity of these sorbents and their stability during thermal cycling. High temperature thermal treatment of TiO_2 and γ-Al_2O_3 in air improved sulfur capacity significantly compared to support particles dried at 110^oC. This was demonstrated in breakthrough experiments carried out using a model fuel consisting of 3500 ppmw benzothiophene in octane. Blank TiO_2, γ-Al_2O_3 and SiO_2 were prepared by following identical steps as with the supported Ag sorbents except that HNO_3 of similar concentration was used for impregnation. The TiO_2 blank showed the highest capacity among the three supports at 19.82 mg/g compared to a capacity of 17.34 mg/g demonstrated by γ-Al_2O_3. However SiO_2 support did not demonstrate this improvement in sulfur capacity following the thermal treatment. Thus calcination only generated active centers on the TiO_2 and γ-Al_2O_3. The calcined TiO_2 support demonstrated a capacity of 19.82 mg/g compared to 5.58 mg/g demonstrated by the dried support. The reason for this improvement in sulfur capacity is presented in Chapter VI.

Ag loading of 4 Wt.% were obtained on the three supports by varying the concentration of the $AgNO_3$ impregnating solution keeping the volume of impregnation equal to the pore volume of the respective supports. Breakthrough for the supported Ag sorbents were observed using JP5 fuel with total sulfur content of 1172 ppmw shown in Figure III.2. At 10 ppmw breakthrough capacity, Ag/SiO_2 showed capacity of 0.49 mg/g

in comparison to 1.87 by γ-Al_2O_3 and 0.82 by TiO_2. However SiO_2 showed the highest saturation capacity of 9.74 mg/g compared to 6.97 by γ-Al_2O_3 and 5.6 by TiO_2.

Sorbent/support	**BET surface area [m_2/g]**	**Pore volume [ml/g]**	**Active metal surface area [m_2/g]**	**Dispersion %**	**Avg. crystal size [nm]**
Ag(4%)/TiO_2	114.2	0.27	6.69	34.2%	3.42
Ag(4%)/γ-Al_2O_3	252.5	0.56	4.62	23.0%	5.11
Ag(4%)/SiO_2	267.0	0.50	3.95	20.3%	5.79

Table III.1. Pore structure and Ag dispersion of 4Wt. % Ag/TiO_2, Ag/SiO_2, Ag/γ-Al_2O_3

O_2 chemisorption and N_2 adsorption were used to determine Ag dispersion and surface characteristics. Oxygen uptake on 4 Wt.% Ag on TiO_2, SiO_2 and γ-Al_2O_3 are shown in Figure III.3. The highest dispersion of Ag was observed on TiO_2 despite both SiO_2 and γ-Al_2O_3 having twice the BET surface area (Table III.1). Even though smaller crystallites have been noted to be prone to sintering in reducing atmospheres at elevated temperatures, TiO_2 was observed to be a substantially more stable support during thermal cycling in oxidizing conditions. Ag dislodged from the surface of SiO_2 and γ-Al_2O_3 was observed on the tubing as well as reactor walls after a few cycles of operation unlike TiO_2. TiO_2 has been reported to be a more stable support for Ag by other researchers as well. Thus TiO_2 was chosen as the primary support material for further desulfurization studies.

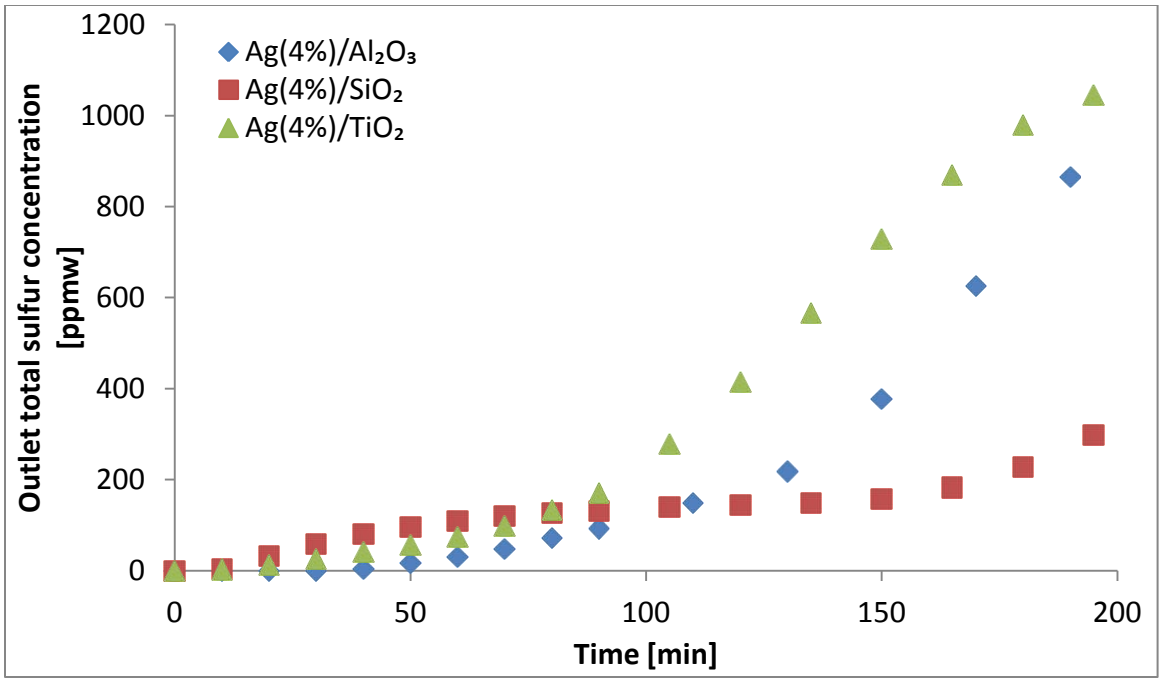

Figure III.2. Breakthrough characteristics of 4 Wt.% Ag supported on TiO_2, γ-Al_2O_3 and SiO_2 for JP5 with a total sulfur content of 1172 ppmw sulfur

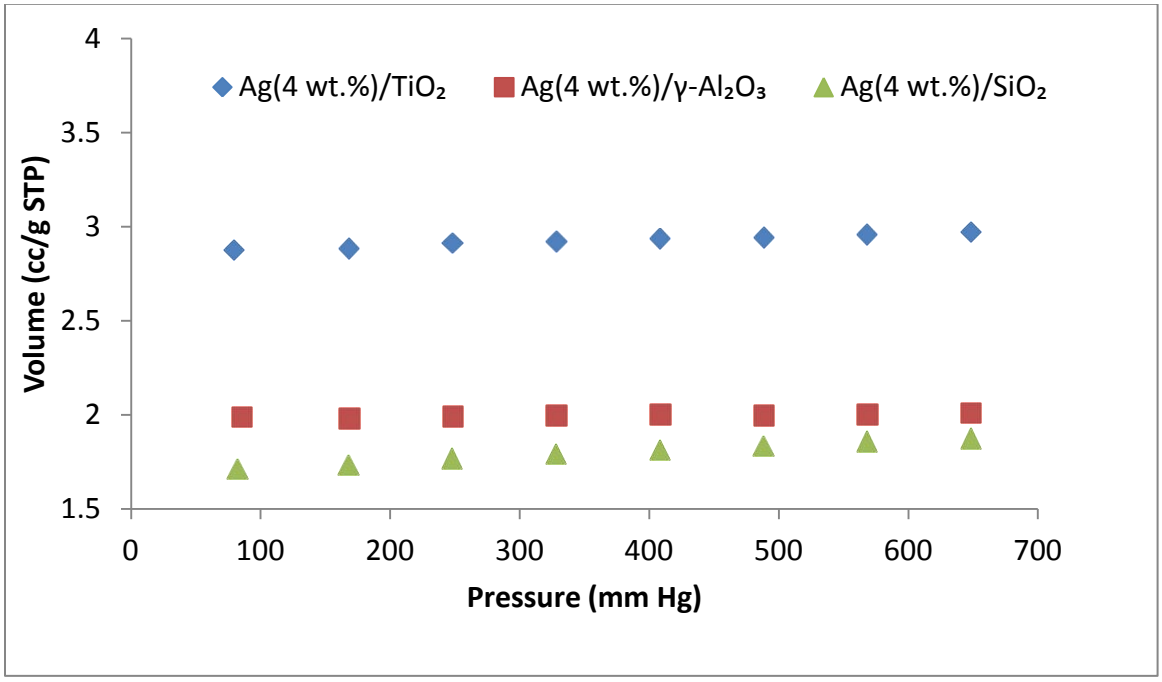

Figure III.3 . Oxygen uptake of 4.0 Wt. % Ag/TiO_2, Ag/SiO_2, Ag/γ-Al_2O_3

III.2.2.2 The effect of pore structure of TiO_2

The pore structure of a sorbent affects the transport or diffusion of large aromatic sulfur species of a fuel between active sites on the interior of the sorbent particle and bulk of the fuel. Thus transport impacts the desulfurization performance as well as the regenerability of the sorbent. Similar to support chemistry, support pore structure also influences the dispersion of metals on the surface. Generally higher surface area supports tend to result in a higher dispersion of the active metals. Larger pore sizes facilitate higher mass transfer rates for the heavy molecular weight sulfur aromatics. Ag (4Wt. %)/TiO_2 was prepared on three types of TiO_2 supports with surface characteristics as listed in Table III.2.

Type	Vendor	BET surface area [m^2/g]	Pore volume [ml/g]	Avg. pore diameter [nm]	Active metal surface area [m^2/g]	Dispersion %	Avg. crystallite size [nm]
1	St. Gobain Nor Pro	114.2	0.27	9.61	6.69	34.4	3.41
2	Alfa Aesar	98.35	0.36	14.59	4.73	24.4	4.83
3	Alfa Aesar	38.48	0.23	24.02	4.61	23.7	4.96

Table III.2. The pore structure and dispersion of Ag sorbents supported on three grades of TiO_2 supports.

The breakthrough performance of three sorbents using a model fuel with approximately 3500 ppmw benzothiophene with n-octane is shown in Figure III.4. Ag

supported on Type 1 TiO_2 demonstrated the highest sulfur capacity of 28.74 mg/g saturation capacity followed by type 2 TiO_2 at 27.87mg/g. Type 3 TiO_2 having the lowest surface area among the three had the lowest sulfur capacity of 9.29 mg/g. Thus the sulfur capacity was observed to be more dependent on of the specific surface area than the pore volume of the sorbent. Higher surface area materials tend to have more defects on the surface leading to better dispersion of metals which results in more active sites. The pore sizes of the three types of TiO_2 used were much larger than the dimensions of the sulfur aromatics in fuels. Thus the pore size of the support did not influence desulfurization performance of the sorbent.

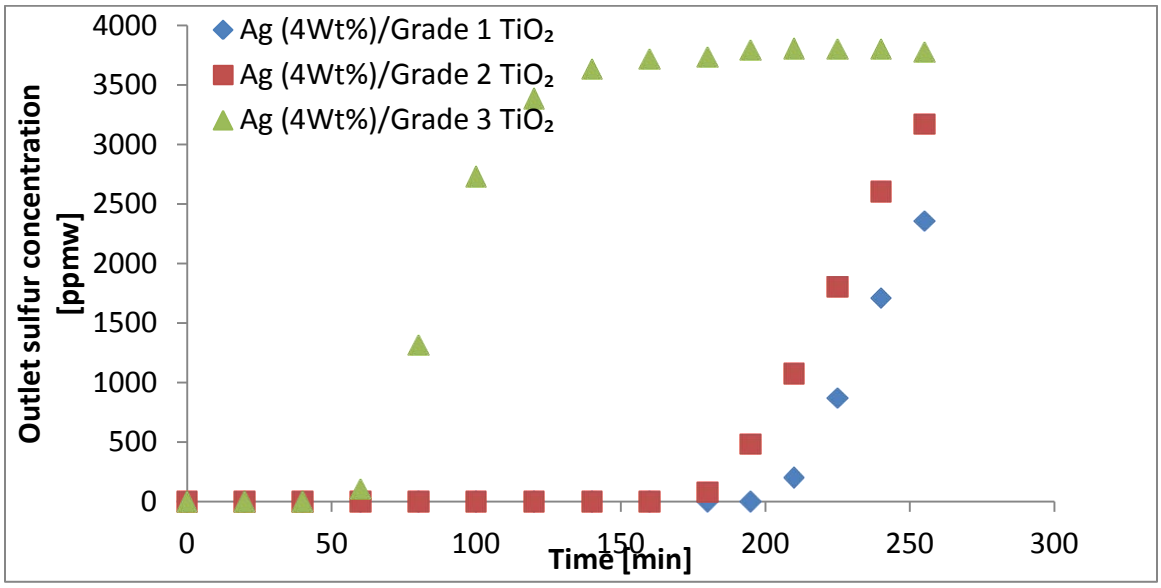

Figure III.4. Breakthrough performance of Ag (4 Wt.%)/TiO_2 using supports with different pore structure for a model fuel containing 3500ppmw benzothiophene in n-octane

III.2.2.3 The effect of Ag loading

The silver loading in the sorbents tested so far were maintained at 4.0 Wt.%. Since metal loading affects its dispersion and influences the interactions with the

support, sorbents with loading varying between 2 and 20 Wt.% were prepared and tested for desulfurization performance. JP5 fuel with a total sulfur content of 1172 ppmw sulfur was used as the challenge. While Ag loading was varied, O_2 chemisorption was used to examine the dispersion of Ag. N_2 adsorption was also used to determine BET surface area and pore volume of the sorbent. Specific surface areas and pore volumes of the sorbents decreased with Ag loading. This indicates a progressive clogging of pores with increasing Ag loading. The effect of silver loading on its dispersion is summarized in Table III.3. Generally increasing metal loading has the effect of reducing its dispersion. This is due to the agglomeration of metal atoms into crystallites. This trend was observed in the case of Ag/TiO_2 sorbents as well. Oxygen chemisorption indicated that the average crystal size increased from 3.4 nm to 6.9 nm when the loading was increased from 4 to 20 Wt.% Ag while the dispersion decreased from 34 to 17%.

Ag loading [Wt.%]	**BET surface area [m^2/g]**	**Pore volume [ml/g]**	**Active metal surface area [m^2/g]**	**Avg. crystal size [nm]**	**Disp. %**
4.00	114.2	0.274	6.69	3.4	34.44
8.00	89.33	0.2303	10.7	4.1	28.66
12.00	79.22	0.2115	12.05	5.3	22.35
20.00	57.92	0.1331	14.31	6.9	17.04

Table III.3. Surface properties of Ag/TiO_2 sorbents with different silver loadings

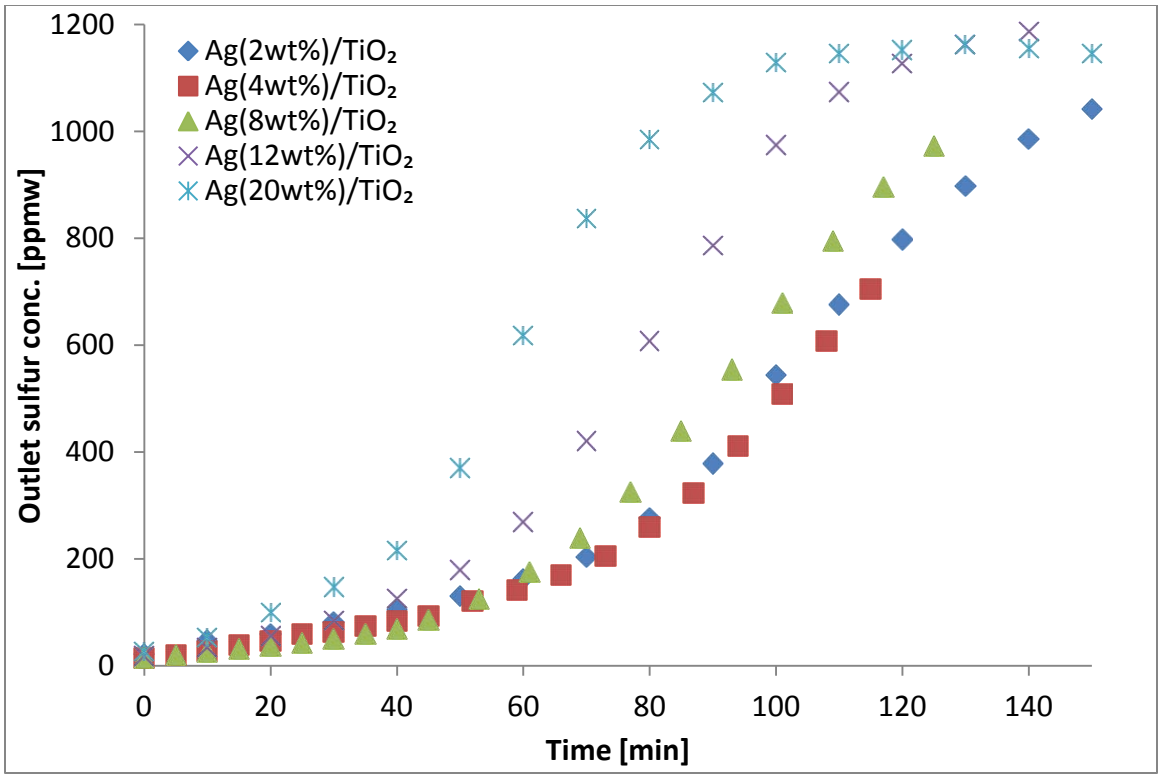

Figure III.5. Breakthrough performance of Ag/TiO_2 sorbent with the Ag loading varied between 2 and 20 Wt.% for JP5 fuel with 1172 ppmw sulfur

From the breakthrough data shown in Figure III.5, the sorbents with lower Ag loadings had the highest sulfur capacity. The difference in sulfur capacity was minimal between 2 and 4% Ag loading with the 4% performing marginally better. The loss in capacity was significantly larger at the higher loadings of Ag. The active Ag surface area increased from 6.69 m^2/g to 14.31 m^2/g between 2 and 20 % loadings. Sulfur capacity was lost despite this increase in Ag surface area. This indicates that the sulfur capacity is associated with a highly dispersed phase of Ag. Loss in sulfur capacity at the higher loadings may also be associated with loss in active desulfurization centers on the support that are shielded by the larger Ag crystallites.

III.2.3 Multi-cycle performance

Sulfur sorbents that operate in the liquid phase have relatively low capacity. It is thus impractical to use a single use sorbent for sulfur removal from hydrocarbon fuels. Regenerability is most cost-effectively carried out using air rather than solvents and reducing gases such as hydrogen. The Ag (4 Wt.%)/TiO_2 sorbent was taken through ten cycles of adsorption in JP5 fuel, regeneration using air. Following an adsorption step, the fluid held-up in the bed was drained downward to the sump. Air at room temperature was used as a blow-down medium for approximately 10 min to remove fuel from the particle interstices. The bed was then heated externally using a furnace to a temperature of 220^0C at a rate of 10K/min and held for 1h. This step ensured the vaporization of fuel held in the pores. Bed temperature was then raised to 450^0C at a rate of 10K/min and held for another two hours. The bed was ready for the next adsorption cycle after cooling down to room temperature in flowing air. The resulting breakthrough curves obtained following the ten regeneration cycles are shown in Figure III.6. Desulfurization performance was uniform for the ten cycles tested.

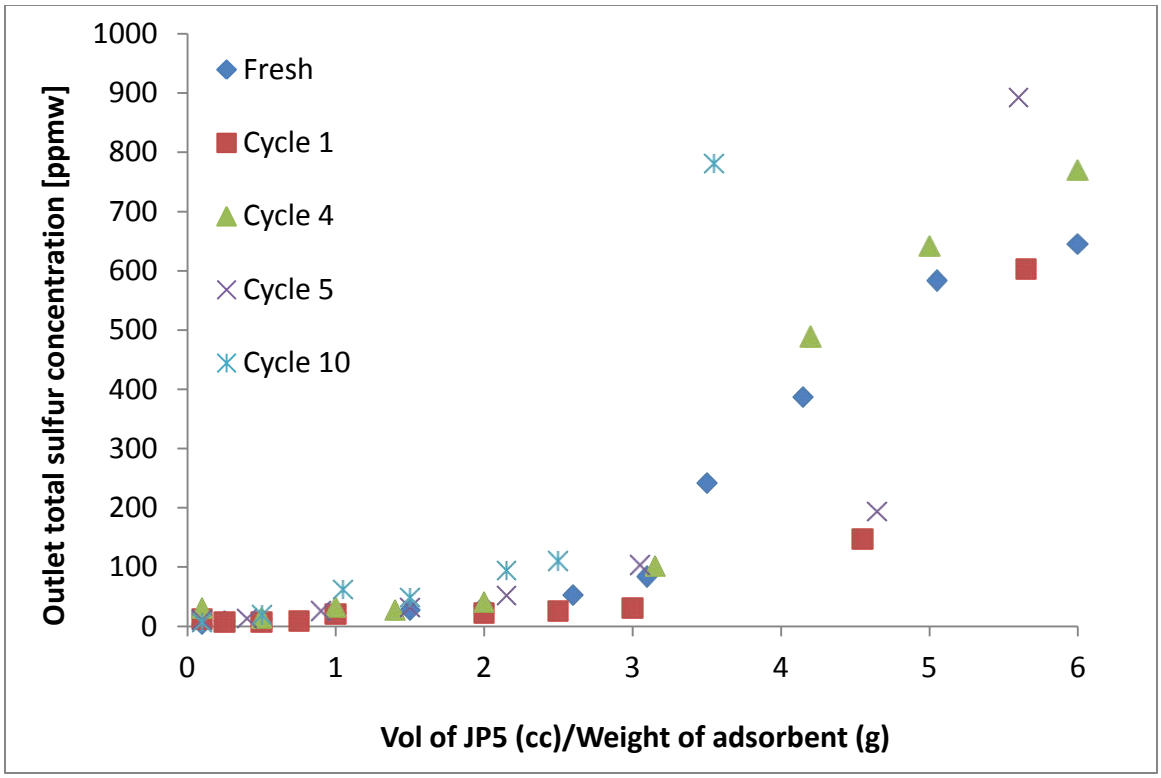

Figure III.6. Multi-cycle performance of Ag/TiO_2 sorbent tested with JP5 fuel; regenerated in air for 10 cycles

III.2.4 Effect of varying fuel composition

The sulfur content of a fuel varies depending on the origin of the crude, refining and blending operations. Refining processes such as hydrocracking and HDS significantly influence the sulfur content. Therefore, JP5, JP8 and a light fraction JP5 with respective sulfur contents of 1172, 630 and 582 ppmw were studied for desulfurization using the Ag(4.0 Wt.%)/TiO_2 sorbent. PFPD chromatograms of these fuels are shown in Figure III.7. Sulfur content varies with the source of the crude and between different batches of the same fuel [101]. The sulfur molecule contributing to approximately 20% of the total sulfur content in JP5 was 2,3 dimethyl benzothiophene. Tri methyl benzothiophenes were found to be in higher concentration in JP8 compared to JP5. From the

chromatograms it was also observed that fractionation of JP5 resulted in the separation of a majority of the heavier sulfur aromatics such as 2,3,4 Trimethyl benzothiophenes (TMBT) to the heavier fraction.

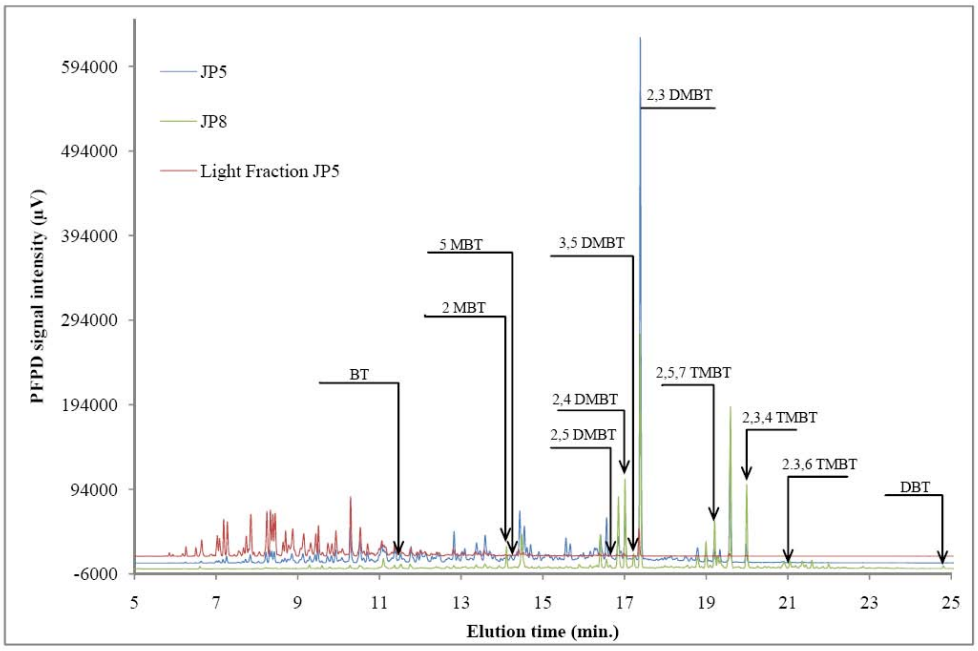

Figure III.7. Chromatograms of JP5, JP8 and light fraction JP5 showing sulfur heterocycles present

Breakthrough characteristics of the fuels using Ag(4 Wt.%)/TiO_2 sorbent are shown in Figure III.8. A summary of sulfur capacities is listed in Figure III.9. At 10 ppmw breakthrough concentration the highest capacity was demonstrated for light fraction JP5 at 4.22 mg/g. Highest saturation capacity was demonstrated for JP5 at 6.32 mg/g. The difference in breakthrough performance between JP8 and JP5 was significant. Analysis of the bed outlet after 30 min. (Figure III.10) shows that the tri-methyl benzothiophenes prevalent in JP8 were not removed by the sorbent resulting in

premature sulfur breakthrough for JP8. Thus fractionation of fuels provides an advantageous separation of sulfur species for adsorptive desulfurization.

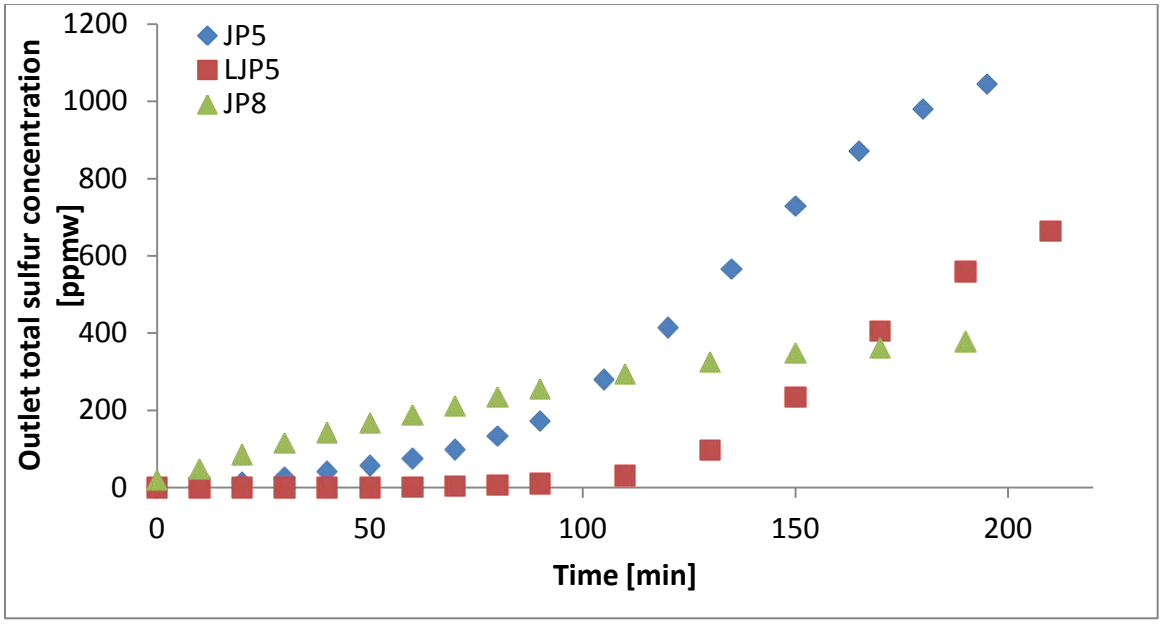

Figure III.8. Performance comparison of Ag (4 Wt.%)/TiO_2 sorbent with JP5 [1172 ppmw], JP8 [693 ppmw] and light fraction JP5 [582 ppmw] fuels.

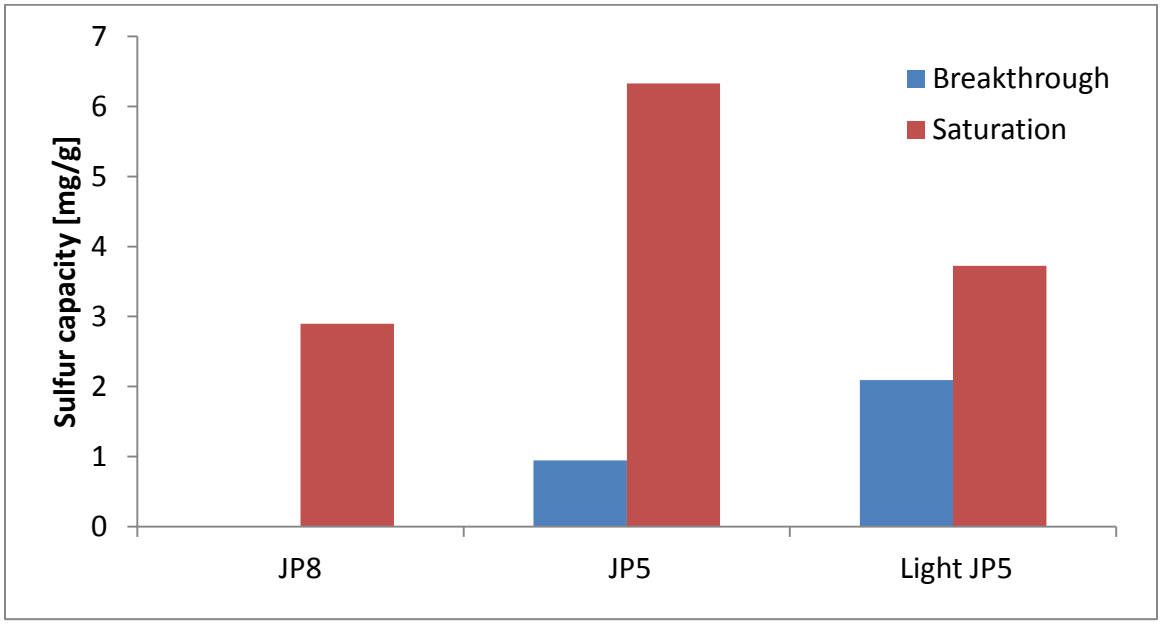

Figure III.9. Sulfur capacities for Ag (4 Wt..%)/TiO_2 sorbent for JP5, JP8 and light fraction JP5

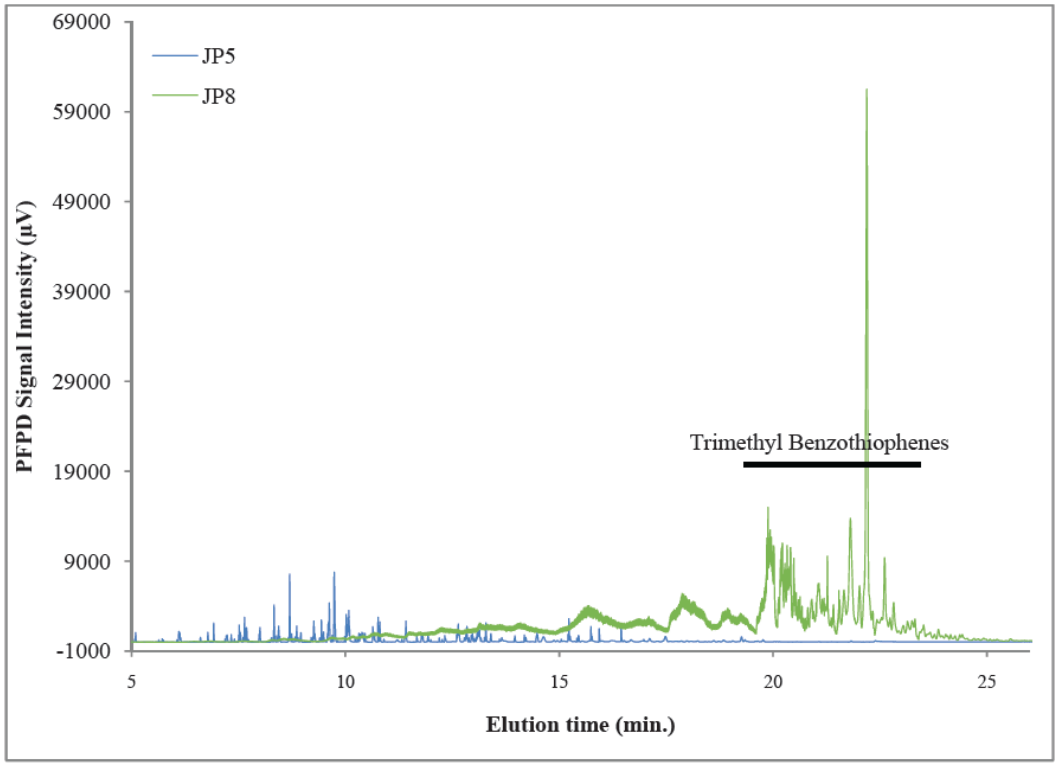

Figure III.10. Chromatograms of bed output after 30 min. showing the higher concentration of Tri-methyl benzohtiophenes

III.3 Conclusions

The high affinity of Ag for sulfur observed in the tarnishing of silver in air was also observed to be true for sulfur in hydrocarbon fuels. The Ag(4Wt..%)/TiO_2 sorbent demonstrated a saturation sulfur capacity of 6.3 mg/g for JP5 (1172 ppmw sulfur) and 2.9 mg/g for JP8 (630 ppmw sulfur) at ambient conditions. Thermal treatment of acidic supports such as TiO_2 and γ-Al_2O_3 was observed to generate desulfurization centers in addition to the sulfur capacity demonstrated by the Ag phase. Higher sulfur capacity was demonstrated by sorbents with higher dispersion of Ag. Therefore the active desulfurization centers are associated with a highly dispersed oxide phase of Ag. Thermal regeneration conditions for the sorbent using air were also established and

demonstrated for 10 cycles with minimal loss in capacity. Differences in desulfurization efficiency were observed with varying fuel chemistry and the respective sulfur aromatics involved. The sorbent showed the best performance with light fraction JP5 due to the lower concentration of tri-methyl benzothiophenes. The mechanism of sulfur removal for these sorbents is will be presented in the following chapters.

IV. Synthesis, Optimization and Characterization of Ag/TiO_2 Sorbents

IV.1 Introduction

Several factors that could significantly affect the desulfurization efficiency of Ag/TiO_2 sorbent were investigated in this chapter. As with any catalytic material, preparation conditions were found to affect the sulfur capacity. Preparation conditions dictate physiochemical properties of the surface, affect the dispersion of active metal and ultimately govern the number of active adsorption centers on the surface. Preparation methods also affect the thermal stability of the sorbent and hence its life over multiple regeneration cycles. Conditions of impregnation, drying and calcination stages were varied and the effect sulfur capacity investigated. Pretreatment of the support is generally carried out during catalyst manufacturing to improve structural integrity, vary surface roughness, induce surface defects and to drive off/introduce water molecules or -OH groups on the surface. Pretreatment of the TiO_2 support was carried out to discern the effect on sulfur capacity.

Some impregnation variables that affect the performance of supported catalytic materials are chemical nature, ionic concentration and volume of the precursor. The

chemical nature and concentration of the precursor affects the dispersion of the metal. The volume of impregnation affects the homogeneity of the active species on the support. Generally higher impregnation volumes have been shown to produce more homogeneous catalysts. Smaller volumes of impregnation have been shown to render the properties of Mo/Al_2O_3 catalysts more sensitive to preparation variables while [102] higher volumes of impregnation generate high concentration gradients during the precursor drying stages and result in lower dispersions. A drying stage is employed to drive precursor solvent from support. In general, drying is carried out at temperatures near or above the boiling point of the solvent or under vacuum. The ratio of the precursor nucleation rate to crystal growth rate determines the crystal size during solvent vaporization [103]. The rate of drying affects the redistribution of the solute on the support. Calcination is generally carried out in an oxidizing atmosphere for precursor decomposition, formation of an oxide species, bonding of the formed oxide to the support, removal of some of the elements introduced during the impregnation step and sintering of the formed oxide species. Generally dispersion has been observed to increase with calcination temperature [104, 105] and then decrease. Higher temperatures lead to sintering of the precursor or the formed oxide and lower the dispersion.

The various oxide phases of Ag present in the sorbent were identified and quantified using thermal and spectroscopic methods. The dispersion of Ag and pore structure of the sorbent were obtained from gas volumetric methods. The effect of metal weight loading on redox behavior of Ag was also investigated. These

measurements along with sulfur adsorption capacities were used to form a better understanding of structure-activity relationships in these materials. Ultraviolet spectrum of sorbents with Ag loading varying between 2 and 20% was studied to identify the different oxidation phases of Ag. Absorption bands were compared to features identified by previous research. Qualitative information on redox properties of the dispersed Ag was obtained from temperature programmed reduction and thermogravimetric measurements. Phase transformations were identified from the thermoreduction profiles and quantified using H_2 consumption.

IV.2 Details of sorbent synthesis

Typical synthesis procedures have been presented in Chapter II. Optimization procedures followed to arrive at the preferred sorbent composition is described in the current chapter. To study the effect of support pretreatment, three sorbent batches of similar composition were prepared differing in only in TiO_2 pretreatment conditions. A batch of sorbent was prepared where TiO_2 particles were treated with moist air (100% RH) prior to impregnation. The resulting moisture uptake was 4.6 Wt.% on a wet basis. Acid pretreatment of the support was also carried out with 15N HNO_3 (imbibed for 8h), washed and dried prior to the impregnation of $AgNO_3$. Ag was dispersed using deposition precipitation as follows. The dried TiO_2 support was impregnated with a 3 Wt.% solution of ammonium carbonate and dried at 110°C for 6h. The $AgNO_3$ precursor was subsequently impregnated followed by drying and calcination. Previously deposited

bicarbonate would serve as nucleation sites for the $AgNO_3$ precursor. The resulting ammonium nitrate would decompose during the drying and calcination steps.

Sorbents were also prepared by varying the precursor volume. Precursor concentration was kept constant at 1M to maintain similar conditions at the solid-liquid interface. The volume of the precursor was varied between incipient wetness and wet impregnation conditions. When the volume of precursor used is the pore volume of the support (V/V=100%), the technique is referred to as incipient wetness (or dry) impregnation. When the support particles are suspended in excess precursor solution followed by a filtration and drying step, the technique is referred to as wet impregnation. Here, wet impregnation was achieved by using precursor solution 2.5 times the pore volume of the support such that the solution formed a distinctive layer over the particles. Impregnation was also carried out in a vacuum chamber wherein the support particles were evacuated to a final pressure of 1 mTorr followed by introduction of precursor through a nozzle.

Sorbent particles dried at 50, 90, 110, 150 and 200°C and tested for sulfur capacity to ascertain the effect of drying rate on sulfur capacity and also characterized for Ag dispersion. The samples were weighed at intervals during the drying process to determine the drying rate. Drying was also carried out in a vacuum chamber (1 mTorr) while the temperature was maintained at 30°C. The vacuum was able to remove only 85% of the precursor solvent from the support following a 6h drying period. Effect of varying calcination temperature (300-600°C) was also determined.

Ultraviolet spectroscopy was carried out on Ag/TiO_2 varying Ag loading between 2 and 20 Wt.%. TPR experiments were carried out in a typical gas chromatographic apparatus using H_2 Thermogravimetric analysis was carried out using a TA Instruments Q50 TGA apparatus.

IV.3 Results and discussion

IV.3.1 Synthesis

Synthesis of the Ag/TiO_2 sorbent followed the general routes for supported catalysts involving impregnation, drying and calcination steps. Metal dispersion on the support depends on the strength of interaction between the precursor and support, stronger interactions resulting in higher dispersions. Both the chemical nature and pH of the precursor affects interactions at the support-precursor interface. The pH of the precursor affects the protonation or deprotonation of the surface which may be used to anchor the metal ion to the surface. The stages of sorbent preparation optimized in this work are impregnation, drying and calcination.

IV.3.1.1 Pretreatment of support

Conditions at the support surface were altered prior to introduction of the precursor in an effort to improve the sulfur capacity as well as thermal stability. Ag was deposited using the deposition precipitation method using ammonium carbonate as a nucleating agent. The effect of moisture on the support surface during impregnation was studied. Breakthrough of benzothiophene in a model fuel was used to compare sulfur capacities.

Figure IV.1), support pretreatment was observed to have a negative impact on the performance of the sorbent. Sulfur capacity of the sorbent prepared through deposition precipitation was closest to that of sorbent prepared devoid pretreatment steps. Moisture pretreatment of TiO_2 reduced the sulfur capacity of the sorbent from 22.3 to 18.6 mg/g. Surface water should only influence the impregnation stage and thus affect the dispersion of the metal. However no marked variation in dispersion or pore structure was observed as compared to other samples (Table IV.1). Water molecules not removed during drying and calcination stages maybe retained on the surface with forces stronger than hydrogen bonding [106]. Therefore moisture introduced during the impregnation stage had a negative influence on sulfur capacity of the sorbent.

Treatment with concentrated acids have been shown to increase surface roughness, increase dispersion of metals and enhance stability of catalytic materials [107]. Pretreatment with concentrated HNO_3 (15N) failed to improve the sulfur capacity of the sorbent. The loss in sulfur capacity corresponded to a significant loss in BET surface area which decreased from 128.9 to 76.6 m^2/g. Increase in the average pore diameter of the sorbent indicated a collapse of smaller pores. Interference of remaining nitrate ions with the precursor would also result in lower Ag dispersion. Loss in sulfur capacity was attributed to these two causes.

Pretreatment Step	BT cap. [mg/g]	SAT cap. [mg/g]	Surface area [m^2/g]	Pore volume [cc/g]	Avg. PD [A]	Metal surface area [m^2/g]	Avg. crystallite size [A]	Dispersion %
Deposition Precipitation	22.30	27.26	115.0	0.3936	136.9	5.13	44.56	26.41
Air at 100%RH	18.58	21.68	130.1	0.4566	140.4	5.38	42.49	27.70
5M Nitric Acid	13.62	15.36	76.6	0.3635	189.8	4.12	55.45	21.23
None	23.54	30.98	115.2	0.3387	117.6	5.76	39.65	29.68

Table IV.1. The effect of pretreatment of the support prior to introduction of the precursor on the properties of the sorbent and sulfur capacity

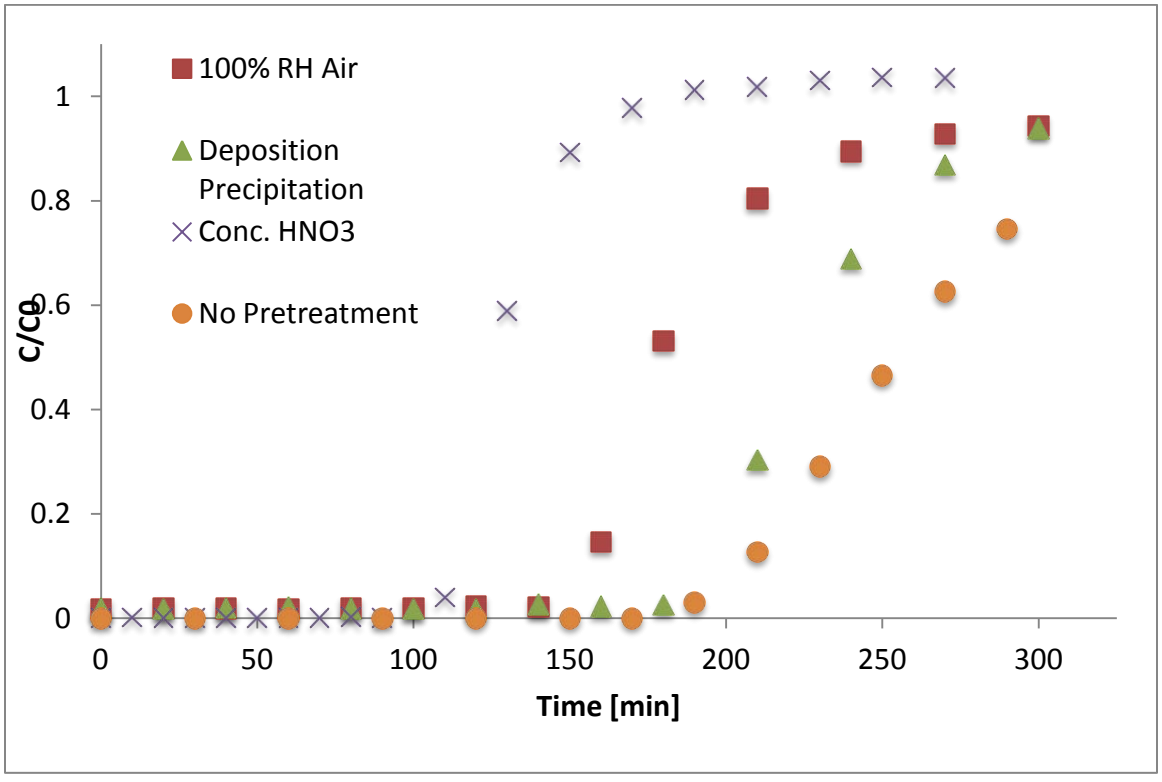

Figure IV.1. Breakthrough of benzothiophene for Ag/TiO_2 sorbents where the TiO_2 was pretreated with moist air, ammonium carbonate (DP), and conc. HNO_3 compared to sorbent prepared without any pretreatment

IV.3.1.2 Effect of impregnation conditions

The volume of impregnation of the precursor is generally optimized with respect to the pore volume of the support. Ag/TiO_2 was prepared and tested with the volume of impregnation varying between incipient wetness and wet impregnation. Breakthrough of benzothiophene for the samples is shown in Figure IV.2. The pore structure and Ag dispersion were measured to correlate sorbent properties with sulfur capacities (Table IV.2). Sulfur capacities of sorbents prepared at incipient wetness and those impregnated with excess precursor (V_{liq}/V_{pore} 145%) were similar. There was a minimal loss in surface area and pore volume between the two sorbents attributed to the increase in Ag loading along with a lowering of average pore size.

Ag/TiO_2 prepared using wet impregnation showed the lowest sulfur capacity. The BET surface area was lower by 62% and the crystal size higher by 18Å between incipient wetness and the wet impregnation. The lowering of surface area did not correspond to the increase in Ag loading. This was explained by the collapse of the support pore structure during wet impregnation. One reason for such collapse is a phenomenon referred to as *decrepitation.* Decrepitation occurs when excess impregnating solution compresses the air inside the pores to high pressures resulting in the disintegration of the pore structure [107-109]. Therefore degradation of pore structure was considered to mainly contribute to the lower sulfur capacity.

Between the samples prepared using incipient wetness, V_{liq}/V_{pore} 145% and wet impregnation, the Ag weight loading increased from 4.0 to 11.5%. However this was not

reflected by a proportional increase in sulfur capacity. In fact the sulfur capacity was observed to be the lowest when the Ag loading was 11.5%. In order to increase the number of adsorption centers on the surface, the additional Ag should be dispersed such that they provide more centers than the corresponding loss in centers on the TiO_2 surface.

Even though vacuum impregnation (VI) generally reduces the effects of decrepitation, in the case of TiO_2 support, the sorbent demonstrated the lowest sulfur capacity. The pore structure of the vacuum impregnated sorbent was not significantly different from the others. However O_2 chemisorption indicated a significant loss in Ag dispersion in the VI samples. Impregnation carried out using a single nozzle would result in non-uniform precursor distributions. Such samples would indicate lower dispersion using gas chemisorption.

The effect of the pH of the impregnating solution on the sorbent performance was also determined. Even though the pH of the precursor changes the conditions on the interface and thus exchange during impregnation, a significant difference was not found between the performances of the sorbents. Therefore the breakthrough data will not be reviewed here.

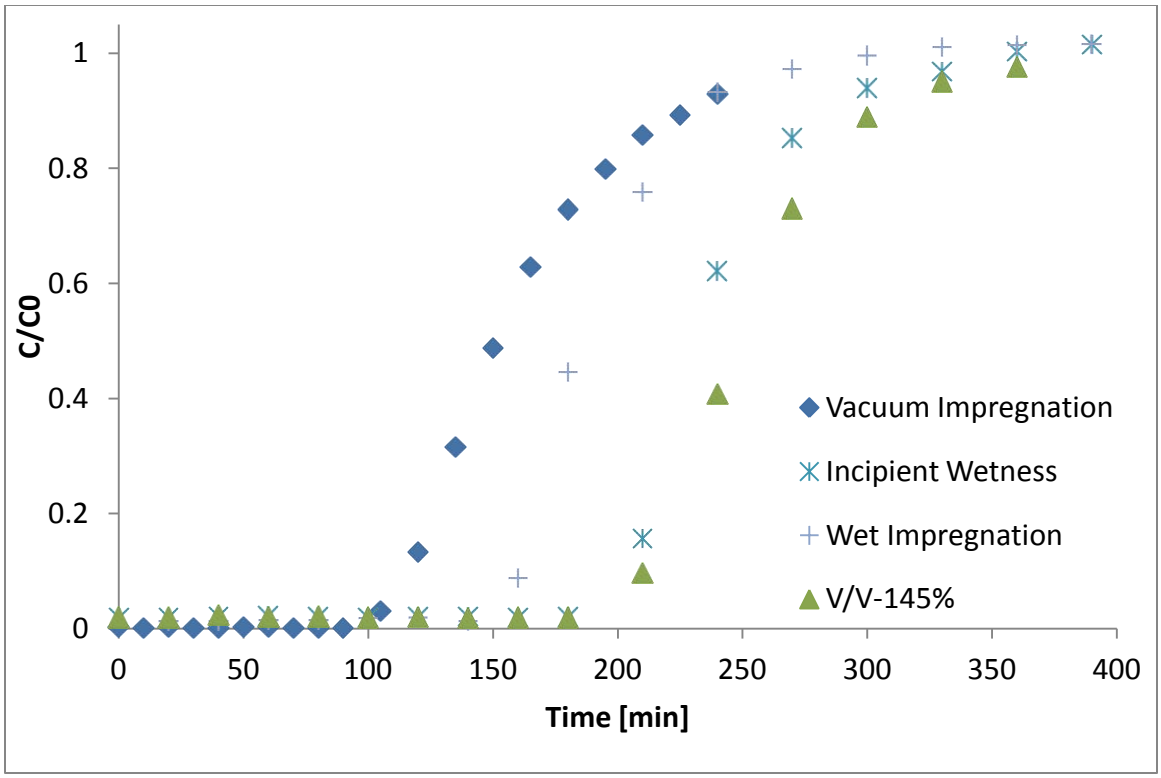

Figure IV.2. Breakthrough of benzothiophene for Ag/TiO_2 sorbents prepared using different impregnation conditions

Imp. condition	Ag Wt.%	Sulfur cap-BT [mg/g]	Sulfur cap-SAT [mg/g]	Surf. area [m^2/g]	Avg. pore size [Å]	Pore vol. [ml/g]	Dispersion %	Avg cry. size [Å]	Metal area [m^2/g]
Incipient	4.00	22.3	28.50	123.3	132.3	0.408	33.36	35.28	7.97
145 V/V%	6.71	22.3	29.74	119.5	118.4	0.354	28.81	40.85	9.38
Wet imp.	11.46	17.97	21.68	77.05	145.9	0.281	22.10	53.26	12.34
Vacuum imp.	4.00	12.39	18.59	118.1	137.1	0.4045	18.44	63.83	3.581

Table IV.2. The effect of impregnation conditions on the sulfur capacity of the sorbent as compared to the pore structure and Ag dispersion

IV.3.1.3 Effect of drying conditions

Drying is considered a crucial stage in preparation of supported catalysts and sorbents. Varying drying conditions produce specific metal profiles on support particles. This property is made use of in catalysis when the reaction rates or selectivity is controlled by diffusion processes. Generally slower drying rates result in a more uniform precursor distribution while faster rates cause migration of the metal away from the center of the particle. Increasing the rate of drying was observed to progressively transform the Mo profile from uniform to a profile resembling an egg-shell on Al_2O_3 supports [102].

Figure IV.3 shows the breakthrough behavior of the sorbents prepared at the varying drying temperatures. Sulfur capacities of the oven dried sorbents between 50 and 200°C were similar. Thus the rate of drying was not a significant factor in the preparation of Ag/TiO_2 sorbents. This indicated a strong interaction between the precursor and exchange sites on the support surface. This indicated minimal migration of ions with the moving solvent front once anchored to surface exchange sites. The similarities were also reflected in the pore structure and Ag dispersion between the samples. Compared to the samples dried in an oven, the vacuum dried sample showed remarkably low sulfur capacity. The sample had a lower specific surface area and Ag dispersion. By monitoring the sample mass during the drying process, it was noted that the vacuum chamber was unable to remove the precursor solution in its entirety. Remaining moisture would result in an acidic environment during $AgNO_3$ decomposition during calcination. Acidic environments cause the degradation of the pore structure as

observed in the case of support pretreatment using concentrated HNO_3. Therefore vacuum drying may only be advantageous when complete solvent removal is possible.

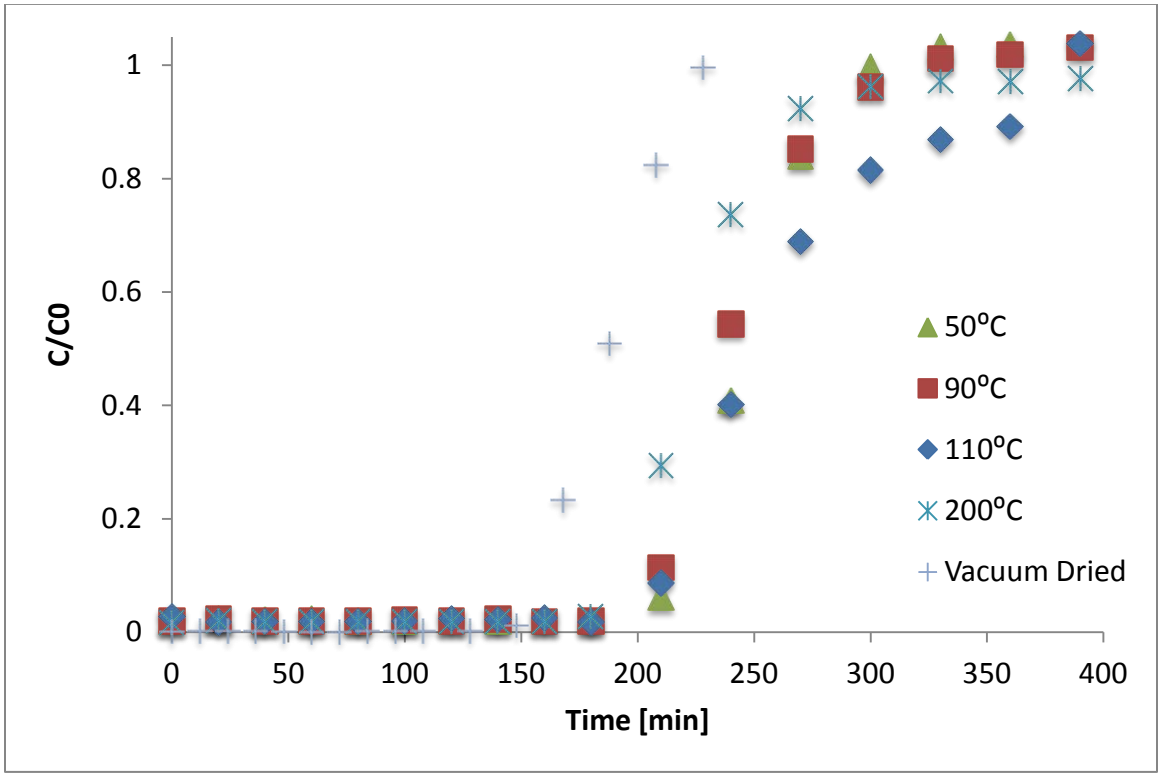

Figure IV.3. The effect of drying rate of the precursor on the sulfur capacity for Ag/TiO_2 sorbents as indicated by breakthrough of benzothiophene in a model fuel

Drying Condition	Surface area [m^2/g]	Pore volume [cc/g]	Avg. PD	Metal surface area [m^2/g]	Avg. crystallite size [A]	Dispersion
50°C	130.5	0.4270	130.8	5.231	43.70	26.93
90°C	133.0	0.4347	130.8	4.779	47.83	24.61
110°C	169.2	0.5584	132.0	4.986	45.84	25.67
Vacuum	113.1	0.3678	130.1	4.508	50.70	23.21

Table IV.3. The effect of precursor drying rate on the pore structure and dispersion of Ag

IV.3.1.4 Calcination conditions

The breakthrough of benzothiophene for the sorbents prepared at the different calcination temperatures are shown in Figure IV.4. The sulfur capacity was observed to decrease with increasing calcination temperature. Sorbents calcined at 500 and 600°C showed a significant loss in sulfur capacity.

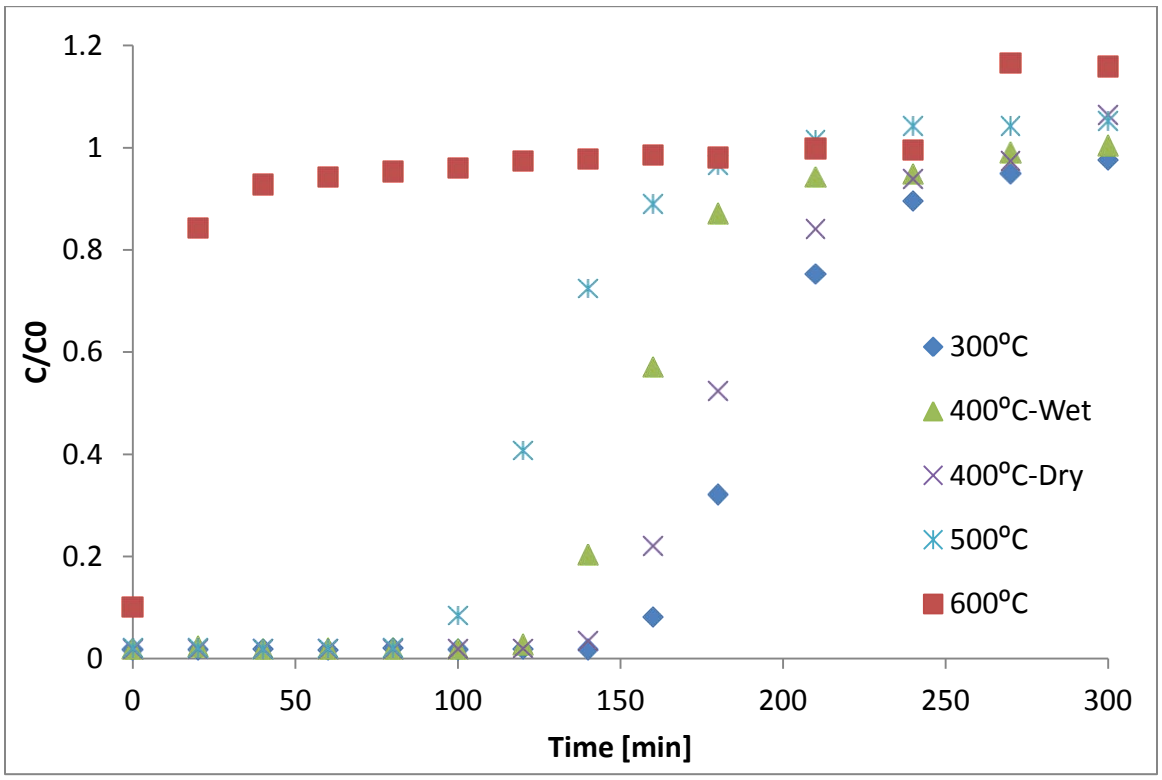

Figure IV.4. The breakthrough performance of Ag/TiO_2 with 3500 ppmw BT in n-octane showing the substantial loss in capacity by the sorbent calcined at 500 and 600°C

A comparison of the surface properties of the sorbents is listed in Table IV.4. A substantial loss in the BET surface area of the sorbent was observed with increasing calcination temperature; decreasing 75% from 128.1 at 300°C to 33.0 m^2/g at 600°C. This trend was also closely followed by the pore volume which was lower by 66%. The average pore size was observed to go through a maximum at 400°C. However such

significant variation was not observed in the dispersion of the Ag in the sorbents calcined at 500 and 600°C. The dispersion was only lower by 36% in the sorbent calcined at 300°C compared to that calcined at 600°C. Again it was observed that the pore structure had a larger impact on sulfur capacity than Ag dispersion.

Calc. Temp. °C	Sulfur cap-BT [mg/g]	Sulfur cap-SAT [mg/g]	Surf. area [m^2/g]	Avg. pore size [Å]	Pore vol. [cc/g]	Disp. %	Avg cry. size [Å]	Active metal surf.area [m^2/g]
300 (2h)	17.35	24.16	128.1	62.68	0.2007	29.16	40.36	5.664
400D (2h)	17.34	22.30	115.2	117.6	0.3387	29.68	39.65	5.764
450 (1h)	11.15	17.35	80.96	156.7	0.3171	23.10	50.96	4.485
450 (3h)	22.30	27.36	110.9	128.1	0.3550	22.23	52.93	4.318
450 (6h)	18.59	21.68	108.1	136.3	0.3685	25.58	46.01	4.968
500 (2h)	11.15	16.11	74.13	95.43	0.1769	25.07	46.94	4.860
600 (2h)	0	1.23	33.05	83.06	0.0686	18.60	63.29	3.612

Table IV.4. The effect of calcination temperature and time on sulfur capacity of Ag/TiO_2 sorbent with respect to the pore structure and Ag dispersion

The surface area decreased with increasing calcination temperatures as a result of the collapse of the pore structure as observed in alumina [110]. Increasing calcination temperatures would also result in the sintering of Ag crystals due to increased mobility of metal ions. The substantial loss in surface area from the reduction in surface roughness or clogging of smaller pores resulted in lowering the sulfur capacity of the sorbent.

The effect of duration of calcination stage was observed for sorbents calcined for 1, 3 and 6h at 400°C. The sulfur breakthrough data is shown in Figure IV.5. Increasing

calcination times had the effect of lowering the sulfur capacity of the resulting sorbent. From the surface characteristics listed in Table IV.4, increasing calcination time was observed to increase the dispersion of Ag. The sorbent with the highest specific surface area (3h) had the highest sulfur capacity followed by 6h and 1h samples. A lower calcination time result in incomplete decomposition of the precursor and was attributed to their lower sulfur capacity. Ideal calcinations conditions were thus established at 400°C for 2h in moisture free air. Longer calcination periods also drive off surface functional groups that might contribute to the sulfur capacity.

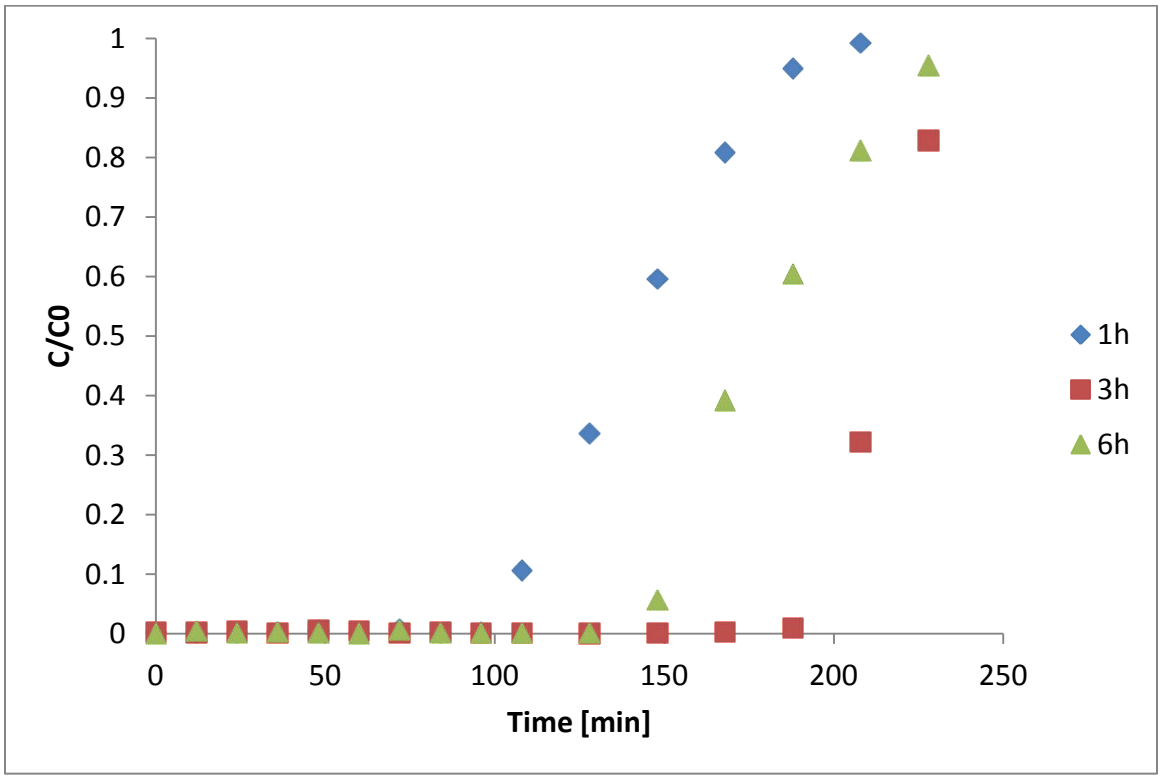

Figure IV.5. Effect of variation in calcination time (1, 3 and 6h) on the breakthrough of benzothiophene for Ag/TiO_2 sorbent

Efforts to increase dispersion of Ag by changing support morphology and conditions at the interface during the impregnation step were not successful. Incipient

wetness impregnation generated high sulfur capacity while wet impregnation was not preferred. Drying conditions did not significantly influence the sulfur capacity of the sorbent. Minimal effect of support pretreatment and drying conditions indicated a strong support-precursor interaction. Even though sorbents calcined at lower temperatures showed better performance, calcination temperature was maintained at 450°C as this was the established regeneration temperature of the sorbent. Thus ideal sorbent synthesis conditions for Ag/TiO_2 were established.

With the sorbent composition and synthesis procedures established, performance was tested with JP5 fuel with a sulfur content of 1172 ppmw sulfur where the sorbent demonstrated consistent sulfur capacity of 7.6mg sulfur/g for 10 adsorption and regeneration cycles. Efforts were consequently made to identify and quantify the composition of the sorbent with respect to the oxidation state of Ag. Information on the chemical composition of the sorbent would provide a better insight on interactions of sulfur heterocycles and adsorption centers.

IV.3.2 Characterization

IV.3.2.1 Ultraviolet absorption

Ultraviolet absorption has been used not only to identify the oxidation state of Ag on supported catalysts but also provide information on the crystal structure/morphology of the Ag phase. UV absorbance bands at 210 and 230 nm have been associated with the electronic transition $4d^{10}$ to $4d^9s^1$ of highly dispersed Ag^+ ions. Bands representing oxidized Ag clusters ($Ag_n^{\delta+}$) of different sizes have been reported at

270-290, 350 and 370-390 nm. Metallic Ag in the form of a film identified at 315 nm and clusters or aggregates at 420-460nm [96, 111-114].

The highly dispersed Ag^{+} species (223nm) were observed on all Ag loaded samples (Figure IV.6). The band intensity reduced with increasing loading [115]. Bands representing oxidized Ag clusters ($Ag_n^{\delta+}$) at 352nm were observed in all the samples also weakening with increasing metal loading until disappearing at loadings greater than 8Wt.%. Thus the UV absorption data conclusively indicated the presence of the oxide phases of Ag while those representing metallic Ag in the form of film or aggregates were absent.

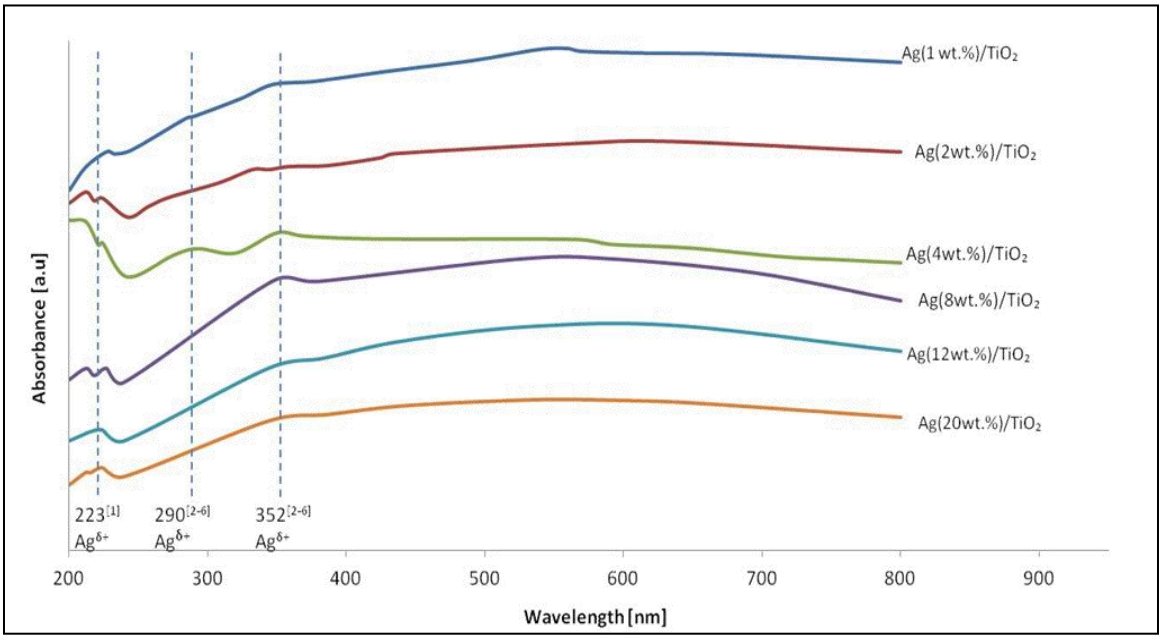

Figure IV.6. Ultraviolet absorption spectra of Ag/TiO_2 sorbents with Ag loading varying between 1 and 12 Wt.%

IV.3.2.2 Thermogravimetric analysis

Qualitative information on the redox behavior of Ag/TiO_2 samples at various Ag loadings was obtained using thermogravimetry. Weight loss profiles of samples without *in situ* pretreatment indicated a gradual weight loss attributed to desorption of water molecules, surface hydroxyls and/or volatile organic compounds. For a sample with 12 Wt.% Ag loading, the initial loss in weight was similar to the blank sample as shown in Figure IV.7. The Ag loaded samples demonstrated a loss in weight at ~550^{o}C which was attributed to the decomposition of the oxide. The reduced sample experienced weight gain at ~250^{o}C indicating Ag oxidation. This feature being absent in the oxidized sample indicated that some of the Ag existed as oxide in the adsorbent. Absence of any features during the cooling cycle indicated the failure of the metal to oxidize. Stronger interactions between the metal and support result in more stable structures.

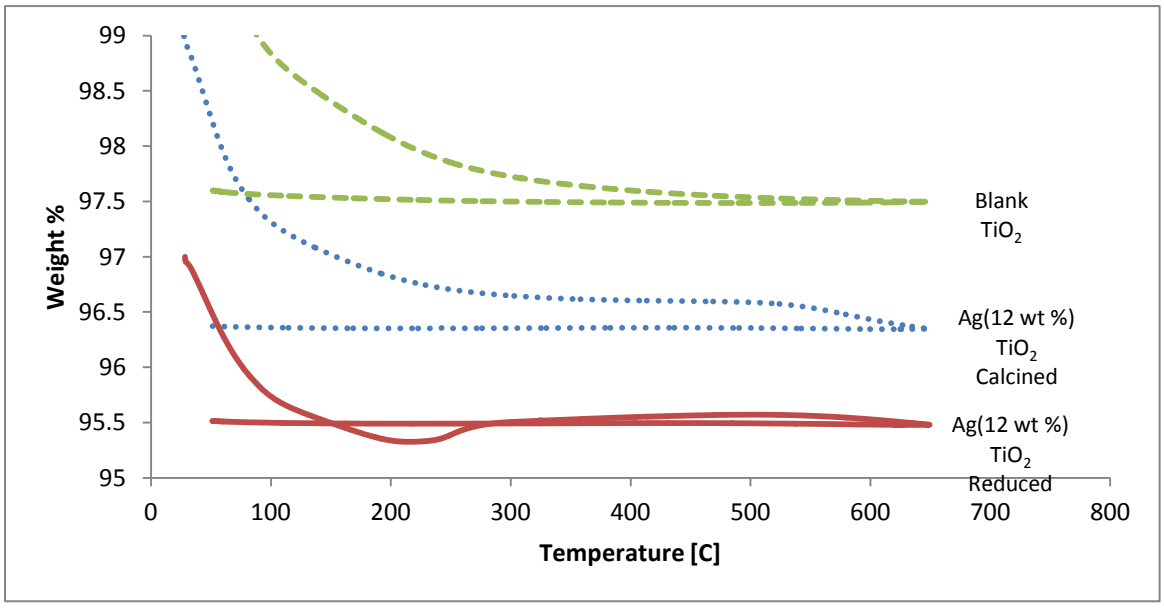

Figure IV.7. TGA profile of calcined and reduced Ag (12 Wt.%)/TiO_2 (*exsitu* 5%H_2/He, 250^{o}C/1h) compared to blank TiO_2 in air

In order to deconvolute the mass changes from loss in moisture from the phase changes in the Ag phase, the samples were heated *in situ* at 400°C for 2h and then cooled to 50°C prior to ramping to 600°C. Pretreatment was carried out in oxidizing (5%O_2/He) and reducing atmosphere (3%H_2/He). No significant mass changes were observed for the samples pretreated in oxidizing atmosphere till 500°C (Figure IV.8). However the blank sample was observed to gain mass between the pretreatment phase and final temperature ramp. This was attributed to moisture uptake as the temperature lowered. The Ag loaded samples did not exhibit this behavior. Decomposition of oxide at ~500°C was evident for samples with weight loading greater than 8%.

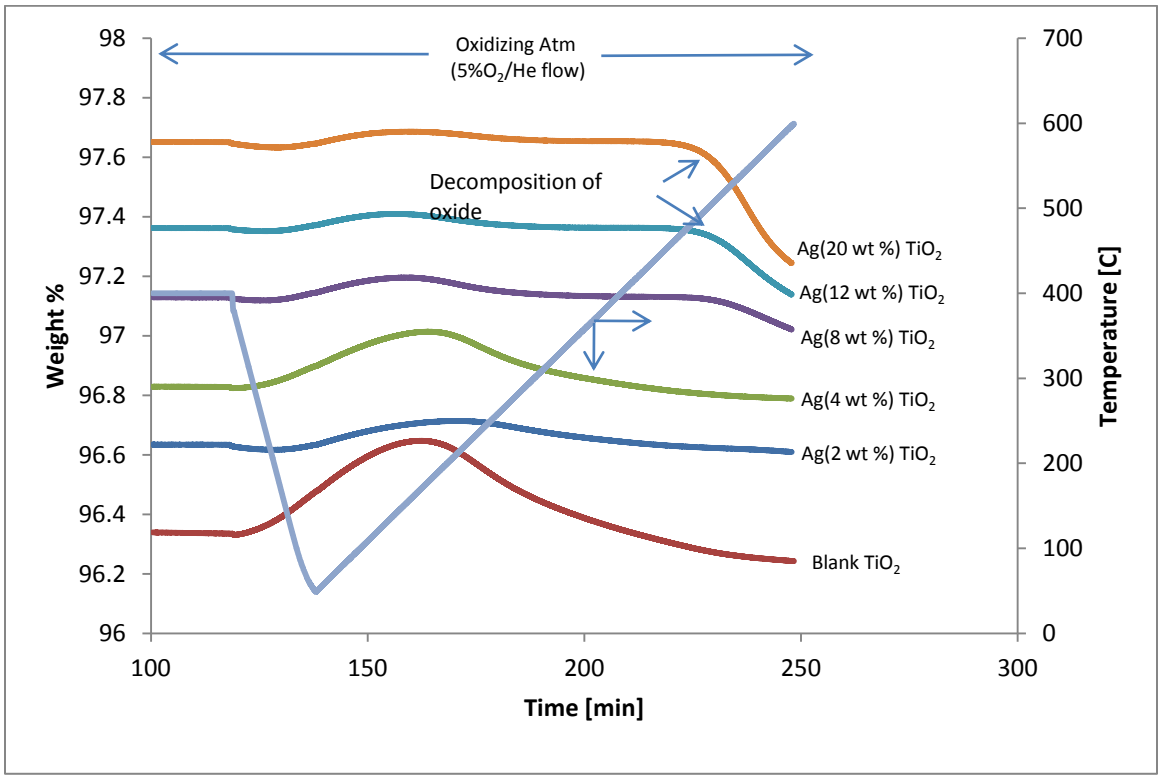

Figure IV.8. Comparison of TGA of Blank TiO_2, and Ag/TiO_2 adsorbents at various Ag loadings in oxidizing atmosphere following *in situ* pretreatment (400°C/2h); ordinate has been offset by for clarity

All the reduced samples indicated more moisture uptake compared to oxidized samples before the final temperature ramp (Figure IV.9). Moisture uptake decreased with increasing Ag loading. This was attributed to the reduction of surface hydroxyl in reducing atmosphere. Ag occupies surface sites occupied by OH groups, more so at higher loadings. Reoxidation of Ag was observed in samples with weight loading greater than 8%. Metal reoxidation was observed at lower temperatures at higher metal loadings. Reoxidation occurred at ~230°C for 8%, ~170°C for 12% and ~150°C for 20%. This also indicated more stable structures at lower loadings.

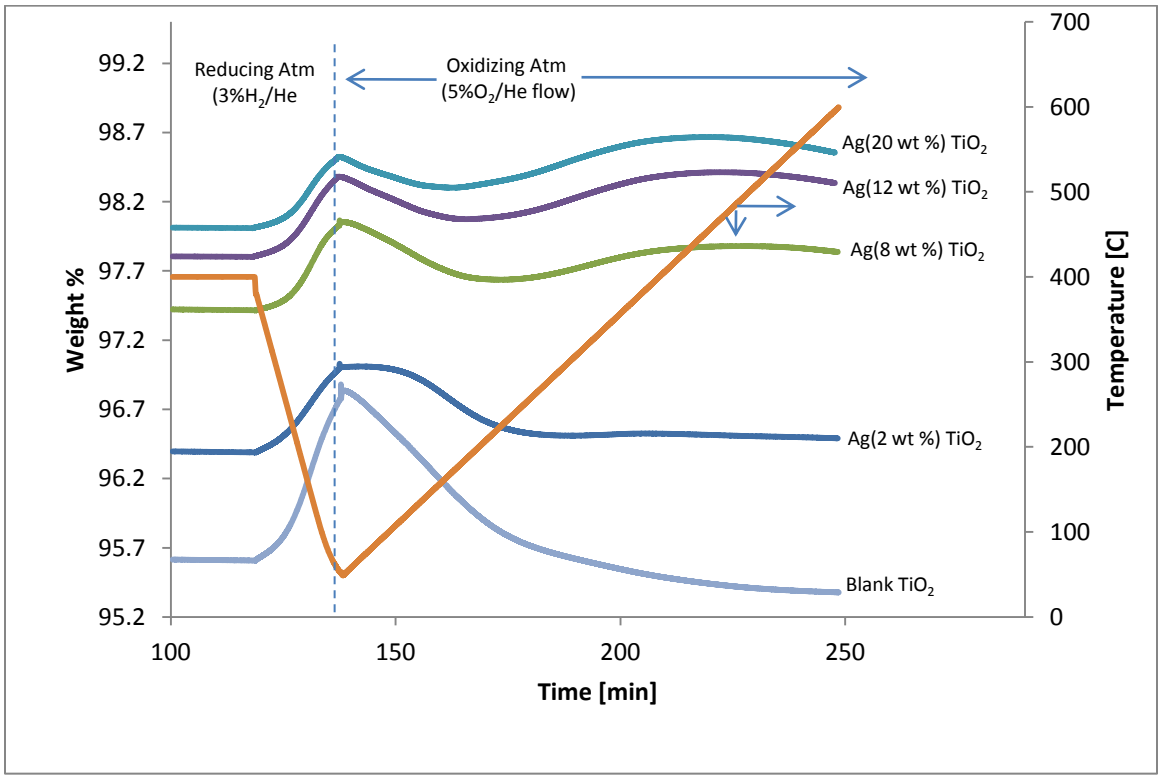

Figure IV.9. Comparison TGA of Ag/TiO_2 adsorbent at various Ag loadings reduced *in situ* at 400°C in H_2 (3% in He); ordinate has been offset for clarity

IV.3.2.3 Temperature programmed reduction

Thermoreduction profiles of Ag/TiO_2 sorbents with varying Ag loadings of 2, 4, 8 and 12 Wt.% were obtained. Reduction profiles of the blank TiO_2 support, Ag_2O and AgO were observed as well to provide background and locate individual maximum. Oxides of copper and nickel were also used to calibrate the H_2 consumption. TPR profiles were complex due to the presence of several reducible species and also due to some overlapping of H_2 desorption signals. Therefore only the main features will be discussed here.

Reduction profiles of the samples are shown in Figure IV.10. The samples with 2% Ag loading showed one maximum at 320°C and two shoulders at 270°C and 390°C. Similar features were also observed for the sample with 4% Ag loading. However the maximum was now shifted to a lower temperature of 300°C and the shoulders shifted to 225°C and 375°C. A significant difference was observed in the reduction profile of the samples with higher Ag loadings. Two of the shoulders observed in the prior two samples were more prominent. The maximum were now observed at 225, 275 and 330°C. There was no shift in the maximum observed in samples with Ag loading at 8 and 12%.

Certain reduction features were observed at temperatures below 143°C. These were not ascribed to Ag species as the pure oxides were observed to reduce at 197°C (AgO) and 270°C (Ag_2O). These features were also not observed on the standard oxides or during the blank TiO_2 runs. Therefore, they were ascribed to represent weakly bound

surface groups that were not removed during the pre-treatment step. The presence of weakly bound surface OH groups have been reported by other researchers as well[106, 116].

The blank TiO_2 showed single maximum at 465°C. This feature was ascribed to the reduction of very stable surface OH groups. Evidence of such strongly bound surface OH groups following high temperature treatment at 350°C have been reported [106]. However this feature was not observed on any of the samples loaded with Ag. This may be explained by selective adsorption of $AgNO_3$ precursor on these strongly bound OH sites during the impregnation step. Previous research has shown that exchange capacity of Pt complexes on silica gels is related to the number of surface OH groups [104].

The single *maximum* observed at the lower loadings was ascribed to the less stable AgO and the following shoulder to the more stable Ag_2O. It was observed that with increasing Ag loading, the maximum shifted to lower temperatures. This is observed when lower loadings result in higher metal dispersion. Highly dispersed metals have a stronger interaction with the support and these oxides are more stable. Also with increasing Ag loading, the shoulder developed into a maximum. Therefore more of the AgO was converted to the more stable Ag_2O with increasing Ag loading. The third shoulder was also observed to disappear at the higher loadings. Similar reduction profiles were observed for the samples with higher metal loadings. Higher loadings result in larger crystallites as most of the nucleation sites are populated. These larger crystals have minimal interactions with the support surface. Thus increasing metal

loading does not affect the reduction profiles beyond a certain point. The H_2 consumption of the samples was estimated using standard samples of Cu and Ni oxides. The reduction temperatures as well as H_2 consumption are listed in Table IV.5. For the analysis, the first and the following shoulder were assigned to AgO (Phase 2) and the 2nd to Ag_2O (Phase 1). The amounts of the two oxide phases were estimated from the H_2 consumption and corresponding stoichiometry. It was observed that as the Ag loading decreased, more of the Ag was present in the oxide phase. At 2% loading, majority of the Ag was in the oxide phase while only 9% of the Ag existed as oxide at 12 Wt.%.

Ag loading [Wt.%]	T_R [^oC]	H_2 con-phase 1 [mmol]	H_2 con.-phase 2 [mmol]	Total H_2 [mmol]	Phase 1 [mg]	Phase 2 [mg]	Total Ag [mg]	% Oxide
2.0	326, 353, 399	0.0045	0.0284	0.0330	1.05	3.53	4.58	102.3
4.0	293, 326, 370	0.0185	0.0052	0.0237	4.29	4.94	4.94	28.8
8.0	284, 316	0.0128	0.0073	0.0201	2.96	2.97	3.87	10.8
12.0	284, 315	0.0101	0.0078	0.0178	2.33	0.96	3.29	9.3

Table IV.5. Estimation of the phases of Ag in the sorbent based on reduction profiles at loadings varying from 2 to 12 Wt.%

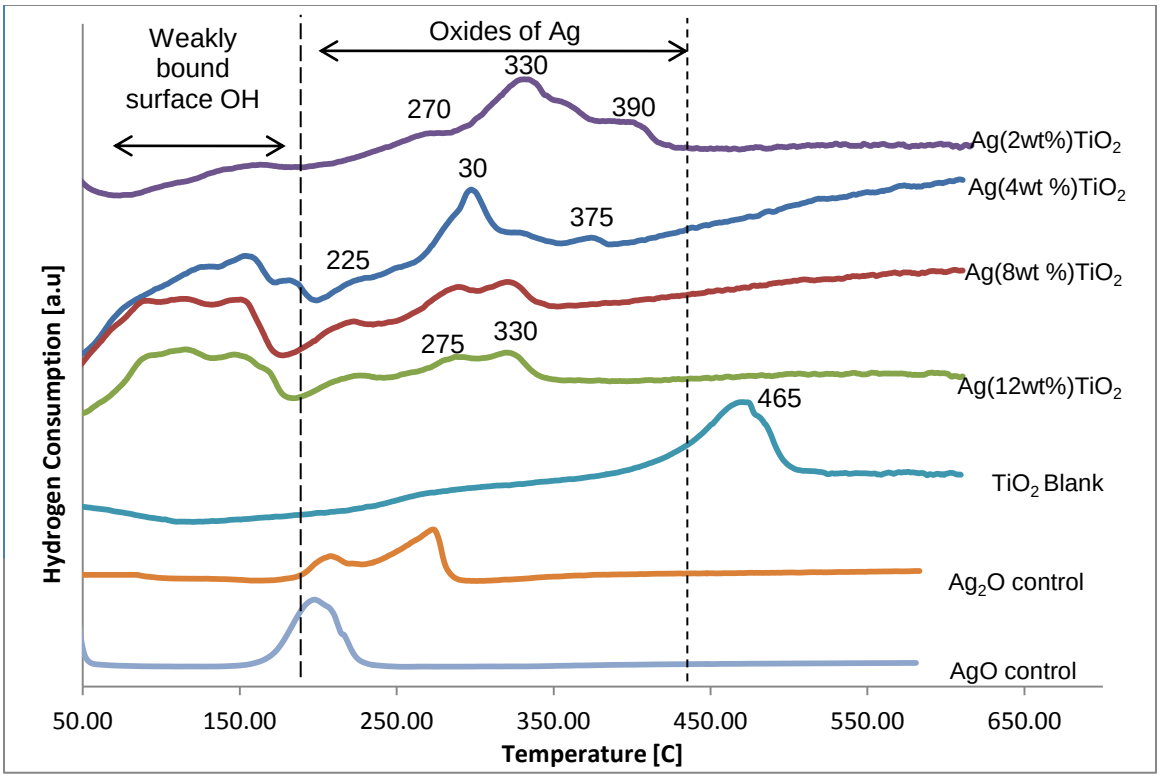

Figure IV.10. Reduction profiles of Ag/TiO_2 samples with Ag loading varying between 2 and 12 Wt.%

No evidence was obtained for the presence of stronger metal support interactions such as the formation of a $Ag\text{-}TiO_2$ complex. Thus the reduction profile indicated that TiO_2 was inert and merely acted as a support surface for Ag.

IV.4 Conclusions

Sulfur capacity of the Ag/TiO_2 sorbent was found to be only mildly dependent on the preparation conditions. The sorbent performance was more sensitive to the conditions that affected the pore structure than the dispersion of Ag such as surface acidity and calcination conditions. Thus the generation and retention of active adsorption centers were more indirectly connected to synthesis steps which were

optimized for maximum sulfur capacity. The absence of marked variation in performance with synthesis conditions makes the composition more amenable to scale-up operations. Characterization of the sorbent composition identified the various oxide phases of Ag present. The extent of oxidation was dependent on the dispersion of Ag which was dictated by the weight loading of Ag. With decreasing Ag loading, more of the Ag existed in the oxide phase. Thermogravimetric analysis also showed that the oxide phases were stable to temperatures of 550°C under oxidative conditions. However higher temperatures resulted in a collapse of smaller pores which lowered the sulfur capacity.

V. Characteristics of Sulfur Removal by Silver-Titania Adsorbents

V.1 Introduction

Ag/TiO_2 adsorbents demonstrated high capacity for sulfur aromatics in fuels at ambient conditions. The adsorbent was thermally regenerable in air over multiple cycles demonstrating a sulfur capacity of 8.5 mg/g over 10 adsorption/regeneration cycles for JP5 fuel (~1200 ppmw sulfur). Sulfur capacity was observed to be affected by fuel chemistry from breakthrough studies using fuels with different sulfur speciation such as JP5 and JP8. A significant variation in selectivity between sulfur heterocycles was noted for the Ag/TiO_2 sorbent. Physiochemical characterization identified that the Ag existed in its oxide phase and the extent of oxidation dependent on the Ag loading.

A marked loss in sulfur capacity was observed between real and model fuels. Sulfur capacity also varies with fuel chemistry especially in the presence of jet fuel additives such as oxygenates and metal deactivators. Variation in the aromatic content and the presence of contaminants also influences the performance of sulfur adsorbents. Elucidating the reason for such loss in sulfur capacity not only facilitates the design of better adsorbents or guard beds to remove deactivating agents but also provide a better

understanding of nature of the active centers. Higher sulfur capacity of $CuCl_2$- γ-Al_2O_3 compared to Cu-Y zeolite has been attributed to the higher selectivity towards oxygenates such as ethanol and MTBE compared to sulfur aromatics [45]. A few compositions reported for adsorptive desulfurization was prepared and tested to provide a comparison to the performance of Ag/TiO_2. The adsorbents were prepared using supports of identical particle size, tested using JP5 fuel at similar flow conditions. Variation in performance from reported data would gauge the influence of factors such as fuel chemistry, particle size and pretreatment steps on sulfur capacity.

Fuel additives impact the performance of sulfur adsorbents more so than the natural variation in fuel chemistry between the different fuels. Additives such as metal deactivators and corrosion inhibitors are designed to interfere with the activity of metallic components. Additives are fuel soluble chemicals added in small amounts to enhance or maintain properties important to fuel performance or fuel handling. Anti-oxidants, metal deactivators, static dissipaters, corrosion inhibitors, icing inhibitors, biocides, thermal stabilizers are common additive components in jet fuels. A fuel system icing inhibitor (FSII) is generally used to prevent the formation of ice at low temperatures encountered at high altitudes, and thus is an essential component of jet fuels. The only FSII approved for Jet A, Jet A1 and US military fuels is di-ethylene glycol monomethyl ether (di-EGME). Metal deactivators are generally used to inhibit the catalytic activity of metals such as copper and zinc against possible oxidation reactions. Alfa-alfa 1- methylethylenediimino-di-ortho-cresol is a common metal deactivator. Electrical conductivity enhancers are used to dissipate static electricity formed due to

friction. The only additive currently approved for use in jet fuel is Stadis 450® whose composition is proprietary. Oxygen in the small amounts of air dissolved in the fuel attacks the reactive compounds in the fuel. Antioxidants prevent this initial attack that can potentially set off a chain of oxidation reactions. Natural antioxidants found in straight run fuels are removed by hydrotreating processes making antioxidants more necessary for treated fuels. The maximum allowed concentration is 24mg/L. The approved antioxidants for aviation fuel are hindered phenols such as 2,6-Di-tert-butyl-4-methylphenol [117]. Breakthrough studies using model fuels comprising of fuel additives and contaminants were carried out to establish the negative influence of these components on the Ag/TiO_2 adsorbent.

When establishing the sulfur capacity of adsorbents with active metal species, sulfur capacity of the blank support structures need be considered as well. Blank supports are ideally tested for sulfur capacity following pre-treatment steps similar to that followed in the preparation of the adsorbent with dispersed metals. Synthesis stages such as impregnation, drying and high temperature treatments influence the concentration of surface functional groups and support pore structure. Sulfur capacity of supports prior to the introduction of active metals has been reported by a few researchers. Kim et al., reported adsorption of several aromatics over activated γ-Al_2O_3 and activated carbon following pretreatment in flowing N_2 at 200^oC for 2h [30]. Sulfur capacity of activated carbon (16.29 mg/g) was significantly higher than that of γ-Al_2O_3 (2.41mg/g) using a model fuel composition of ~300 ppmw total sulfur. Velu et al., reported sulfur capacity of HY zeolite obtained by calcination of NH_4Y zeolite at ~500°C

[37] to be comparable to Y type zeolites ion exchanged with Cu, Ce etc. A comparison of sulfur capacities was also reported by Takahashi et al., between Cu-Y and Na-Y zeolites [87]. These studies indicate that a good part of the sulfur capacity of an adsorbent may reside in the virgin support structure. The nature of interactions between sulfur molecules and the active centers on the support may vary from the interactions with active metals. Therefore sulfur capacities of TiO_2 Al_2O_3 and SiO_2 dried and calcined at 450^oC were studied in this chapter.

In this chapter, efforts were made to differentiate the sulfur capacity of the support structures from that of the metal loaded samples. The influence of various transition metal components on sulfur capacity was studied. Comparison of sulfur capacity of Ag/TiO_2 was made with other reported compositions for adsorptive desulfurization. The influence of fuel additives, structure of sulfur molecules and the effect of competitive adsorption was also studied for Ag/TiO_2 adsorbent.

V.2 Results and Discussion

V.2.1 Sulfur capacity of supports

Sulfur capacity of supports such as SiO_2, Al_2O_3 and TiO_2 are generally established as received or following a simple drying procedure. These steps are carried out to ensure removal of surface moisture and adsorbed organic volatiles. Our work indicated that the supports often exhibit significant adsorption capacity for sulfur when taken through a series of thermal treatments. Addition of metals has been shown to enhance the sulfur capacity of supports such as Cu on Y Type zeolites and Pd on Al_2O_3.

Interactions of sulfur molecules with the support structure maybe varied from that with incorporated metals.

A comparison of sulfur capacity was thus made for TiO_2, Al_2O_3 and SiO_2 that were dried (110°C/6h) and blank samples that were impregnated with dilute HNO_3, died (110°C/6h) and calcined (450°C/2h) in air. Breakthrough of benzothiophene in a model fuel (3500 ppmw in n-octane) using untreated (dried) samples are shown in Figure V.1 . Sulfur capacity of dried TiO_2, SiO_2 and Al_2O_3 were minimal. Breakthrough data for blank samples showed a marked improvement in sulfur capacity for Al_2O_3 and TiO_2 samples, while SiO_2 demonstrated a minor loss in sulfur capacity (Figure V.2).

Therefore the thermal treatment was responsible for the generation of active centers for sulfur capture on Al_2O_3 and TiO_2 structures. Such improvement in sulfur capacity may result from the loss or modification of strongly bound ad-molecules on the surface, generation of oxygen vacancies or incorporation of surface functional groups. Generation of surface acidity from bronsted sites may also be considered. This was suggested by the distinct behavior of SiO_2 compared to Al_2O_3 and TiO_2. Previous reports have indicated the absence of surface acidity on SiO_2 surfaces compared to Al_2O_3 and TiO_2. Rajagopal *et al.* reported that the surface of SiO_2 contains OH groups that are weakly basic or neutral compared to Al_2O_3 [118]. Decomposition of water molecules on TiO_2 surfaces to form surface hydroxyls have been reported [119]. Generation of bronsted acidity on TiO_2 surfaces dependent on preparation conditions have been reported [120]. OH group concentration on Al-Y zeolites has been observed to maximize

at a calcination temperature of 350°C and decrease beyond 550°C [118]. Active bronsted acid sites may be formed from decomposition of adsorbed water molecules during the calcination step on Al_2O_3 and TiO_2.

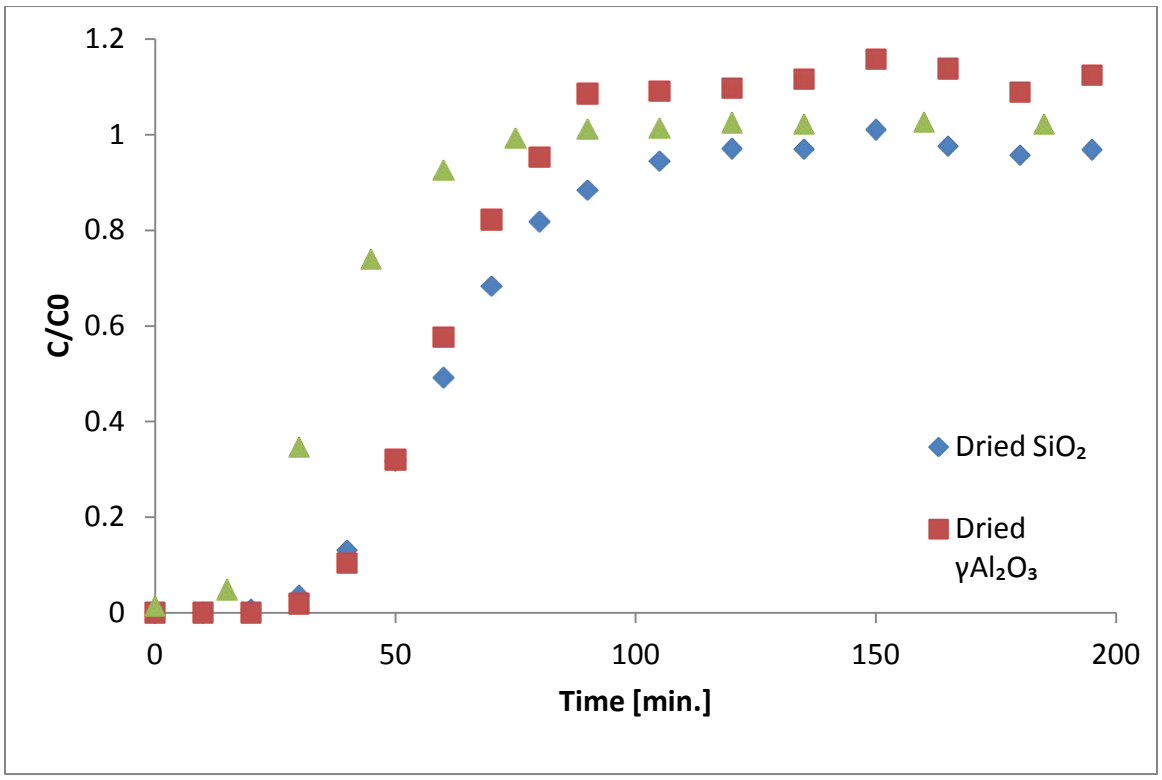

Figure V.1. Breakthrough of benzothiophene (3500 ppmw)/n-octane for dried TiO_2, dried SiO_2 and Dried γ Al_2O_3; dried at 110°C for 6h.

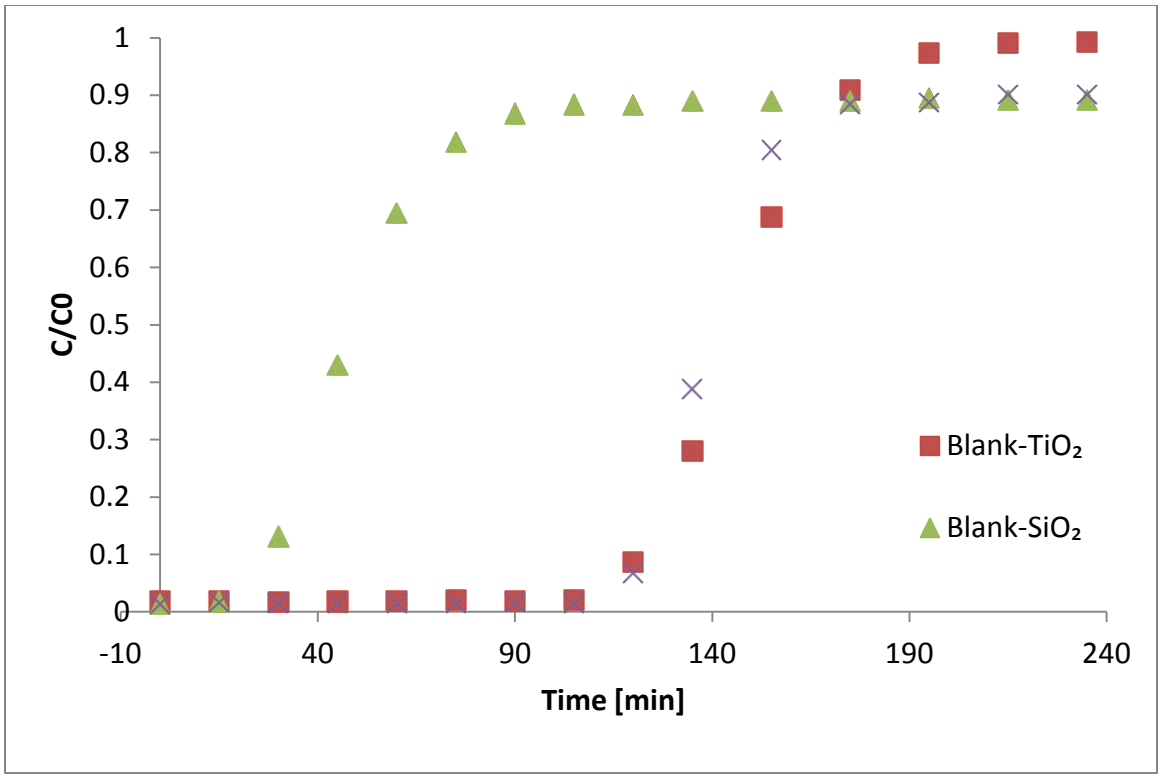

Figure V.2. Breakthrough of benzothiophene (3500 ppmw)/n-octane for Blank TiO_2, Blank SiO_2 and Blank γ Al_2O_3; the blanks prepared through impregnation of dilute HNO_3, dried (110°C/6h) and calcined (400°C/2h)

V.2.2 Comparison with other transition metals and Ag /TiO_2

Liquid phase sulfur adsorbents generally contain transition metal components. Therefore they exhibit an inherent affinity for sulfur heterocycles and rely on metal-sulfur aromatic interaction. Therefore these materials go through reduction (or auto-reduction) pretreatment [30, 87, 121, 122]. However, our previous work indicated a higher sulfur uptake for supported Cu, Ni, Mn and Ag oxides (without reduction step) on SiO_2 {Nair, in-press #624}. Among the metals tested Ag demonstrated the highest sulfur affinity. Here Fe, Cu, Mn, Ga and Ag were dispersed on TiO_2 at a weight loading of 4% and sulfur affinity established from breakthrough of benzothiophene (3500±10 ppmw) in n-octane shown in Figure V.3. The sulfur capacities estimated from the

breakthrough data is presented in Table V.1. Ag demonstrated a saturation sulfur capacity of ~42 mg BT/g followed by Mg at ~39mg/g.

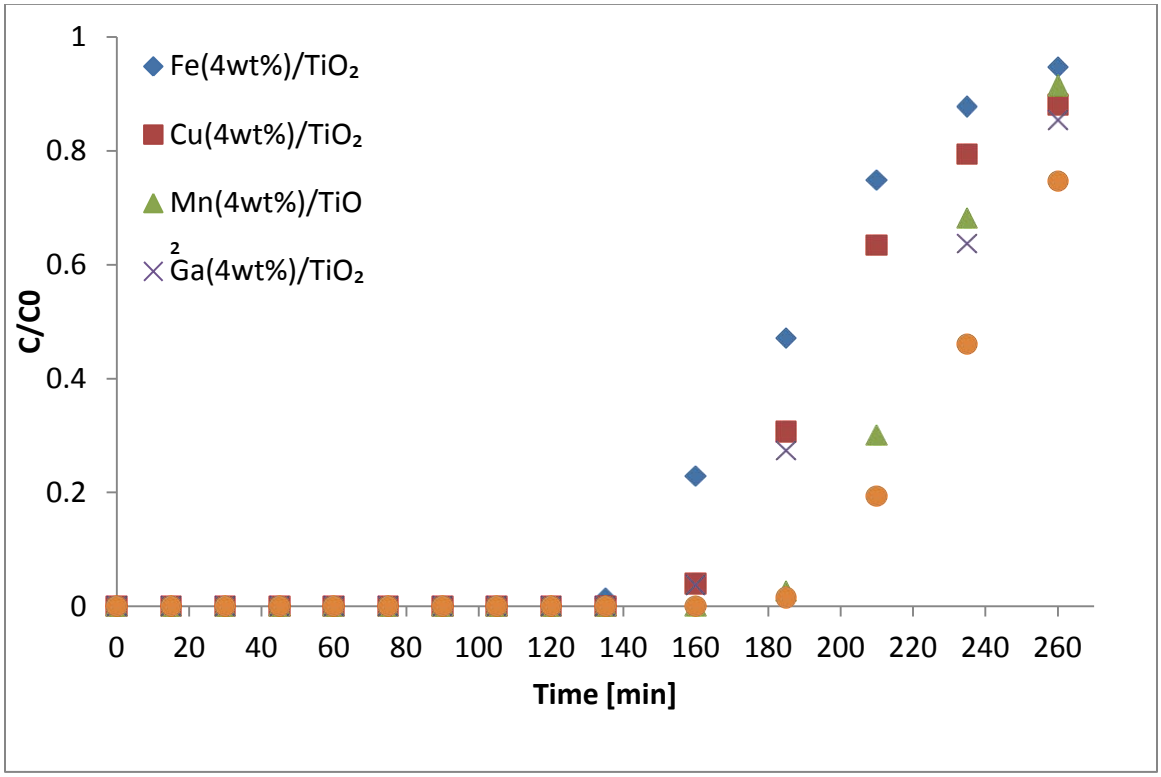

Figure V.3. Breakthrough of benzothiophene (3500 ppmw)/n-octane for 4%Wt. of various metals shown supported on TiO_2, dried (110°C/6h) and calcined (400°C/2h)

Active metal	BT time [min]	Sulfur cap-BT [mg/g]	$t_{½}$ [min]	Sulfur cap-SAT [mg/g]
Fe	134	23.5	187	32.7
Ga	151	26.4	215	32.6
Cu	151	26.4	198	34.7
Mn	180	31.5	222	38.9
Ag	183	32.0	238	41.7

Table V.1. Sulfur capacity of 4 Wt.% of various transition metals supported on TiO_2 estimated from breakthrough of Benzothiophene (3500±10 ppmw) in n-octane

Support	Dried		Blank		4 Wt. % Ag loaded	
	Sulfur cap-BT [mg/g]	Sulfur cap-SAT [mg/g]	Sulfur cap-BT [mg/g]	Sulfur cap-SAT [mg/g]	Sulfur cap-BT [mg/g]	Sulfur cap-SAT [mg/g]
TiO_2	2.10	6.1	13.6	18.3	32.0	41.7
Al_2O_3	5.25	10.0	13.9	17.4	35.9	43.4
SiO_2	4.20	10.7	1.9	6.2	7.4	12.1

Table V.2. Sulfur capacity of Blank and Ag loaded TiO_2, Al_2O_3 and SiO_2

Breakthrough data for supports loaded with 4% Ag is shown in Figure V.4. The addition of Ag improved the sulfur capacity of supports, including SiO_2 as listed in Table V.2 . Therefore, the Ag phase consisted of active adsorption centers independent of TiO_2.

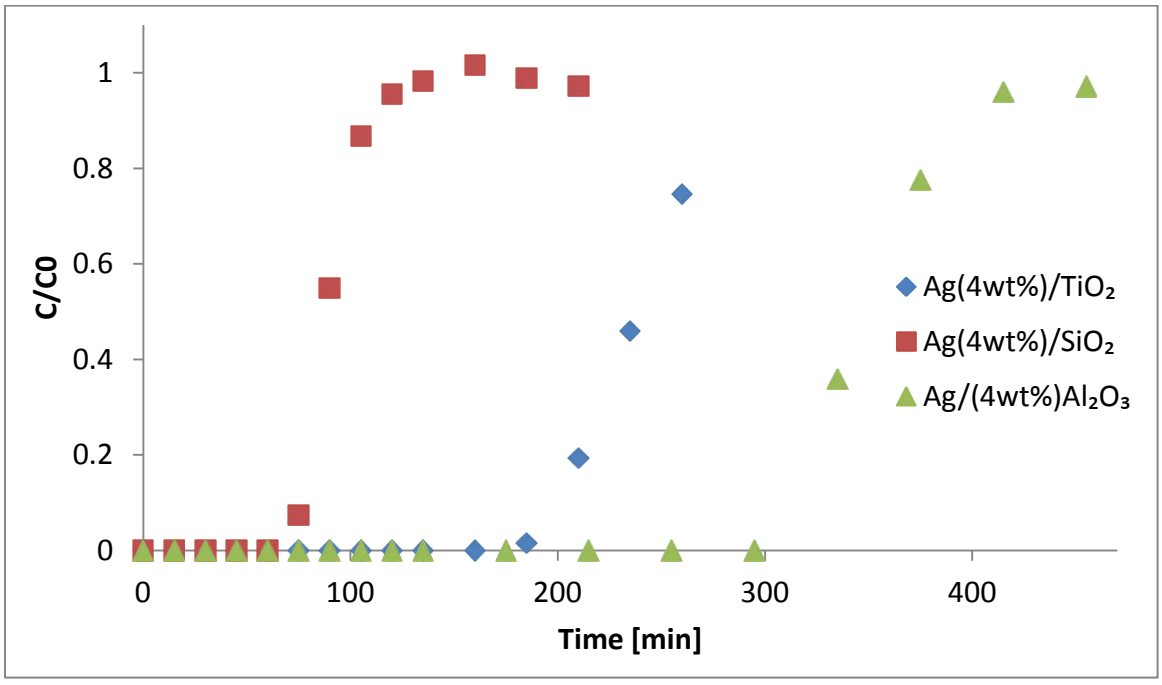

Figure V.4. Breakthrough of benzothiophene (3500 ppmw)/n-octane for Ag (4 Wt.%)/TiO_2, Ag (4 Wt.%)/ γAl_2O_3 and Ag (4 Wt.%)/SiO_2

Even though the Ag loading was 4 Wt.% on all the Ag loaded samples, improvement in sulfur capacity with the addition of Ag was higher for Al_2O_3 compared to TiO_2. This was attributed to the higher dispersion of Ag on Al_2O_3 compared to TiO_2 primarily due the higher specific surface area of Al_2O_3. Even though Al_2O_3 showed higher sulfur capacity, TiO_2 was chosen as the preferred support for this application as it was observed to be more stable over multiple cycles of thermal regeneration {Nair, in-press #624}. Variation in surface acidity with addition of metal ions to a support has been reported in the past. Rajagopal et al. have reported the generation of new bronsted sites and simultaneous decrease in lewis sites on Al_2O_3 surfaces with increasing MoO_3 loading[118]. Thus addition of Ag and changing surface acidity of TiO_2 and Al_2O_3 was attributed to the higher sulfur capacity of Ag loaded samples.

V.2.3 Performance Comparisons

For performance evaluation of some reported adsorbents, breakthrough tests were conducted on Cu ion-exchanged Y-type zeolite, $PdCl_2$(~12 Wt.%)/Al_2O_3, Ag(4 Wt.%)/TiO_2 at similar conditions. The breakthrough performance of the adsorbents is shown in Figure V.5 and sulfur capacities listed in Table V.3. Ag(4 Wt.%)/TiO_2 demonstrated a breakthrough capacity of 1.73 mg/g compared to 2.88 mg/g by $PdCl_2$(~12 Wt.%)/Al_2O_3 at 20 ppmw breakthrough threshold. Breakthrough sulfur capacity of Cu-Y was 0.58 mg/g while Selexorb CDX demonstrated negligible capacity. Among the tested adsorbents, Ag(4 Wt.%)/TiO_2 maybe preferred due to the simple synthesis procedure, absence of activation steps and more importantly facile thermal regenerability using air as a stripping medium.

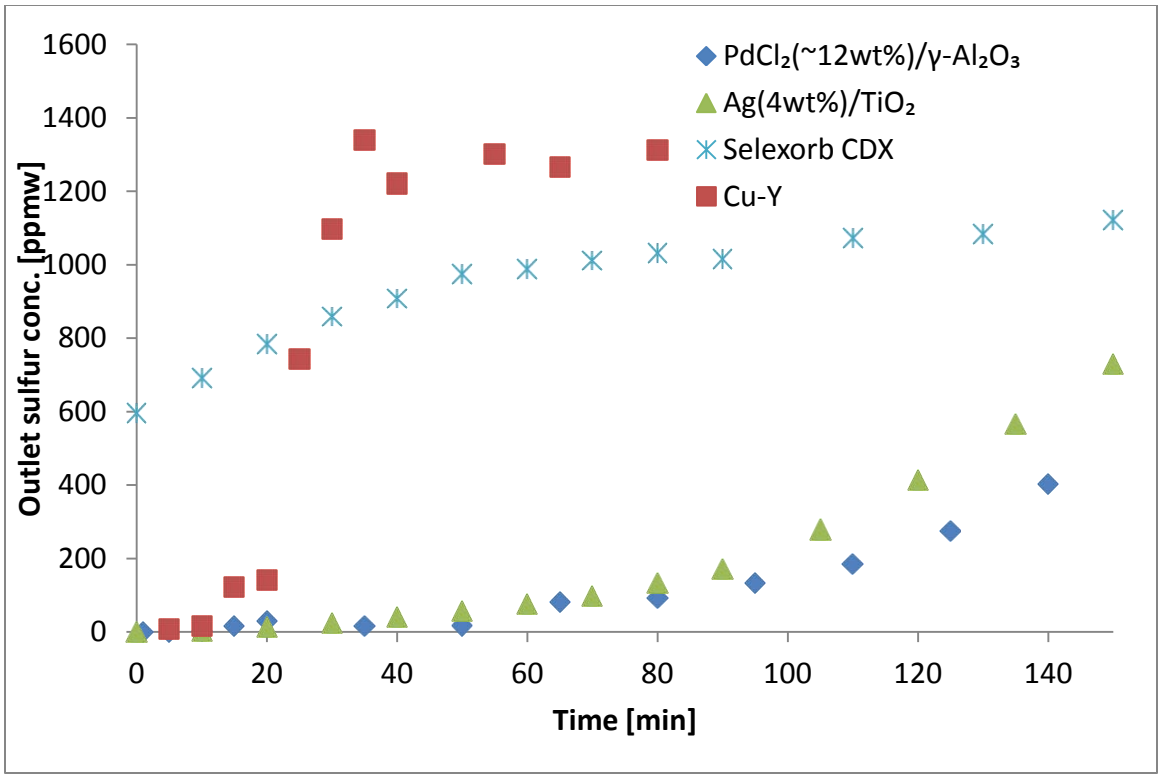

Figure V.5. A comparison of desulfurization performance of Ag(4 Wt.%)/TiO_2, $PdCl_2$(~12 Wt.%)/Al_2O_3, Cu-Y zeolite, Ag(4 Wt.%)/TiO_2 and Selexorb CDX using JP5 fuel with 1172 ppmw sulfur at identical testing conditions and particle size

Adsorbent	BT time* [min]	Sulfur cap-BT [mg/g]	$t_{½}$ [min]	Sulfur cap-SAT [mg/g]
Selexorb CDX	NA	NA	0	0.20
Cu-Y	10	0.58	25	1.50
$PdCl_2/\gamma$-Al_2O_3	50	2.88	165	9.67
Ag/TiO_2	30	1.73	140	8.20

Table V.3. A comparison of sulfur capacity obtained from breakthrough data for Ag(4 Wt.%)/TiO_2, CuY-type zeolite, and $PdCl_2$(~12 Wt.%)/Al_2O_3 using JP5 fuel (1172 ppmw sulfur) as challenge

Loss in sulfur capacity of various adsorbents has been reported while using real fuels as challenge. Comparison of breakthrough between JP5 fuel and benzothiophene (3500±10 ppmw) in a model fuel composition for Ag(4%)/TiO_2 at similar test conditions

is shown in Figure V.6. It may be observed that the adsorbent exhibited higher sulfur capacity for the model fuel compared to JP5. The breakthrough curve was sharper in the case of model fuel which was attributed to transport issues with real fuel. The factors that result in the lower breakthrough performance maybe arise from the chemistry of natural fuels which includes competitive adsorption between a multitude of sulfur aromatics, sulfur-free aromatics and the presence of additives in the fuel. The impact of some of these components in fuel on the performance of Ag/TiO_2 was further explored.

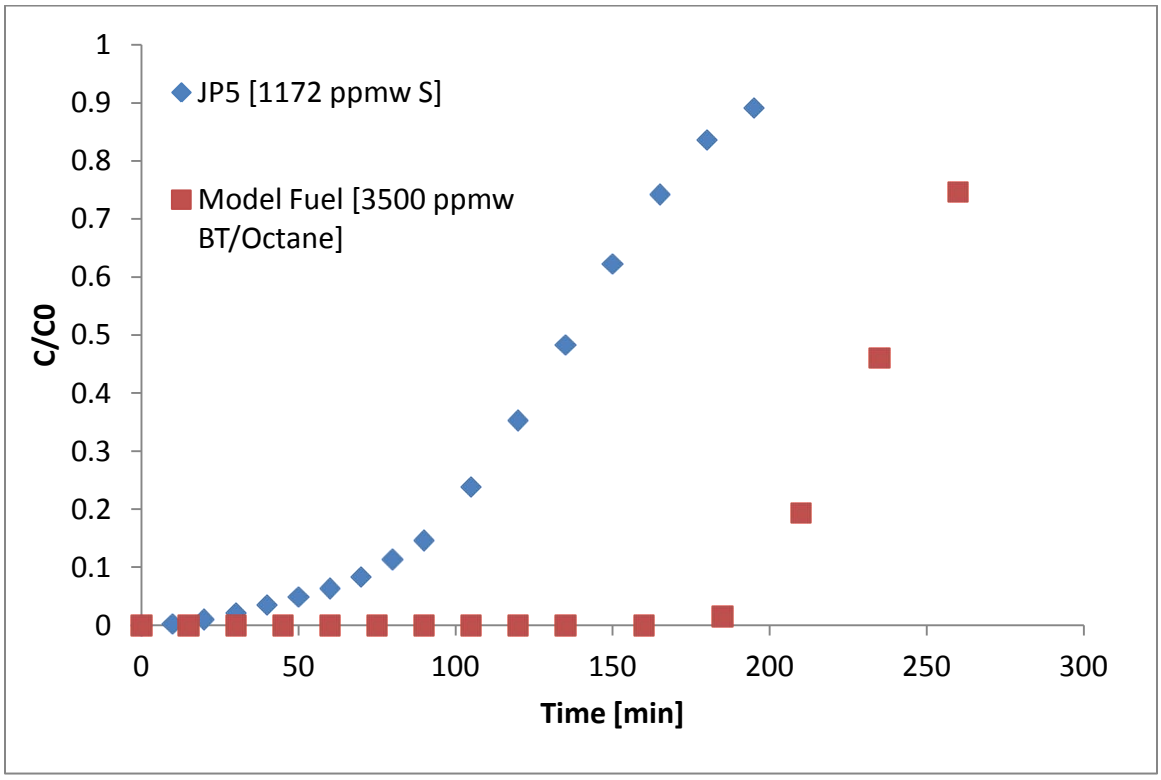

Figure V.6. Breakthrough of sulfur in JP5 (1172 ppmw) compared to that of benzothiophene (3500ppmw) in octane using the Ag(4 Wt.%)/TiO_2

V.2.4 Additives

Several components in a fuel might be responsible for lowering the sulfur capacity of adsorbents. The competition from non-sulfur containing aromatics would be

significant source as many fuels contain up to 16% aromatic compared to a maximum of a few percent of sulfur. Another factor would be additives present in fuels such as oxygenates, antioxidants, antistatic agents and metal deactivators. Understanding the effect of additives on sulfur adsorption process not only addresses the practical issue of application of such adsorbents for use on real fuels but also address the chemical nature of interactions at adsorption interface. Model fuels containing three components were prepared for this study. The first component was benzothiophene (3500±10 ppmw). The second component was a fuel additive and n-octane was the solvent. Breakthrough of benzothiophene was used to determine the effect of the second component on desulfurization using Ag(4Wt.%)/TiO_2. The additives/contaminants studied were ethanol (15% Vol) used as an oxygenate in fuels, Alfa-alfa 1- methylethylenediimino-di-ortho-cresol [MD] (15ppmw) used as a metal deactivator, 2,6-Di-tert-butyl-4-methyl phenol [AO] (15 ppmw) used as an antioxidant and water (100 ppmw), a common contaminant. From the breakthrough data presented in Figure V.7, it was observed that additives reduced the sulfur capacity of the adsorbent. Ethanol in the fuel completely deactivated the sorbent. Therefore for fuels with added ethanol, these adsorbents may not be applicable. The MD also led to reduction in sulfur capacity. This may be attributed to the interference of hydroxyl group of alcohol/cresol with benzothiophene or active centers on the surface. The marked difference between ethanol and toluene (both 15Vol %) in the fuels indicated the same effect. A comparison of sulfur capacity of the adsorbent in the presence of toluene indicated the significant impact of aromatic content of fuels on adsorbent performance. The effect of AO was not as marked as that of MD (both at 15

ppmw) even though both contain phenolic groups. This was attributed to the presence of nitrogen atom in the diimino groups on MD. The MD molecule is therefore more basic in comparison with AO and therefore considered to strongly interact with surface acidic groups. Trace amounts of water molecules have been known to form H_3O^+ ions with bronsted centers [123, 124]. This interaction may explain the loss in sulfur capacity in the presence of water.

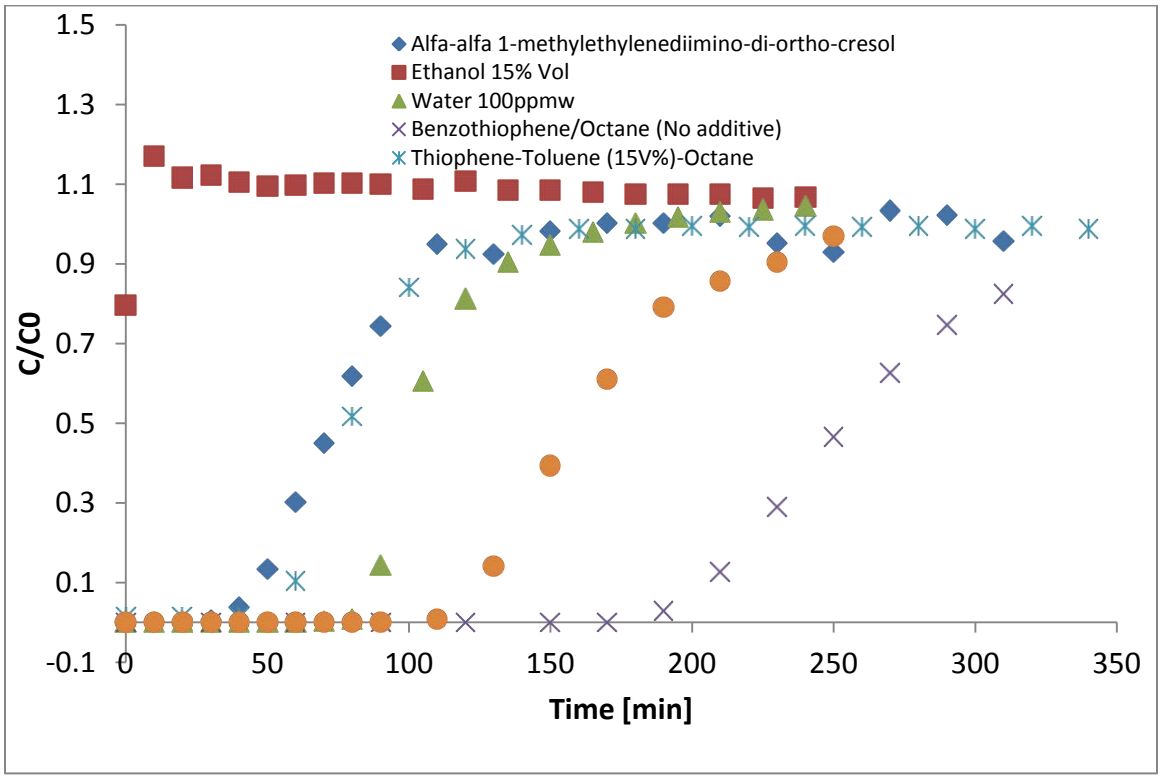

Figure V.7. The breakthrough of benzothiophene (3500 ppmw) for Ag(4 Wt.%)/TiO_2 using model fuels also containing (i) 15 ppmw of antioxidant 2,6-Di-tert-butyl-4-methylphenol (ii) 15 ppmw of metal deactivator Alfa-alfa 1- methylethylenediimino-di-ortho-cresol (iii) Ethanol 15.0 Vol% (iv) 100 ppmw water and (v)Toluene 15 Vol%

V.2.5 Competitive adsorption

Model fuel compositions are generally used as challenge fuels in the evaluation of sulfur adsorbents as they eliminate issues with real fuels such as competitive

adsorption between sulfur species, other aromatics and fuel additives. However, competitive adsorption maybe used to gain insight on mechanism of sulfur adsorption. Breakthrough characteristics would not only clarify the primary interactions between the sorbent and solute molecules but also indicate the secondary interactions between surface ad-layers. Breakthrough of three sulfur heterocycles viz. thiophene (0.572 g/l), benzothiophene (0.913g/l) and dibenzothiophene (1.253 g/l) were observed using Ag/TiO_2 sorbent in a model fuel composition; the total sulfur concentration was 0.08mol/l. For primary interactions between the sulfur atom and the sorbent, this study would isolate the effect of the structure of sulfur aromatic during competitive adsorption.

Multi-component sorption has been classified as quite a formidable subject handled by elaborate models, rules of thumb and extensive experimentation. Computer simulations have been hampered by complex theory, lack of suitable equilibrium data or prediction methods for multiple components. Therefore only qualitative inferences will be attempted here. If each component of the mixture is assumed to follow Henry's law, then each component maybe considered to propagate independent of others resulting in a sequence of discontinuous and sharp fronts during both adsorption and desorption. Generally light components breakthrough initially followed by heavy components. Lighter and intermediate components may rise above its feed concentration. This behavior is predominant in systems following the Langmuir adsorption model [125].

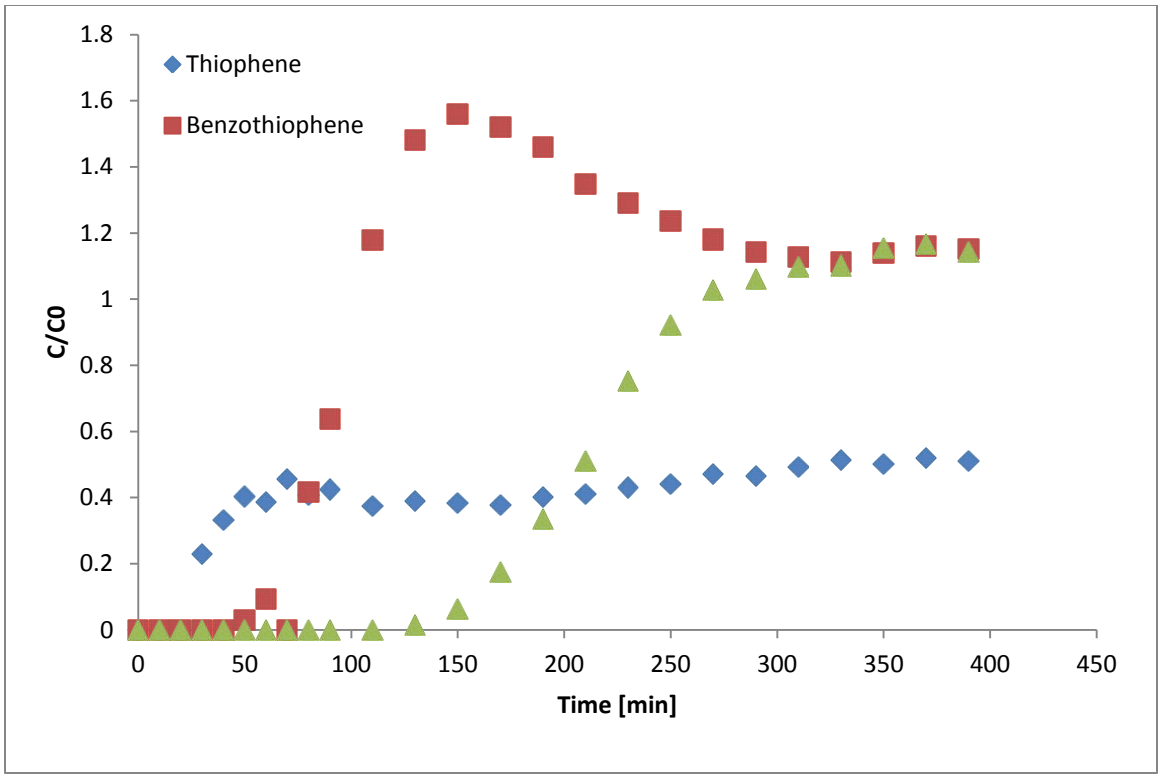

Figure V.8. Breakthrough of thiophene (0.572 g/l), benzothiophene (0.913g/l) and dibenzothiophene (1.253 g/l) for Ag (4 Wt.%)/TiO_2 from a model fuel containing all three species in n-octane; total sulfur content of ~0.08 mol/l

This characteristic behavior of systems following the Langmuir model was also noted for the case of BT and DBT (Figure **V**.8). BT broke through prior to DBT and the concentration remained 20% above the inlet, typical of multi-component adsorption. The observation explained by the displacement of adsorbed BT molecules by DBT. This was also indicated by the lowering of BT concentration from 1.6 C0 to 1.2 C0 simultaneous to the breakthrough of DBT. Therefore prior to breakthrough, DBT replaced BT on the surface.

Thiophene despite being the lightest component and breaking through before BT and DBT, did not follow the expected trend. Once the outlet concentration approached

~50% of inlet, further breakthrough did not occur within the duration of the experiment. This observation maybe explained by the variation in size between the solute molecules. Even though thiophene broke through initially due to the lower strength of interaction with the sorbent, it was able to access active centers amid larger molecules of BT and DBT on the surface. Multi-component sulfur adsorption using the Ag/TiO_2 sorbent thus followed the general characteristics of the Langmuir model. BT and DBT were removed more efficiently than thiophene. The odd behavior of thiophene was associated with its molecular size. Early breakthrough of sulfur using real fuels compared to model fuels may therefore be attributed to competition among solute molecules. Eliminating interactions among the solutes makes the analysis of the adsorption system simpler. Therefore breakthrough of individual sulfur aromatics was also pursued.

V.2.6 Structure of sulfur heterocycle

The structure of the sulfur heterocycle with respect to the number of aromatic rings as well as the presence of alkyl side chains affects the interactions with adsorption centers on the adsorbent. Challenge fuels with methyl thiophene (MT), benzothiophene (BT), dibenzothiophene (DBT) and 4,6 DMDBT in n-octane were tested for desulfurization performance using the Ag (4 Wt.%)/TiO_2 sorbent. Sulfur concentration of the fuels was 0.08 mol/l. Breakthrough characteristics are indicated in Figure V.9. The sulfur capacity was observed to vary as MT<4,6 DMDBT<BT<DBT. Therefore the presence of aromatic ring (π electron density) increased the interaction between the sulfur species and the adsorption centers as observed in the earlier case of multi-component adsorption. A significant loss in capacity was observed for 4,6 DMDBT

compared to DBT. The lowering of sulfur capacity as a result of methyl groups on 4,6 DMDBT was attributed to the reduction in π electron density on the aromatic ring. From the above data it was noted that larger aromatics are generally more effectively removed with π electron interaction playing a significant role.

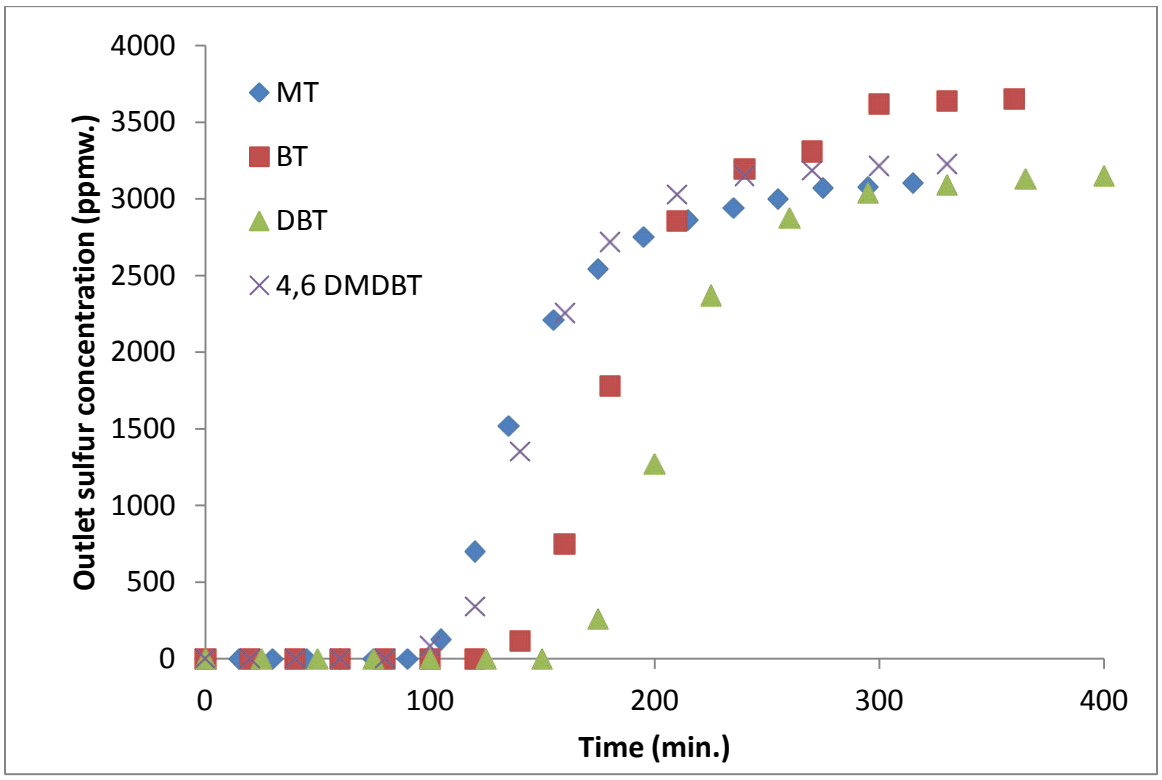

Figure V.9. Breakthrough of methyl thiophene (MT), benzothiophene (BT), dibenzothiophene (DBT) and 4,6 dimethyl dibenzothiophene for Ag(4%)/TiO_2 in a model fuel with identical sulfur concentration of 0.08mol/l

Several distinctions can be drawn between the individual and multi-component breakthrough behavior of these sulfur aromatics. Sulfur capacity was higher for species during the individual adsorption due to higher equilibrium sorbent capacity at higher sulfur concentrations (Table **V**.4). Sulfur concentration reached a plateau at levels below the feed concentration in the individual adsorption before rising to the inlet levels.

However the outlet levels were noted to rise above the inlet concentration during multi-component adsorption.

	Thiophene/M-thiophene 3500/807.9±10ppmw [mg T-MT/g]		Benzothiophene 3500/1289.5±10 ppmw [mg BT/g]		Dibenzothiophene 3500/1769.7±10 ppmw [mg DBT/g]	
	Sulfur cap-BT	**Sulfur cap-SAT**	**Sulfur cap-BT**	**Sulfur cap-SAT**	**Sulfur cap-BT**	**Sulfur cap-SAT**
Competitive adsorption	0.286	-	2.28	5.02	8.14	17.23
Individual adsorption	11.15	29.12	14.86	35.93	18.59	39.64

Table V.4 . Sulfur capacity of the Ag/TiO_2 sorbent for various sulfur aromatics during individual and competitive adsorption

The role of surface acidity on the activity of these sulfur adsorbents are currently being pursued in our laboratories. The effect of calcination conditions on surface acidity and corresponding changes in sulfur capacity is being investigated using NH_3 adsorption, titration of bronsted sites and temperature programmed desorption of NH_3. These findings will be presented in future publications.

V.3 Conclusions

Sulfur adsorption using Ag /TiO_2 adsorbent was attributed to acidity of these materials arising from bronsted centers. Strongly acidic surfaces such as TiO_2 and γ-Al_2O_3 demonstrated considerable sulfur capacity compared to neutral surfaces such as SiO_2. Addition of bronsted sites by transition metal oxides increased sulfur capacity of all

supports. Ag/TiO_2 demonstrated comparable sulfur capacities with other reported adsorbent compositions. Fuel additives were found to have a negative impact on the sulfur capacity. Interaction of basic additives with acidic adsorption centers was attributed for deactivation of the adsorbent. Competitive adsorption demonstrated that the lighter sulfur aromatics breakthrough initially followed by heavier components. The displacement of lighter molecules was also observed. Heavier sulfur aromatics were captured more effectively by the adsorbent.

VI. The Role of Hydroxylated Surfaces in Sulfur Adsorption

Supported Ag based adsorbents for sulfur removal were active in the oxidized state in contrast with the majority of reported adsorbents that are active reduced. This accounted for their regenerability in oxidative conditions. The absence of activation steps also makes the materials easier to handle and transport, simplifying regeneration procedures. Therefore the mechanism of sulfur adsorption would vary from that reported for a majority of adsorbents.

XPS and TPR measurements showed that Ag was present as an oxide. TPR indicated that more of the Ag was present in the oxide phase at lower loadings. Therefore, the majority of the species at the adsorption interface was in the oxide state. Oxygen chemisorption indicated that larger crystals existed at higher Ag loadings. It was also observed that the lowering of Ag dispersion did not lower the sulfur capacity of the adsorbent significantly.

Further investigation into the activity of these adsorbents revealed that Al_2O_3 and TiO_2 contributed to the sulfur capacity even in the absence of Ag. It was observed that the sulfur capacity was generated by the calcination step during synthesis and was absent in the "dried" samples. However sulfur capacity of SiO_2 did not improve following the calcination step. Previous research also indicated the correlation between

calcination and surface acidity [99]. This indicated that surface acidity might play a significant role in sulfur adsorption in these materials. Addition of Ag to Al_2O_3, TiO_2 as well as SiO_2 improved sulfur capacity. Studies have shown that metal impregnation on to support surfaces augments acidity [126, 127].Metal ions such as Cr, Fe and Co has been demonstrated to increase the surface acidity of activated carbons [128, 129]. Modification of Al_2O_3, SiO_2 and MgO with other oxides have been reported to influence their acid/base properties as well [129].

Sulfur selectivity of the adsorbent varied significantly with fuel chemistry. Adsorption behavior was complicated by competitive adsorption between various sulfur heterocycles. Model fuels are generally used to eliminate these effects while observing the mechanism of sulfur removal. The effect of sulfur-free heteroatoms with a similar structure was carried out to probe electronic interactions at the adsorptive interface. Polarizable molecules like alkenes or aromatic hydrocarbons can screen a large spectrum of specific surface interactions. Molecules with electron-donor characteristics will permit the characterization of acceptor properties of most reactive surface sites [130]. Adsorption capacity was observed to improve with the addition of aromatic rings to the solute molecule which indicated π interactions as a considerable influence on the adsorption capacity. Observations so far indicated a significant contribution of surface acidity to sulfur removal; a detailed analysis was attempted in this chapter.

A linear relationship has been observed between surface acidity and photocatalytic activity of TiO_2 generally influenced by surface area, crystal structure,

density of surface OH groups etc. [73]. Surface cations (Ti^{n+}) possess an uncompensated positive charge (Lewis acid) and interact with molecules with free electron pairs. The coordinatively unsaturated oxygen atoms on the other hand are lewis bases and adsorb acidic molecules. Oxygen vacancies are less common in anatase due to higher under-coordination of π atoms formed upon removal of bridging oxygen. This low coordination makes these vacancy sites very reactive and terminal OH groups move to these sites [131]. Dissociative adsorption of water is preferred on TiO_2 surfaces compared to the molecular one, especially at low coverages [132]. On TiO_2, OH groups may either be acidic or basic [74]. Simulations of adsorption on TiO_2 have shown that only hydroxylated surfaces are occupied by organic molecules [133]. Therefore sulfur adsorption using TiO_2 based sorbents is likely to be caused by either Lewis or Bronsted acidity of the surface. Measurement of surface acidity therefore becomes necessary to relate to sulfur capacity.

NH_3 chemisorption is used to measure acidity of surfaces. It is a strong base and is readily adsorbed on strong and weak acid sites resulting from anion vacancies, lewis and bronsted sites and used as a probe molecule to test the acidic properties of metal oxide surfaces [77-80]. A range of interactions have been observed between NH_3 and oxide surfaces. NH_3 is chemisorbed on electron deficient metal atoms through the overlap of free electron pair on NH_3 and the vacant orbital of the cation. IR spectroscopy has revealed that NH_3 adsorbs strongly on two kinds of Ti(IV) sites [134]. Strong adsorption occurring at low NH_3 coverage has been attributed to specific Lewis acid-base adducts formed between NH_3 and Ti^{4+}. Strength of interaction weakens at higher

coverage due to repulsive lateral interaction between adjacent NH_3 molecules [135]. On a hydrated surface, NH_3 binds to a proton of a hydroxyl group through hydrogen bonding [134-136]. Dissociation of NH_3 on contact with an oxide surface resulting in the formation of surface NH_2 (or NH) and additional OH species has also been observed [137]. Complete transfer of protons to the NH_3 molecules from bronsted sites to produce adsorbed NH_4^+ ions is also common on anatase [79]. The presence of ammonium ions on the surface upon NH_3 absorption generally indicates the presence of Bronsted centers.

NH_3 chemisorption accounts for all surface acidity. Estimation of bronsted acid sites was carried out using standard acid base titration method [81] using 2,6-Lutidine as a probe and Hammett indicators [82-84]. The measurement of surface acidity using probe molecules is a well established and effective method [78, 138-141]. 2, 6-Lutidine is a stearically hindered amine and is preferentially adsorbed on proton acid sites even in presence of strong Lewis acid sites, thus acts as a good adsorbate for the bronsted acid sites [85, 86]. The effect of activation temperature and addition of Ag phase to Al_2O_3, TiO_2 and SiO_2 on bronsted acidity was established. Sulfur capacities were determined using JP5 fuel.

Sulfur removal using silver based sorbents is postulated through three mechanisms; the formation of a sulfide on the surface [59-62], strong chemisorption [63-65], physisorption or a combination thereof. These mechanisms differ by the strength of interaction between the sulfur heterocycle and the active center. Multi-layer

sulfide formation is a possible mechanism as observed in the tarnishing of silver objects in air. High selectivity for trace amounts of sulfur in fuels also points to strong chemisorption. Sulfur removal maybe a result of Van der Waal's interactions between sulfur heterocycles and active centers.

A majority of industrial adsorption processes are designed based on physical adsorption. Mechanisms such as π complexation have been used to explain sulfur removal by Cu-Y type zeolites [142, 143]. Variation in electron density of aromatic ring brought about by the sulfur atom has been attributed to the higher adsorption selectivity of these materials. These interactions are stronger than reversible van der waal interactions. The lone pair of electrons on the sulfur atom conjugates with π electrons on the aromatic ring. The d orbitals on the Cu atom back donate electron density to anti-bonding π orbitals (π*) of the sulfur rings resulting in π bonding between the solute and Cu atoms [66]. Higher HDS activity of BT has been attributed to the non-uniform electron distribution compared to DBT. Adsorptive desulfurization selectivity has been observed to increase with increasing electron density on the sulfur atom [47].

This chapter discusses the estimation of the proton acid sites of Al_2O_3, TiO_2 and SiO_2 with and without Ag and calcined at various temperatures by standard acid base titration method [81] using 2,6-Lutidine as a probe and Hammett indicators [82-84].Sulfur capacity of the materials were determined using JP5 fuel with a total sulfur content of 1172 ppmw. The measurement of Surface acidity using probe molecules is a well established and effective method [78, 138-141]. 2, 6-Lutidine was chosen as the

basic probe molecules because the sterically hindered amine is preferentially adsorbed in proton acid sites even in presence of strong Lewis acid sites, thus acts as a good adsorbate for the Bronsted acid sites [85, 86]. The proton donating surface acidity was determined for various supports also considering the effect of thermal treatments.

VI.1 Results

VI.1.1 Influence of the hetero atom

From a comparison of breakthrough characteristics of several sulfur species in model fuel compositions as well as JP5, it was observed that sulfur capacity of Ag/TiO_2 was influenced by the structure of the sulfur heterocycle. Breakthrough studies using sulfur free solute molecules containing other heteroatoms would provide further information on the nature of interactions and adsorption selectivity of the sorbent. This data may be then correlated to the chemical nature of the active centers.

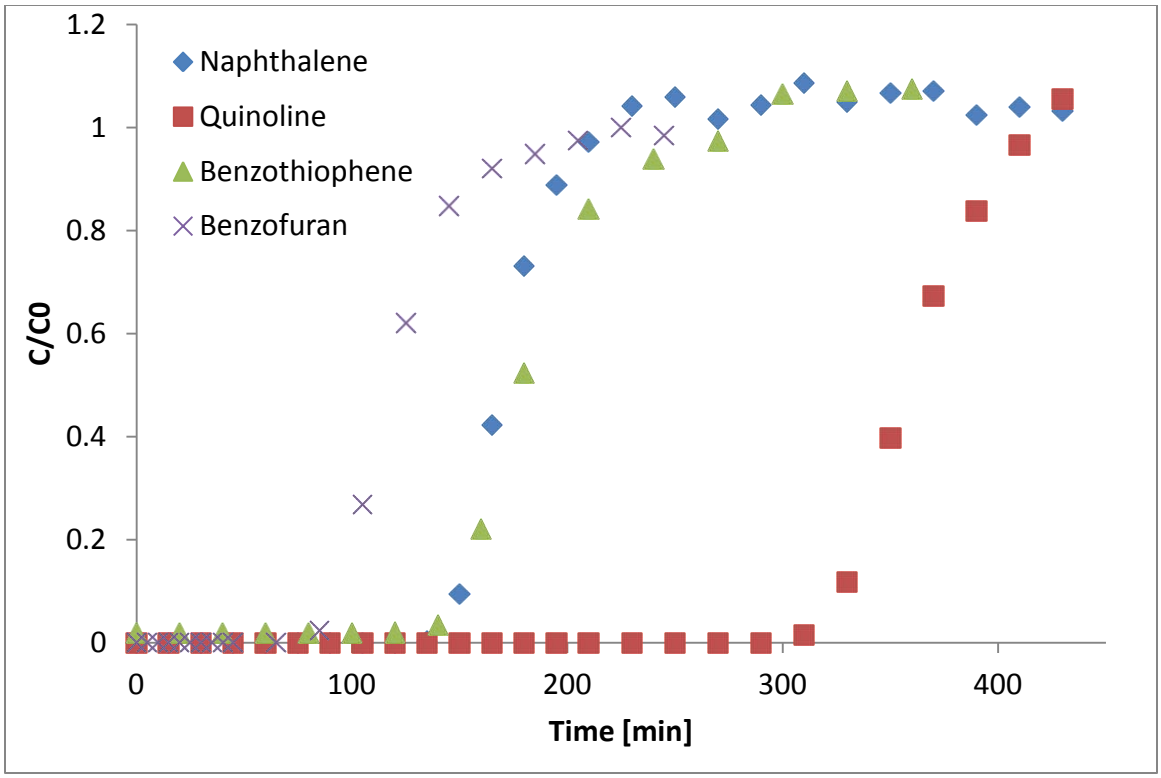

Figure VI.1. The effect of electron density on the heteroatom on adsorption efficiency of Ag(4 Wt.%)/TiO_2 established from breakthrough of 3500±10 ppmw naphthalene, quinoline, benzothiophene and benzofuran

Breakthrough of benzothiophene, quinoline, naphthalene and benzofuran over Ag/TiO_2 sorbent is shown in Figure VI.1. These solutes were selected based on their structural similarity to benzothiophene; in quinoline, the sulfur atom replaced by nitrogen, in benzofuran by oxygen and naphthalene had no heteroatom. The initial concentration of each specie was 3500 ppmw in n-octane. The highest saturation capacity was observed for quinoline (44.60 mg/g) followed by benzothiophene (22.30 mg/g) and naphthalene (20.44 mg/g). The lowest capacity was exhibited toward benzofuran (14.62 mg/g). Thus the affinity of the active center toward the heteroatom may be listed in the order N>S>O which corresponded to the order of electronegativity of these atoms. Therefore electron rich or basic molecules have higher affinity for the

active center which indicates that the active center is acidic or electron deficient in nature.

VI.1.2 The influence of acidic centers on sulfur adsorption

The acidity of the solute molecule influences its adsorption on the Ag/TiO2 adsorbent. Therefore the effect of the acidity of the surface on sulfur adsorption was to be ascertained. The Ag/TiO_2 sorbent was treated with probe molecules NH_3, pyridine, 2, 6 lutidine, CO and Trimethyl Chlorosilane (TMCS) for this purpose. The sorbent particles were saturated with the probe molecules as explained earlier and sulfur capacity established using JP5 fuel as challenge.

Two sets of breakthrough studies were carried out on the samples;. the first set on blank TiO_2 and the second on samples loaded with Ag. In order to distinguish the effect of probe molecules on the support devoid of the Ag phase, activated Al_2O_3 and TiO_2 were treated with NH_3 and breakthrough behavior observed. Sulfur capacity of 'dried' samples was also determined for comparison purposes. Pretreatment of the blank TiO_2 samples with NH_3 deactivated the active centers completely (Figure VI.2(a)). Similar deactivation was also observed on the Al_2O_3 support (Figure VI.2(b)).

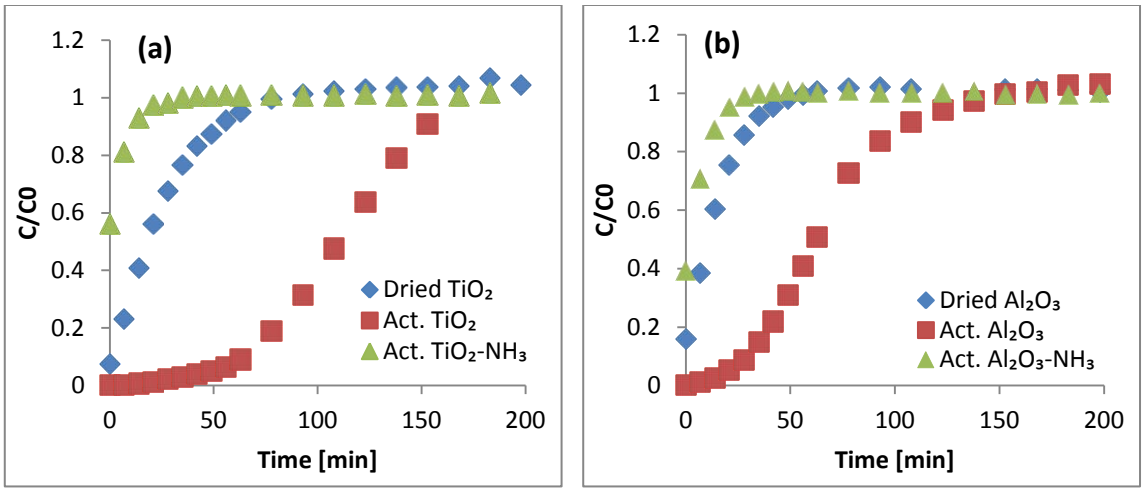

Figure VI.2 . The effect of poisoning of acidic adsorption centers using NH_3on activated (a) TiO_2 and (b) Al_2O_3 on sulfur adsorption capacity indicated by breakthrough tests using JP5 fuel (1172 ppmw sulfur) as challenge

On the samples loaded with Ag, all the probe molecules acted as poisons. The poisons had three effects on the performance of the sorbent; the first group reduced the sulfur capacity of the sorbent permanently, the second group completely deactivated the sorbent and the third group also deactivated the sorbent, but reversibly. This behavior was explained based on the strength of interaction between the acidic center and the basicity of the probe molecule. The more basic of the probe molecules irreversibly deactivated the acid centers while the less basic had a milder interaction and was replaced by the sulfur aromatics during desulfurization (Figure VI.3).

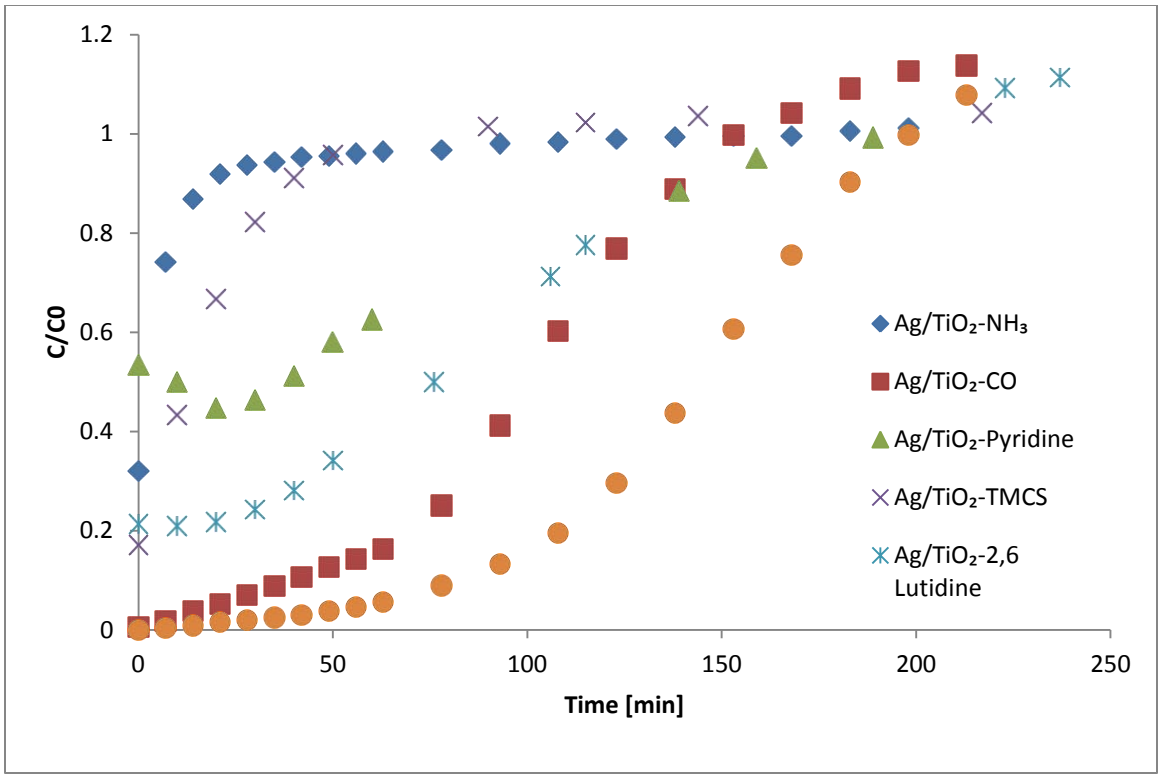

Figure VI.3. The effect of poisoned acidic centers on Ag(4%)/TiO_2 with probe molecules of varying acidity on desulfurization using JP5 fuel (1172 ppmw sulfur) as challenge

Even though CO was able to completely deactivate blank TiO_2, much of the sulfur capacity was retained when the same was carried out on the Ag loaded sample. This indicated that the acidic centers on TiO_2 blank were no deactivated by CO. Because CO is a much milder base compared to NH_3 and thus would only interact with stronger of acid sites. NH_3 and TMCS completely and irreversibly deactivated the sorbent. This interaction with TMCS indicates that the sulfur removal centers are single hydroxyl groups.

Pyridine and 2, 6 lutidine demonstrated a reversible interaction, pyridine being the stronger among the two. They are common probe molecules used in the study of surface acidity [85]. 2,6 lutidine is almost selectively adsorbed on bronsted sites while

pyridine reacts with bronsted and lewis sites [144]. Methyl groups on the aromatic stearically hinder the nitrogen atom so that the molecule fails to interact with Lewis sites. 2,6 lutidine only interacts with bronsted sites because the hydroxyl groups extend away from the substrate surface and make the interaction possible. Both pyridine and 2, 6 lutidine treated samples showed no breakthrough capacity for sulfur. The sorbent was inactive during the initial phase of breakthrough. However, with time the sulfur molecules were able to displace the active centers populated by both pyridine and 2, 6 lutidine, more easily in the case of 2, 6 lutidine.

From the above breakthrough behavior, not only was the acidic nature of the active center reiterated but their bronsted nature consisting of mainly single hydroxyl groups.

VI.1.3 Infrared spectroscopy

Identification of surface functional groups resulting from interactions with probe molecules may provide further information on the nature of the active center. The IR region corresponds to the energies of vibrations and rotations of molecules. Therefore configuration of aggregates of atoms or functional groups on a surface may be associated with absorption of IR radiation over certain frequency intervals. The sorbent particles were exposed to probe molecules and then IR spectra were examined for signatures of characteristic surface groups.

NH_3: Infrared spectra of TiO_2 support, activated TiO_2, and Ag/TiO_2 sorbent was compared following treatment with probe molecules NH_3, pyridine and trichloro methyl

chlorosilane (TMCS). Spectrum of activated TiO_2 was compared to that of activated TiO_2 and Ag/TiO_2 samples treated with NH_3 shown in Figure VI.4. All the samples showed an absorption band at 1620 cm^{-1}. This band has been associated with the OH bending (υ_2) vibration of residual adsorbed water. Studies have shown that monomeric water has its υ_2 vibration at 1600 cm^{-1}, dimeric water at 1620 and polymeric water at 1633 cm^{-1} [106]. Therefore there was an abundance of dimeric water species on the surface. Also noted was that the intensity of this feature was lower in samples that were pretreated with the probe molecules. OH stretching vibrations typically observed at 3700$cm^{-1}$was absent in all the samples possibly due to low instrument sensitivity.

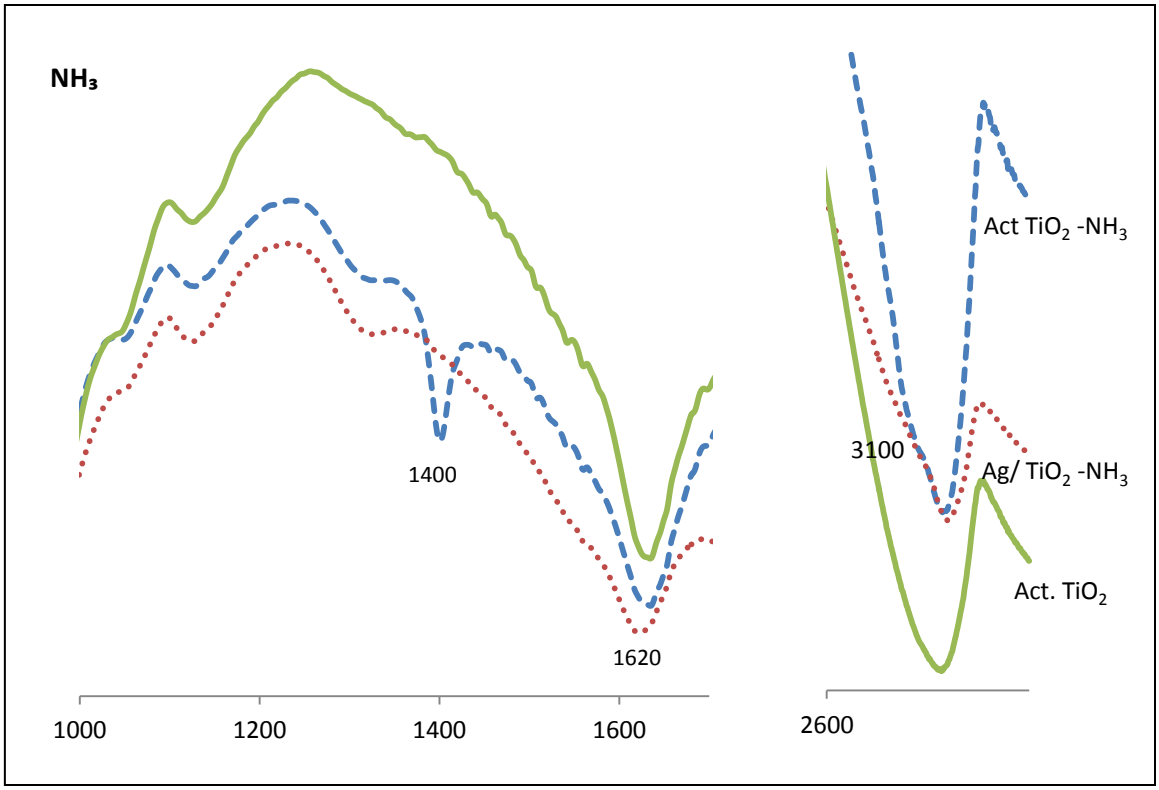

Figure VI.4. IR Spectra of activated TiO_2, activated TiO_2 treated with NH_3 and Ag(4 Wt.%)/TiO_2 treated with NH_3

The presence of ammonium ions on the surface upon NH_3 absorption generally indicates the presence of Bronsted centers. Four bands at 3399, 3355, 3249 and 3514 cm^{-1} have been reported for NH_3 adsorbed on anatase surfaces [145]. On the TiO_2 sample treated with NH_3, a broad band at 3450 was observed as well as shoulders at 3100 and 3200 cm^{-1}. The bands were shifted by 50 cm^{-1} from what has been previously reported as shown in Figure VI.4. These bands have been attributed to the υ_1 and υ_3 stretching vibrations of NH_3 bound to two different types of Lewis acid sites. The strong band observed at 1400cm^{-1} has been reported to be the $\upsilon_4(\delta_{as})$ asymmetric deformation vibration of the NH_4^+ species on surface bronsted sites [146]. This indicates the protonation of part of the adsorbed NH_3 and the presence of bronsted acid sites on the sample surface [147]. Thus IR spectroscopy and NH_3 adsorption was able to identify bronsted sites on the sorbent surface. However the species was not observed on samples loaded with Ag. This is possible when these bronsted sites are occupied by the $AgNO_3$ precursor during sorbent synthesis. Similar highly stable species were observed in thermoreduction profiles of activated TiO_2 samples which were absent in the Ag loaded samples.

Trimethyl Chlorosilane (TMCS): TMCS reacts selectively and completely with single surface hydroxyl groups and also a small fraction of interacting surface hydroxyls as well. Single hydroxyl groups with the oxygen atoms facing away from the plane of the surface lattice will react 1:1 with methyl chlorosilanes [148]. Generally there are three types of surface OH groups; free, geminal and hydrogen bonded. Only free and geminal OH groups are the active centers that react with TMCS. Hydrophilic networks formed

among OH groups deter the hydrogen bonded centers from reacting with TMCS. Bands indicating the presence of CH_3 groups *viz.* 1255 (CH_3 symmetric deformation) and 1449 (CH_3 non symmetric deformation) were observed shown in Figure VI.5(a). The band at 2963 cm^{-1} attributed to surface attached TMCS groups [149] was also observed on the Ag/TiO_2 samples treated with TMCS.

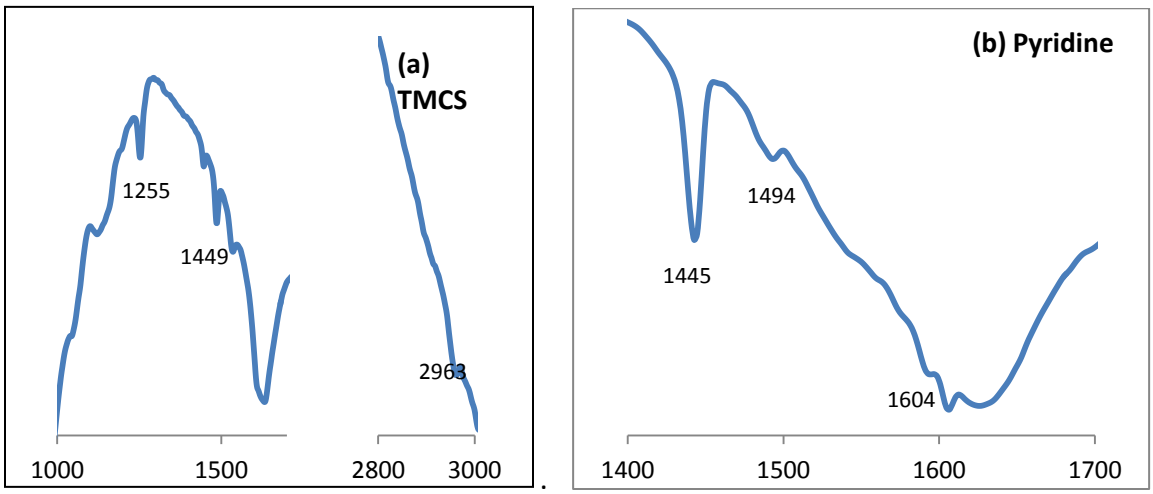

Figure VI.5. IR adsorption features of (a) surface attached TMCS and (b) ligated pyridine molecules adsorbed on Ag(4 Wt.%)/TiO_2

Pyridine: The adsorption of pyridine on a surface generally involves the formation of hydrogen bonds between isolated hydroxyl groups and the nitrogen atoms of adsorbed pyridine molecules. The band at 1592cm^{-1} in particular is characteristic of pyridine which is adsorbed on an oxide via hydrogen bonding interactions with surface hydroxyl groups [150]. The band at 1608 cm^{-1} due to the υ_{8a} vibration of pyridine molecules is characteristic of pyridine coordinatively ligated to electron deficient Lewis acid sites on the surface. The band at 1445 cm^{-1} arises from the υ_{19b} vibration of pyridine molecules [151]. It has been reported that the spectra of anatase exposed to

pyridine contains four bands at 1613, 1575, 1494 and 1445 cm^{-1} assigned to 8a, 9b, 19a and 19b ring vibrations of ligated pyridine respectively and confirm lewis acid sites on the surface [145, 152]. In the samples of the Ag/TiO_2 with pryridine adsorbed, bands were observed at 1445, 1494 and 1604 cm^{-1} as shown in Figure VI.5(b). These bands confirm the presence of Lewis acid sites.

VI.1.4 Ammonia chemisorption

NH_3 uptakes by the samples were used to gauge their acidity. Since NH_3 interacts with both Lewis and Bronsted sites, these measurements represent the total surface acidity. The samples were calcined *in situ* (400^oC), cooled to the analysis temperature (175^oC) prior to obtaining the isotherms. NH_3 uptake of SiO_2, Al_2O_3 and TiO_2 was obtained. The amount of chemisorbed NH_3 was obtained from isotherms representing combined and weak adsorption as explained earlier (Figure VI.6).

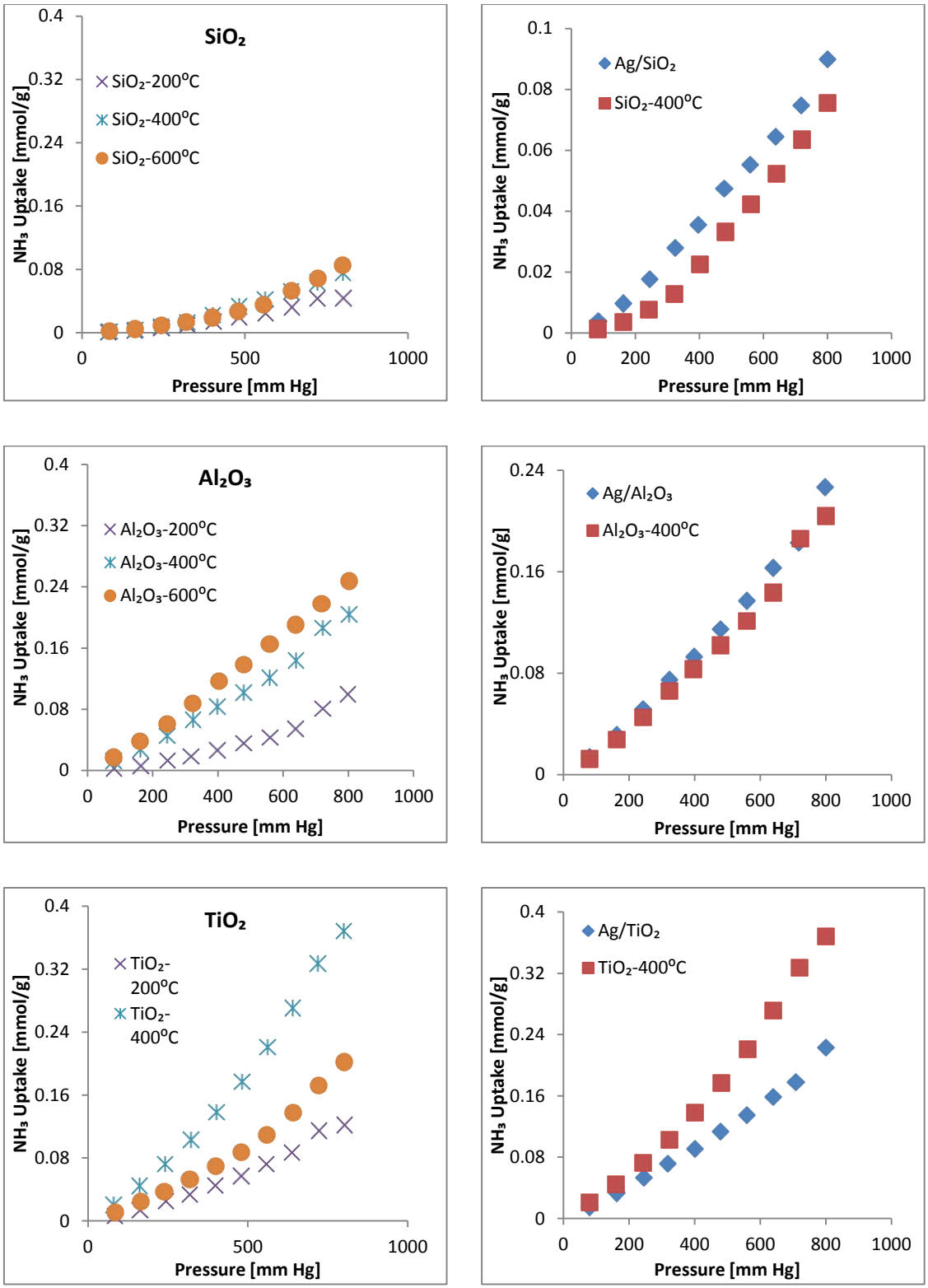

Figure VI.6. Ammonia adosrption isotherms of SiO_2, Al_2O_3 and TiO_2 samples calcined in air at 200, 400 and 600°C compared to Ag(4 Wt.%)/SiO_2, Ag(4 Wt.%)/Al_2O_3 and Ag(4 Wt.%)/TiO_2 samples calcined at 400°C; Isotherms obtained at 175°C

It was observed that smallest NH_3 uptake occurred on the SiO_2 sample. This confirmed the earlier observation that the surface of SiO_2 was non-acidic. Increasing calcination temperature to 600^oC did not significantly impact NH_3 uptake. NH_3 uptake on Al_2O_3 on the other hand was significantly higher than SiO_2. NH_3 uptake of TiO_2 was higher than on Al_2O_3. Increase in calcination temperature from 200 to 400^oC resulted in an increase in NH_3 uptake higher than that observed on Al_2O_3. However, unlike Al_2O_3 increase in calcination temperature to 600^oC decreased NH_3 uptake. This was attributed to the higher stability of Al_2O_3 pore structure during thermal treatments. Previous work on the TiO_2 support had indicated a significant loss in surface area for calcination temperatures above 500^oC [153].

The addition of Ag to SiO_2 and Al_2O_3 resulted in an increase in NH_3 uptake as shown in Figure VI.6. However for TiO_2 the NH_3 uptake decreased with the addition of Ag to the surface. The Ag phase may occupy acid sites on the support. The Ag phase consists of acid sites as well. When the number of acid sites added by the Ag phase is greater than the sites removed due to its deposition, then the total acidity increases. In the case of TiO_2 the net acidity was lower.

We hypothesize that sulfur adsorption occurs on bronsted acid sites; both on TiO_2 support and Ag_xO phase. NH_3 adsorption cannot differentiate between bronsted and lewis sites. Efforts were made to use potentiometric titration with bases as described in the following section.

VI.1.5 Potentiometric titration

Introduction of probe molecules to the surface prior to adsorption studies indicated that bronsted centers play a substantial role in sulfur adsorption. it was therefore necessary to establish bronsted acidity from overall acidity measured indicated using NH_3 adsorption. Bronsted sites were selectively titrated using 2,6 lutidine solution for this purpose.

NH_3 chemisorption indicated that activation in air increased surface acidity. The effect of activation on bronsted acidity of Al_2O_3, TiO_2 and SiO_2 were studied. Pre-dried samples were calcined at various temperatures and titrated with the base. Saturation sulfur capacities of the samples were obtained using JP5 fuel. Calcination temperature of TiO_2 was limited to 550^oC as the pore structure collapsed at higher temperatures [153].

The pKa of the methyl yellow indicator is +3.3. The pKa of samples that required no titer (indicated as zero µmoles/g) was greater than +3.3. It was observed that with the increase in activation temperature, the concentration of Bronsted acid sites increased (Figure VI.7). Activation temperature of Al_2O_3 was higher (250^oC) compared to TiO_2. The concentration of proton donating acid sites on Al_2O_3 surface was higher compared to TiO_2. Previous research has indicated that Al_2O_3 mostly comprises of Bronsted sites while Lewis sites dominates TiO_2 [154]. SiO_2 was basic after calcination at 450°C and had very little impact on its sulfur adsorption capacity. An identical trend was observed from NH_3 chemisorption experiments presented earlier. The order of supports

samples in terms of the concentration of proton donating surface acid sites was: Al_2O_3 > TiO_2 > SiO_2. Sulfur adsorption capacity of the samples using JP5 fuel was measured to correlate with the measured bronsted acidity shown in Figure VI.7. The relationship between calcination temperature and proton donating surface acidity as well as sulfur removal capacity was evident.

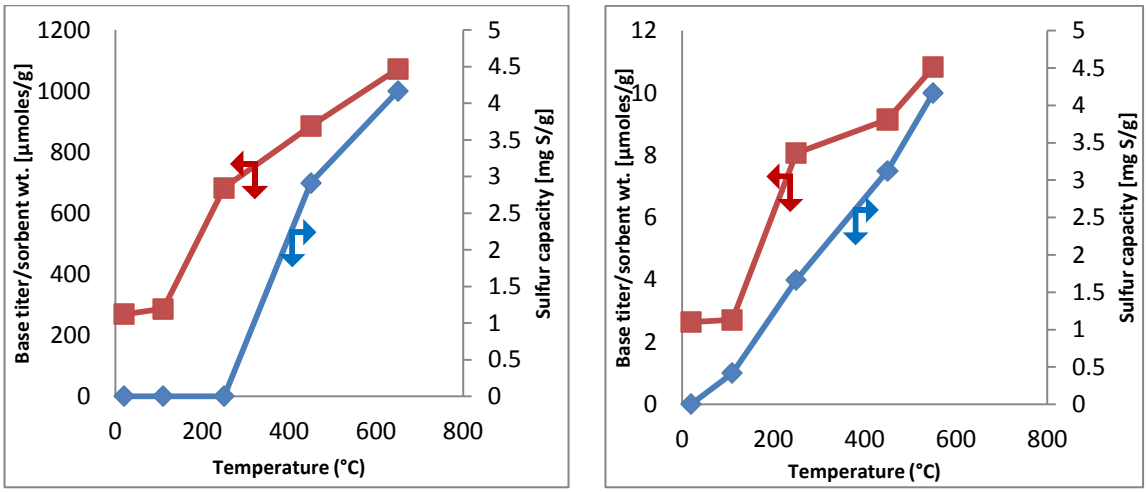

Figure VI.7. The relationship between bronsted surface acidity measured by potentiometric titration and sulfur adsorption capacity using JP5 fuel (1172 ppmw sulfur) as challenge for activated (a)Al_2O_3 and (b)TiO_2 at various activation temperatures

The effect of addition of the Ag phase to TiO_2 on the bronsted acidity was also established. The amount of base required to neutralize samples of Ag(4 Wt.%)/SiO_2, Ag(4 Wt.%)/Al_2O_3 and Ag(4 Wt.%)/TiO_2 was determined using titration listed in Table VI.1. There was a considerable increase in the amount of base required for neutralization which demonstrates that metal impregnation enhanced surface acidity.

VI.2 Discussion

Activated Al_2O_3 and TiO_2 demonstrated a sulfur capacity of c.a. 0.15mmol/g using a challenge of 3500 ppmw benzothiophene in n-octane. Addition of Ag phase increased the sulfur capacity from 0.15 to 0.3 mmol/g as shown in Figure VI.9(a). NH_3 chemisorption indicated that activated Al_2O_3 and TiO_2 were considerably more acidic than SiO_2. A comparison of NH_3 uptake at 760mm between activated supports and Ag loaded samples is shown in Figure VI.9(b). The acidity was acquired during activation process and increased with increasing activation temperature. However this was not observed when high temperatures resulted in the collapse of pore structure as in TiO_2. Addition of Ag phase resulted in a modest increase in the acidity of Al_2O_3 and SiO_2 while witnessed a decrease in the case of TiO_2. Similar trends were observed on bronsted acidity measurements by titration. Bronsted acidity increased with activation temperature as well. Addition of Ag increased the bronsted acidity of TiO_2 and SiO_2 but that of Al_2O_3 did not vary. Generation of bronsted acidity during calcination is a result of defect mediated dissociation of water molecules on oxygen vacancies or lewis centers. Water molecules exist on the surface of supports as in various configurations such as hydronium ions, dimers etc. held together by hydrogen bonding. High temperature treatments can drive off surface water and OH groups resulting in lewis sties. Increasing surface temperature may also convert vicinal OH groups to either geminal or isolated OH groups. Such changes to surface water indicated schematically in Figure VI.8 significantly increases surface acidity and are reflected in NH_3 chemisorption and titration measurements.

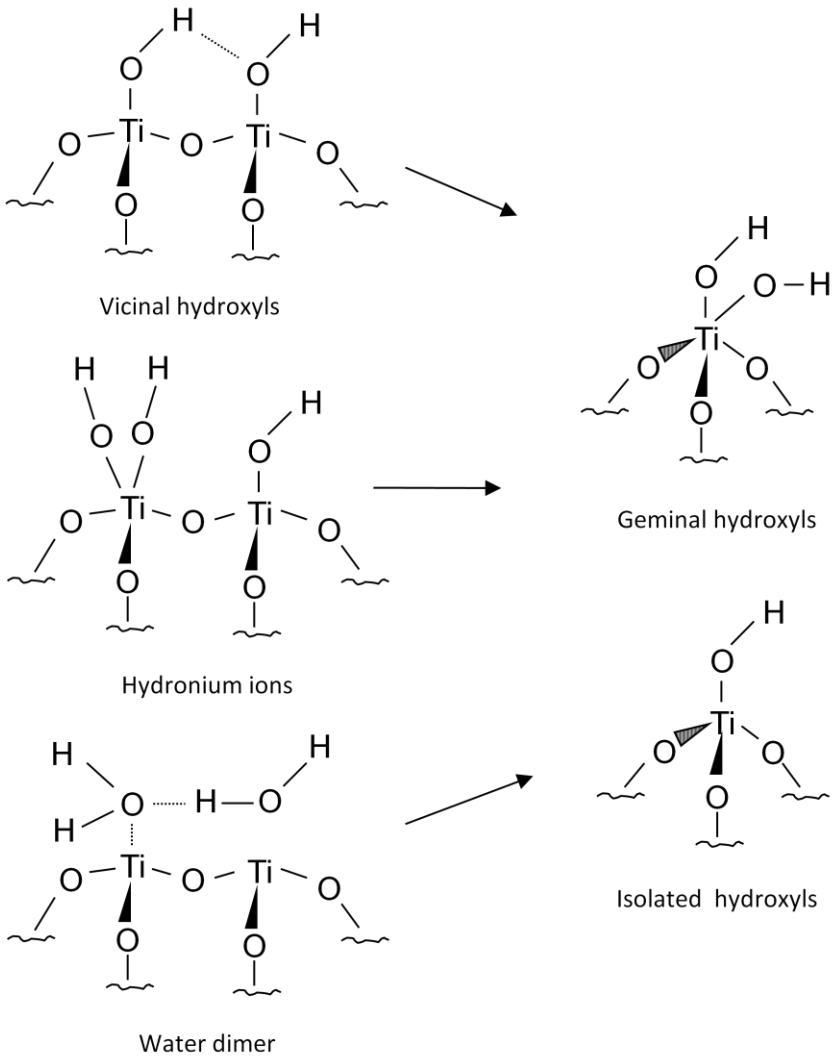

Figure VI.8. Conversion of vicinal OH, hydronium ions and water in dimeric form to geminal and isolated OHs

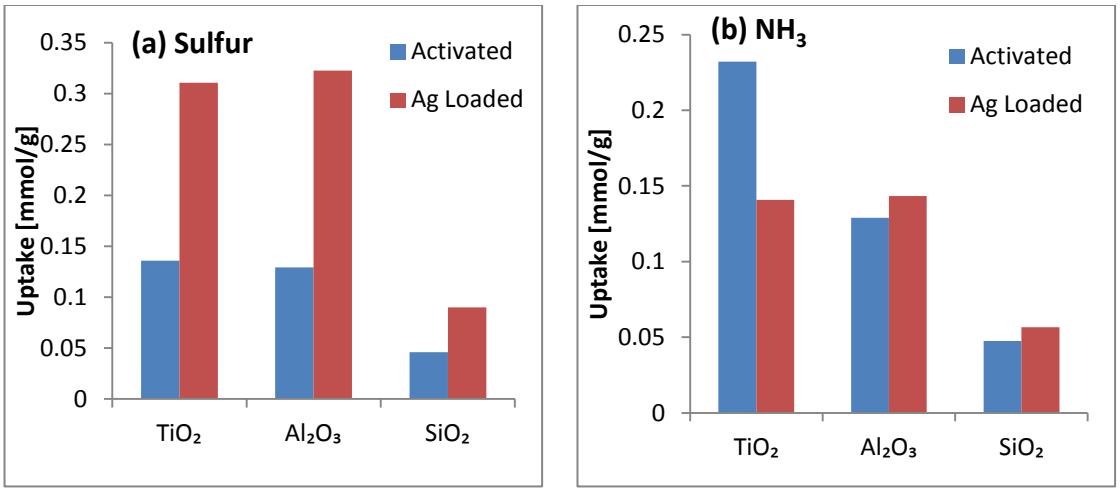

Figure VI.9. A comparison of (a) sulfur adsorption capacity and (b) NH_3 uptake between activated TiO_2, Al_2O_3 and SiO_2 supports and samples loaded with 4 Wt.% Ag

TPR measurements had indicated the removal of strongly bound acidic groups on activated TiO_2 by the addition of the Ag phase. Similar observation was also made from IR spectra of NH_3 treated samples. Therefore Ag occupies acidic sites on the surface. It is also clear from the titration data that Ag phase consists of additional bronsted centers. Therefore there would be a net increase in surface acidity when bronsted acidity added by the Ag phase is higher that the acid sites occupied by the dispersed Ag. A comparison of bronsted acidity between activated and Ag loaded samples is listed in Table VI.1. Bronsted acidity of the TiO_2 sample increased from 7.5 to 100 µmol/g and that of SiO_2 from 0 to 225 µmol/g for SiO_2. The bronsted acidity of Al_2O_3 remained unchanged at 700 µmol/g.

Sorbent	2, 6-Lutidine titer/sorbent Wt. [µmoles/g]	
	Activated	Ag Loaded
TiO_2	7.5	100
Al_2O_3	700	700
SiO_2	0.0	225

Table VI.1. Bronsted acidity of activated (450^oC/2h) and Ag loaded supports obtained from titration measurements

Sulfur adsorption in these materials is postulated through an interaction between the π electrons of the aromatic solute and the acidic OH groups on the surface a schematically represented in Figure VI.10.

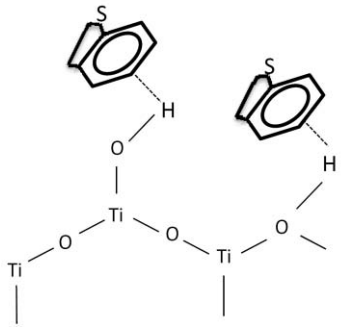

Figure VI.10. Adsorption of benzothiophene through interaction between π electrons and proton on surface OH group

VI.3 Conclusions

Active sulfur adsorption centers on supported Ag sorbents were acidic in nature. This was confirmed using several techniques. The adsorption selectivity among aromatic species was observed to be quinoline>naphthalene~benzothiophene>benzofuran following their order of basicity. The poisoning effect of probe molecules on adsorption of benzothiophene was NH_3>TMCS>Pyridine>2,6 Lutidine>CO also in the order of their

basicity. IR signatures of surface complexes with lewis and bronsted acid sites were observed on samples treated with the above mentioned probe molecules. Surface acidity was measured by NH_3 chemisorption and bronsted acidity using titration with 2,6 lutidine. Activation in air increased the bronsted surface acidity from 0 to 10 μmol/g between calcination temperatures 20 and 550^{o}C and the addition of Ag to the TiO_2 surface increased acidity from 5 to 100 umol/g. Therefore bronsted acid centers account for the sulfur adsorption capacity of these materials.

VII. Equilibrium of Sulfur Aromatics Over Ag/TiO_2 Sorbents

VII.1 Introduction

To understand the strength of adsorption, equilibrium isotherms of several sulfur aromatics were observed on the Ag/TiO_2 sorbent at different temperatures. The equilibrium data maybe recalled for the design of sulfur sorption units based on the Ag/TiO_2 sorbent or to gain a better understanding of the nature of sulfur removal. Adsorption isotherms have been reported for thiophenic sulfur compounds from binary solutions in n-octane on Cu-Y zeolites and $PdCl_2$ impregnated on activated carbon both in liquid and vapor phase [155]. Flow calorimetric and thermogravimetric analysis were also used to study the adsorption of thiophene compounds on NaY zeolites [156, 157]. Adsorption data was fitted to the Langmuir-Freundlich single solute isotherm [155, 158]. Isotherm data thus obtained was correlated with 3 isotherm models, Langmuir, Freundlich and Fritz-Schlunder isotherm models using a non-linear regression analysis. These models have been used to represent adsorption on activated carbon in aqueous environments [159]. Generally, the Langmuir isotherm adequately represents adsorption at low concentrations. The model has successfully represented adsorption isotherms for pollutant solutes [160]. The expression is represented by Equation VII-1.

$$q = \frac{K_{1L}C}{1 + K_{2L}C}$$ Equation VII-1

Where q (mg/g) is the amount in the solid phase, C (mg/l) is the initial sulfur concentration and K_{1L} and K_{2L} (l/g) are the Langmuir constants. The Freundlich isotherm considers the adsorption surface to be heterogeneous and that the energy of adsorption varies as a function of surface coverage represented by Equation VII-2.

$$q = k_F C^{n_1}$$ Equation VII-2

Where k_F is the Freundlich constant mg/g(mg/l)^n and n_1 represents the heterogeneity factor. The constant k_F is the related to the adsorption capacity while $1/n_1$ to the adsorption intensity. Freundlich's isotherm best represents the data when more than a monolayer coverage of the surface exists and the site is heterogenous with different binding energies. The model also assumes an unlimited supply of unreacted sites. 1/n is usually less than 1 because sites with the highest binding energy are utilized first, followed by weaker sites and so on [161].

The Fritz-Schlunder model [162] was developed to represent multi-solute adsorption where simpler adsorption models were inadequate and is represented by Equation VII-3.

$$Y_i = \frac{a_{i0} X_i b_{i0}}{ci + \sum_n^{i=1} aij \, X_j{}^{bij}}$$ Equation VII-3

Y_i is the amount of solute *i* adsorbed per unit weight of adsorbent at equilibrium concentration X_i in a solution containing *n* solutes. For a single solute system the expression reduces to the four parameter model represented by Equation VII-4.

$$q = \frac{k_1 C^{n1}}{1 + k_2 C^{n2}} \qquad \text{Equation VII-4}$$

The fit of equilibrium data to these adsorption models was observed. When a model represents adsorption data adequately, the underlying postulates maybe considered to be applicable to the system.

VII.2 Adsorption Equilibrium

Adsorption isotherms describe the equilibrium between the solute and active centers, bring molecular insight to the interactions at the interface as well as facilitate the scale-up of adsorption processes. Equilibrium sulfur concentrations of 4 sulfur aromatics viz. thiophene (Figure VII.1), benzothiophene (Figure VII.2), dibenzothiophene (Figure VII.3) and 4,6 dimethyl dibenzothiophene (Figure VII.4) on Ag/TiO_2 sorbent was established at 22, 40 and 60±2^oC. Experimentally measured equilibrium data were fitted to the proposed isotherms using the Levenberg-Marquardt (LM) algorithm

The Langmuir and Fritz Schlunder model was a good fit for isotherms obtained for the sulfur aromatics in most conditions, however thiophene was an exception. It was also observed that the Freundlich model least correlated to the equilibrium data. Therefore adsorption conditions laid out by Langmuir maybe more applicable to the Ag/TiO_2-sulfur system than by Freundlich. Each adsorption site captures a maximum of

one solute molecule and multi-layer adsorption is unlikely. It also suggests that all adsorption sites are equivalent with a minimal interaction between adsorbed molecules. The surface is likely to be homogenous and the energy of adsorption not influenced by the surface coverage. This would also imply that during adsorption, there are a limited number of unreacted sites.

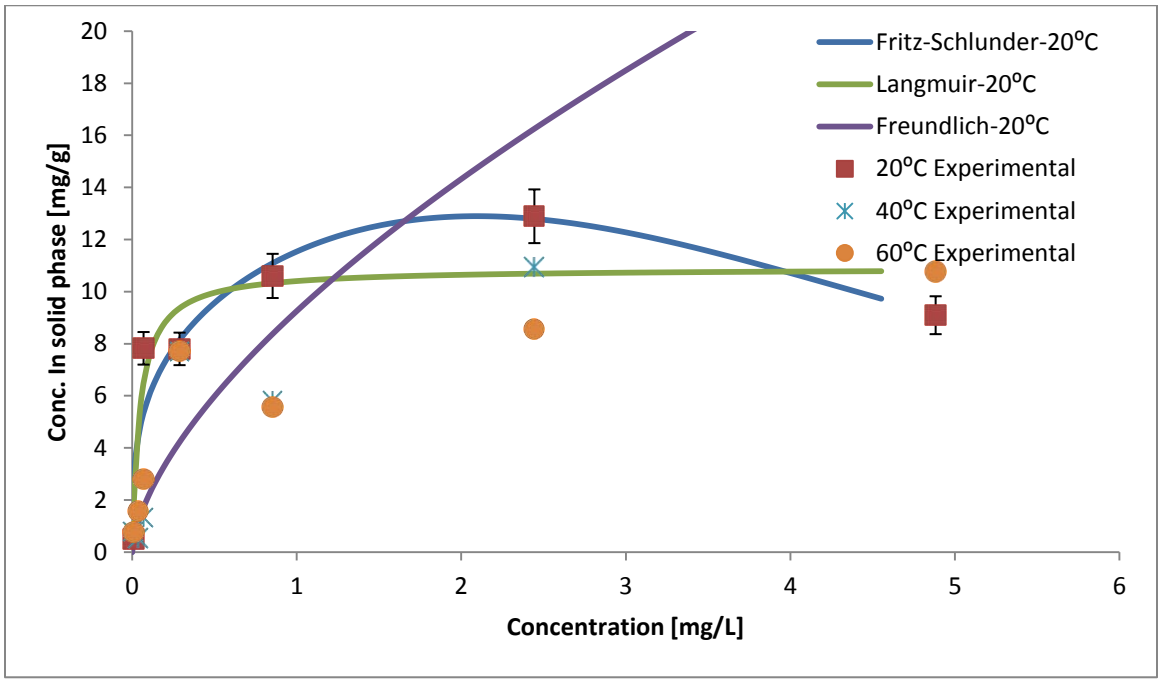

Figure VII.1. Equilibrium sulfur concentrations for thiophene using Ag/TiO_2 sorbent at 20, 40 and 60°C and Fritz-Schlunder, Langmuir and Freundlich isotherm model fits at 20°C

Other inferences may also be made from equilibrium data. Chemical reaction with the Ag phase resulting in the formation of a sulfide was unlikely. The applicability of Langmuir adsorption model indicates that the majority of sulfur was removed through chemisorption.

Equilibrium data for thiophene was not represented adequately by any of the adsorption models. This indicated an interaction atypical of the other solutes as observed during multi-solute adsorption and was attributed to the smaller molecular size of thiophene and the ability to access sites not accessible by the bigger solute molecules. It was also observed that the capacity of the sorbent averaged around 8 mg/g at the higher concentrations for all the sulfur aromatics at the different temperatures. This indicated that the adsorption maybe considered irreversible when operating conditions are below 60°C. Higher temperatures only had the effect of reducing the capacity of the sorbent in the case of 4,6 DMDBT, again attributed to the presence of alkyl groups.

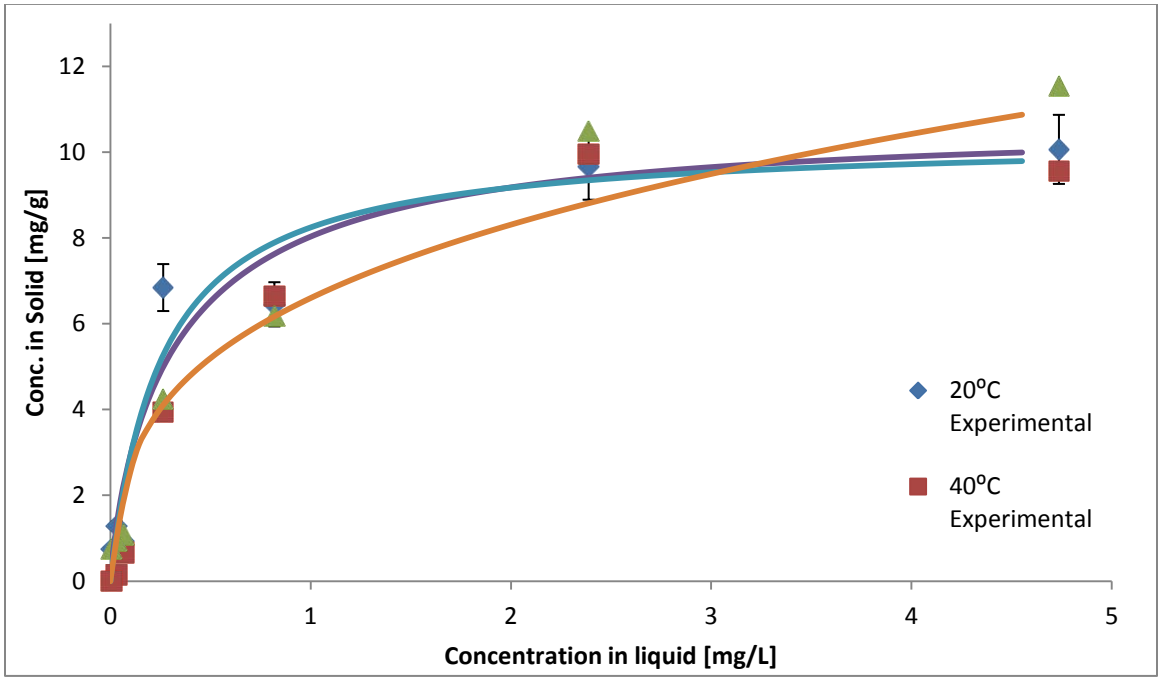

Figure VII.2. Equilibrium sulfur concentrations for benzothiophene using Ag/TiO_2 sorbent at 20, 40 and 60°C and Fritz-Schlunder, Langmuir and Freundlich isotherm model fits at 20°C

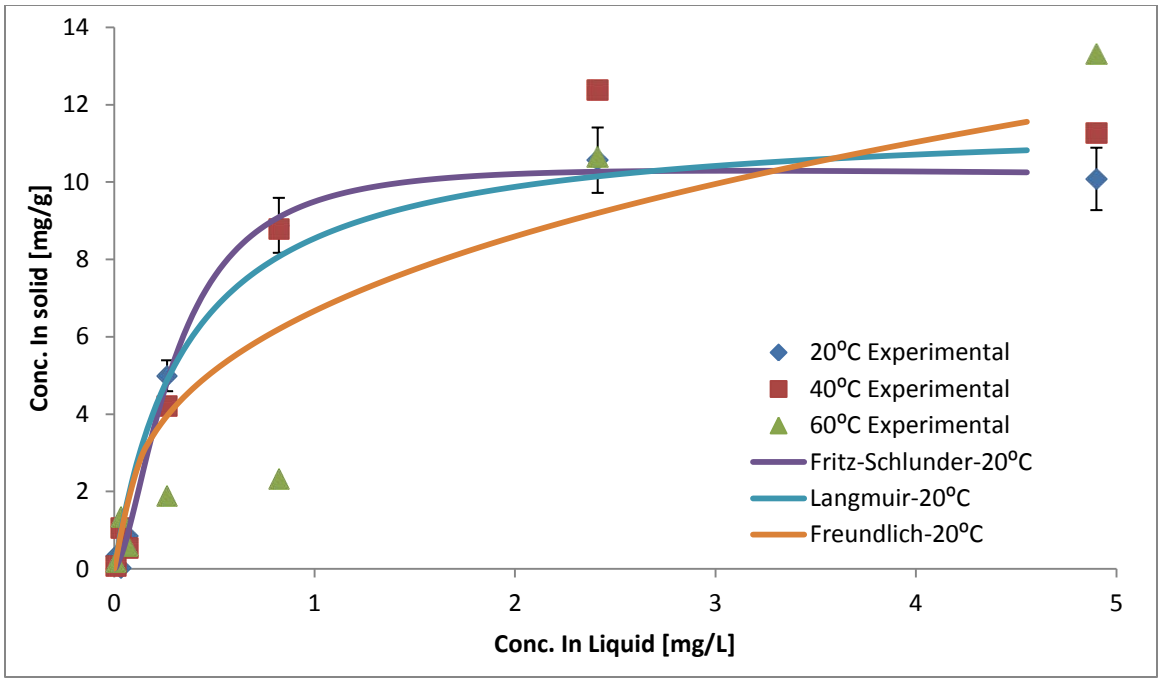

Figure VII.3. Equilibrium sulfur concentrations for dibenzothiophene using Ag/TiO_2 sorbent at 20, 40 and 60°C and Fritz-Schlunder, Langmuir and Freundlich isotherm model fits at 20°C

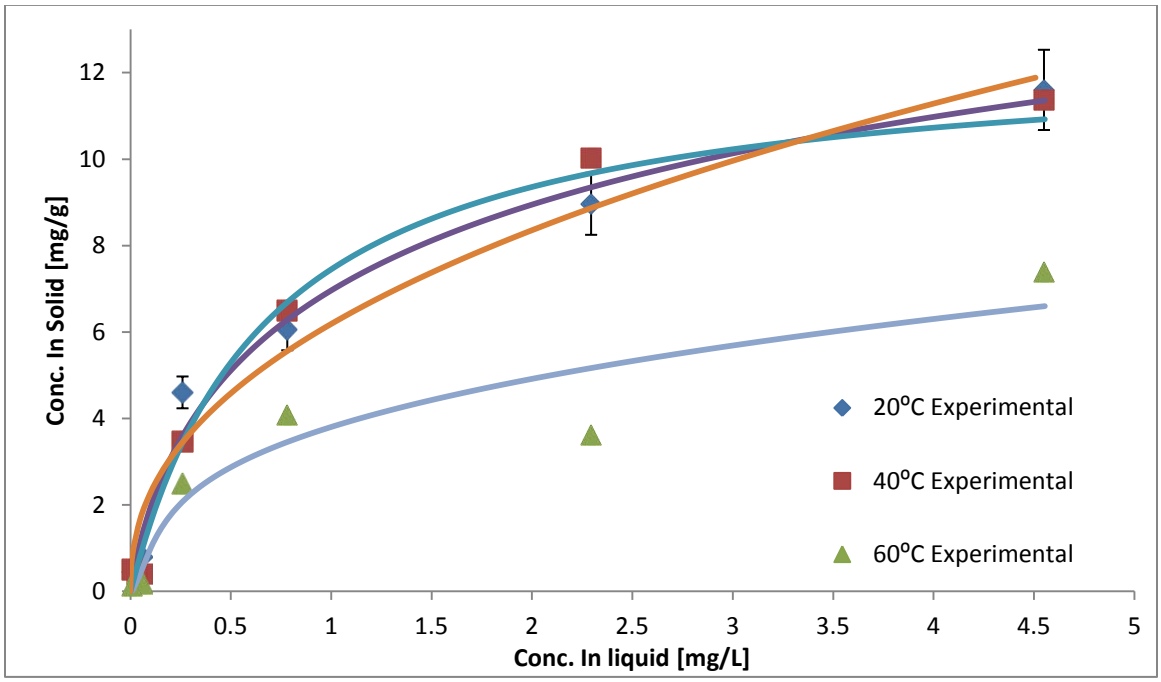

Figure VII.4. Equilibrium sulfur concentrations for 4,6 dimethyl dibenzothiophene using Ag/TiO_2 sorbent at 20, 40 and 60°C and Fritz-Schlunder, Langmuir and Freundlich isotherm model fits at 20°C

	Langmuir			Freundlich			Fritz-Schlunder				
	K_L	a_L	R^2	K_F	n_F	R^2	K_S	b_1	a_S	b_2	R^2
Thiophene											
20	**231.08**	**21.20**	***0.85***	**9.26**	**0.17**	**0.63**	**11.82**	**0.29**	**0.02**	**2.38**	**0.87**
40	**38.47**	**3.49**	***0.86***	**7.53**	**0.42**	**0.84**	**67.09**	**1.14**	**7.06**	**9.95E-01**	**0.87**
60	**62.15**	**6.55**	***0.87***	**6.83**	**0.30**	**0.87**	**76.61**	**0.93**	**9.08**	**0.79**	**0.89**
Benzothiophene											
20	**40.79**	**3.94**	**0.94**	**6.70**	**0.32**	**0.88**	**24.18**	**0.80**	**2.01**	**0.84**	**0.93**
40	**20.77**	**1.84**	**0.99**	**5.90**	**0.40**	**0.91**	**13.98**	**0.72**	**0.80**	**1.23**	**0.99**
60	**18.26**	**1.37**	**0.98**	**6.51**	**0.41**	**0.97**	**7.35**	**0.54**	**0.03**	**1.89**	**0.99**
Dibenzothiophene											
20	**31.71**	**2.71**	**0.97**	**6.78**	**0.35**	**0.85**	**65.92**	**1.56**	**5.94**	**1.60**	**0.99**
40	**26.15**	**1.91**	**0.97**	**7.25**	**0.38**	**0.88**	**14.42**	**0.93**	**0.46**	**1.44**	**0.99**
60	**5.91**	**0.22**	**0.95**	**4.75**	**0.68**	**0.95**					
4,6 Dimethyl dibenzothiophene											
20	**18.29**	**1.46**	**0.97**	**6.19**	**0.43**	**0.97**	**20.96**	**0.89**	**2.01**	**0.74**	**0.98**
40	**16.32**	**1.21**	**0.99**	**6.18**	**0.45**	**0.96**	**22.56**	**1.17**	**2.01**	**1.10**	**0.99**
60	**9.85**	**1.38**	**0.87**	**3.39**	**0.46**	**0.89**	**199.59**	**1.92**	**51.49**	**1.57**	**0.91**

Table VII.1. Adsorption constants obtained from regression analysis of isotherm data for Ag/TiO_2 sorbent

VII.3 Conclusions

Isotherms for all the sulfur aromatics were of Type I classification indicating favorable adsorption. Good match to Langmuir model indicated monolayer adsorption with one active site associated with one solute molecule adsorbed. This also indicated that the sulfur removal was primarily as a result of chemisorption. The strong interaction was also evident as there was minimal difference between uptakes at lower and higher temperatures.

VIII. Conclusions and Recommendations for Future Work

VIII.1 Conclusions

Conclusions regarding various aspects of sulfur removal using supported Ag sorbents have been presented at the end of each chapter. An overview of all research activities conducted will be mentioned here. Several inventions, materials and analysis methods have been developed as a part of this research. The notable achievements are:

1. A novel sorbent for sulfur removal from liquid feed stocks at ambient conditions was developed
2. Thermal regeneration conditions in air was established and demonstrated for such materials for the first time in reported literature
3. The sorbent formulation is the only reported for being active in the oxide state
4. The sulfur sorption capacity of acidic supports in the absence of active metals and the mechanism for the 'activation' step has not been reported by previous research
5. A PLC controlled liquid auto-sampling equipment was designed and custom built for the purpose of carrying out breakthrough experiments

6. The role of acidic surface functional groups in sulfur sorption from liquid fuels have been overlooked by previous research
7. A new method for the poisoning of adsorption sites with probe molecules to provide a better understanding of molecular surface interactions was developed

The silver sorbent developed during the course of this research is the only commercially viable composition for desulfurization of liquid hydrocarbon fuels. Ease of synthesis, availability of raw materials, use of large particle sizes, absence of activation steps or high purity gases for pre-treatments and low cost are some of the characteristics that render the sorbent more practical than others. Regenerability is the property that allows an adsorption process to transform from a batch to a continuous process. Regenerability achieved using air as a stripping medium is viable compared to the use of solvents for desorption as required for other popular sorbents. The fact that thermal regeneration can be carried out using exhaust gases from internal combustion engines in mobile applications and using steam in refinery settings also allows for integration of the desulfurizer into available utilities.

Several sorbents in literature used Al_2O_3 to support active metals. These studies overlooked the sulfur capacity of blank Al_2O_3 and failed to separate sulfur capacity exhibited by the active metal from it. Identification of the role of surface acidity in sulfur removal is a significant breakthrough. The above mentioned omissions by previous researchers have introduced ambiguities in understanding molecular interactions at the

surface. The presence of hydroxyl groups at the adsorption interface and their interaction with sulfur aromatics is a significant finding of the current research. The use of probe molecules to selectively deactivate active centers on the surface is another notable contribution of current research. This method maybe used not only in the study of sorbents but also in the field of catalysis. The method allows for understanding chemistry of surfaces and the relationship with reactions on various active sites.

VIII.2 Recommendations for future work

VIII.2.1 Development of new materials

The knowledge that sulfur adsorption is brought about by acid sites can be utilized to improve the performance of Ag based sorbents as well as develop new materials. Generation of surface defects play a significant part in the 'defect induced dissociation of water' mechanism proposed for the generation of acidic surface hydroxyl groups. Oxide structures with surface defects are formed using techniques such as treatment with strong acids, thermal cycling and the like. Synthesis of new mixed oxide supports (Al_2O_3/SiO_2 or Al_2O_3/TiO_2) also may be used to develop materials with a highly defected surface. The knowledge that the addition of metal oxides such as Ag_xO further increases the concentration of bronsted acidity may be applied to other metals such as W_xO, Nb_xO, Cd_xO, Cr_xO. These metals may only be required as a dopant in a two-component active metal matrix to generate surface defects. The use of high surface area supports has been demonstrated to improve sulfur capacity. Application of high surface

area activated carbon needs to be investigated with regeneration carried out at relatively low temperatures to limit oxidation.

VIII.2.2 Surface analysis of Ag phase

Even though a variety of techniques were employed to analyze the surface structure and chemistry of the Ag phase, a complete understanding of the surface is lacking. The failure to detect diffraction features of the Ag phase on samples with relatively high loadings of Ag (14 Wt.%) possible due to small crystallite size need further investigation. One such method would be to induce crystallite growth thermally. Samples at various weight loading of Ag may be cycled through an oxidation and reduction process in the presence of moisture to induce smaller crystallites to coalesce. XRD analysis of subsequent material will confirm the size of these crystallites and may be compared with O_2 chemisorption data. Another set of studies would involve efforts to completely oxidize the Ag phase in a high energy system such as by using plasma followed by analysis using temperature programmed reduction. Increased H_2 uptake will further confirm the proposed morphology of the Ag phase.

VIII.2.3 *In situ* InfraRed studies for mechanistic details

Even though the contribution of surface hydroxyls to sulfur adsorption was established, direct spectroscopic evidence for the 'activation' step was not obtained. This was mainly because of the limited scope of transmission spectroscopy. TiO_2 has high atomic density and thus is quite opaque to the IR beam. Reflective IR spectroscopy may yield better resolution of bands representing OH groups on the surface. IR

spectroscopy conducted *in situ* during thermal treatment would provide conclusive evidence on the decomposition of water molecules on the surface and rearrangement to form acidic OHs.

VIII.2.4 Temperature programmed desorption

Temperature programmed desorption of probe molecules such as NH_3 has been used in catalysis to estimate the thermodynamics of surface interactions. Desorption profiles of these molecules with respect to temperature would provide a deeper understanding of the energetic of molecular interactions at the surface.

VIII.2.5 System level design of desulfurization unit

Several designs have been proposed for desulfurization units based on sorption using liquid feed stocks. However, designs for units regenerated thermally are scarce because sorbents that are thermally regenerable have not been prevalent. The main issue with a system involving high regeneration temperatures would be heat transfer. Designs involving multiple adsorbent beds on a rotary system as shown in Figure VIII.1 passing sequentially thorough an adsorption section (at ambient conditions) followed by a regeneration section (at high temperature) have been built. Such a system, even though feasible, has several moving parts involves high temperature parts is prone to failure.

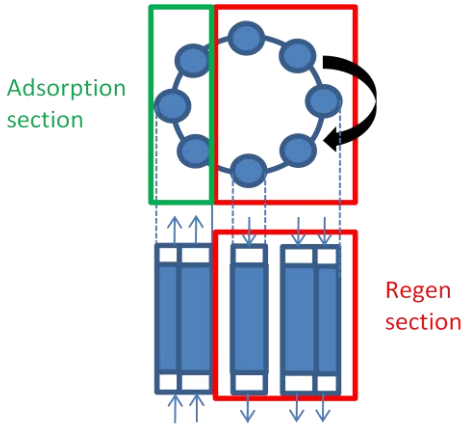

Figure VIII.1. Rotary multi-bed design for desulfurization of liquid fuels

An alternative design would mimic a TEMA style heat exchanger wherein the tube side would hold the sorbent particles and shell side would be used to provide thermal energy for regeneration as shown in Figure VIII.2.

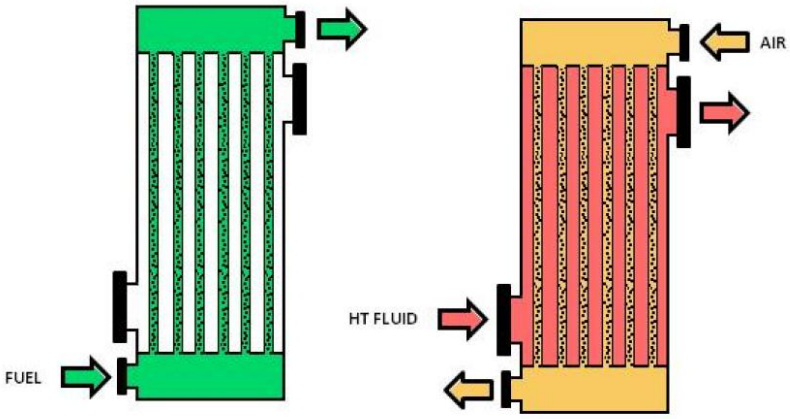

Figure VIII.2. Multi-tube bank design for a desulfurizer with adsorbent on the tube side and heat transfer fluid on the shell side

High temperature streams such as exhaust gases from internal combustion engines or superheated steam maybe applied on the shell side based on the application. Designs and vendors for such a unit would be readily available compared to an exotic

design based on multiple beds. These designs may then be integrated to commercial refining operations or portable power applications using process simulation application such as Aspen. Such an analysis will provide detailed understanding on the thermal load and ultimately the cost effectiveness of desulfurization units based on sorption.

An effective desulfurization composition for hydrocarbon fuels was developed. Performance comparisons with other sorbents indicated high sulfur capacity. The sorbent composition was regenerable over multiple cycles. Synthesis conditions significantly affected desulfurization efficiency and correlations between surface structure and sulfur capacity was established. Oxidation state and dispersion of the Ag phase on the support was characterized in detail. The influence of surface acidity and role of Bronsted centers on sulfur adsorption was established. Development of materials with higher sulfur capacity would result in the growth of commercial adsorptive desulfurization units.

References

[1] Gasoline sulfur standards. [cited 2009 12-15-2009]; Available from: http://www.epa.gov/oms/standards/fuels/gas-sulfur.htm.

[2] Stern, I. D. Global sulfur emissions from 1850 to 2000. Chemosphere 2005; 58: 163-75.

[3] Inoue, S., Takatsuka, T., Wada, Y., Hirohama, S., Ushida, T. Distribution function model for deep desulfurization of diesel fuel. Fuel 2000; 79: 9.

[4] Ali, F. M., Al-Malki, A., El-Ali, B., Martinie, G., Siddiqui, N. M. Deep desulphurization of gasoline and diesel fuels using non-hydrogen consuming techniques. Fuel 2006; 85: 1354-63.

[5] Garcia-Gutierrez, L. J., Fuentes, A. G, Hernandez-Teran, E. M., Murrieta, F., Navarrete, J., Jimenez-Cruz, F. Ultra-deep oxidative desulfurization of diesel fuel with H_2O_2 catalyzed under mild conditions by polymolybdates supported on Al_2O_3. Applied Catalysis A: General 2006; 305: 15-20.

[6] Liu, S., Wang, B., Cui, B., Sun, L. Deep desulfurization of diesel oil oxidized by Fe (VI) systems. Fuel 2008; 87: 422-8.

[7] Mei, H., Mei, W. B, Yen, F. T. A new method for obtaining ultra-low sulfur diesel fuel via ultrasound assisted oxidative desulfurization. Fuel 2003; 82: 405-14.

[8] Campos-Martin, M. J., Capel-Sanchez, C. M., Fierro, G. Highly efficient deep desulfurization of fuels by chemical oxidation. Green Chem 2004; 6: 557-62.

[9] Ma, X., Zhou, A., Song, C. A novel method for oxidative desulfurization of liquid hydrocarbon fuels based on catalytic oxidation using molecular oxygen coupled with selective adsorption. Catal Today 2007; 123: 276-84.

[10] Defilippis, P., Scarsella, M. Functionalized hexagonal mesoporous silica as an oxidizing agent for the oxidative desulfurization of organosulfur compounds. Ind Eng Chem Res 2008; 47: 973-5.

[11] Grossman, J. M., Lee, K. M., Prince, C. R., Garrett, K. K., George, N. G., Pickering, J. I. Microbial desulfurization of a crude oil middle-distillate fraction: Analysis of the extent of sulfur removal and the effect of removal on remaining sulfur. Appl Environ Microbiol 1999; 65: 181-8.

[12] Klein, J. Biological processing of fossil fuels. Appl Microbiol Biotechnol 1999; 52: 2-15.

[13] Ma, T., Tong, M., Zhang, Q., Liang, F., Liu, R. Screening, identification of the strain FDS-1 for microbial desulfurization specially and its use in diesel oil desulfurization. Weishengwu Xuebao 2006; 46: 104-10.

[14] Mcfarland, L. B., Boron, J. D., Deever, W., Meyer, A. J., Johnson, R. A., Atlas, M. R. Biocatalytic sulfur removal from fuels: Applicability for producing low sulfur gasoline. Critical Reviews in Microbiology 1998; 24: 99 - 147.

[15] Zakharyants, A. A., Murygina, P. V., Kalyuzhnyi, V. S. Biodesulfurization of dibenzothiophene and its derivatives. Uspekhi Sovremennoi Biologii 2005; 125: 104-14.

[16] Rang, H., Kann, J., Oja, V. Advances in desulfurization research of liquid fuel. Oil Shale 2006; 23: 164-76.

[17] Song, C. An overview of new approaches to deep desulfurization for ultra-clean gasoline, diesel fuel and jet fuel. Catal Today 2003; 86: 53.

[18] Qi, R., Wang, Y., Li, J., Zhao, C., Zhu, S. Pervaporation separation of alkane/thiophene mixtures with pdms membrane. J Membr Sci 2006; 280: 545-52.

[19] Qi, R., Zhao, C., Li, J., Wang, Y., Zhu, S. Removal of thiophenes from n-octane/thiophene mixtures by pervaporation. J Membr Sci 2006; 269: 94-100.

[20] Qi, R., Wang, Y., Chen, J., Li, J., Zhu, S. Pervaporative desulfurization of model gasoline with ag2o-filled pdms membranes. Sep Purif Technol 2007; 57: 170-5.

[21] Qi, R., Wang, Y., Li, J., Zhu, S. Sulfur removal from gasoline by pervaporation: The effect of hydrocarbon species. Sep Purif Technol 2006; 51: 258-64.

[22] Sughrue, L. E., Johnson, M. M., Dodwell, W. G., Reed, E. L., Bares, E. J., Gislason, J. J., Morton, W. R., Malandra, L. J. Desulfurization and sorbents for same. US patent.6656877.

[23] Gislason, J. J., Schmidt, R., Welch, B. M, Simon, E. D., Morton, W. R. Desulfurization of cracked gasolines and diesel fuels using cadmium oxide and a promoter. US patent application.20040007130.

[24] Price, G. A., Gislason, J. J., Dodwell, W. G., Morton, W. R., Parks, D. G. Desulfurization of hydrocarbon stream using novel compositions containing manganese oxide. US patent.7105140.

[25] Simon, E. D., Morton, W. R., Schmidt, R., Gislason, J. J., Welch, B. M. Reduced-valence metal-promoted niobium oxide and tantalum oxide as petroleum desulfurization sorbents. US patent.2004040887.

[26] Morton, W. R., Gislason, J. J., Welch, B. M., Simon, E. D., Schmidt, R. Promoted gallium or indium oxides as bulk and supported desulfurization catalysts for petroleum feedstocks. US patent application.2004063578.

[27] Morton, W. R., Gislason, J. J., Schmidt, R., Welch, B. M. Desulfurization and novel compositions for same. US patent.7220704.

[28] Morton, W. R., Gislason, J. J., Schmidt, R., Welch, B. M. Reduced-valence metal-promoted molybdenum oxide and tungsten oxide as petroleum desulfurization sorbents. US patent application.2004040890.

[29] Khare, P G. Novel sorbents for desulfurization of gasoline or diesel fuel. US patent.6683024.

[30] Kim, H. J., Ma, X., Zhou, A., Song, C. Ultra-deep desulfurization and denitrogenation of diesel fuel by selective adsorption over three different adsorbents: A study on adsorptive selectivity and mechanism. Catal Today 2006; 111: 74-83.

[31] Velu, S., Ma, X., Song, C., Namazian, M., Sethuraman, S., Venkataraman, G. Desulfurization of jp-8 jet fuel by selective adsorption over a Ni-based adsorbent for micro solid oxide fuel cells. Energy Fuels 2005; 19: 9.

[32] Ma, X., Sprague, M., Song, C. Deep desulfurization of gasoline by selective adsorption over nickel-based adsorbent for fuel cell applications. Ind Eng Chem Res 2005; 44: 5768-75.

[33] Herna´Ndez-Maldonado, A. J., Yang, F. H., Qi, G., Yang, R. T. Desulfurization of transportation fuels by π-complexation sorbents: Cu(i)-, ni(ii)-, and zn(ii)-zeolites. Applied Catalysis B: Environmental 2005; 56: 17.

[34] Wang, Y., Yang, H. F., Yang, T. R., Heinzel, M. J., Nickens, D. A. Desulfurization of high-sulfur jet fuel by π-complexation with copper and palladium halide sorbents. Ind Eng Chem Res 2006; 45: 7649-55.

[35] Bhandari, M. V, Ko, H., Chang, P. G., Jung, H., Sang-Sup, C., Soon-Haeng, K. Desulfurization of diesel using ion-exchanged zeolites. Chem Eng Sci 2006; 61: 2599-608.

[36] Hernández-Maldonado, J. A., Yang, T. R. New sorbents for desulfurization of diesel fuels via π-complexation. AIChE J 2003; 50.

[37] Velu, S., Ma, X., Song, C. Selective adsorption for removing sulfur from jet fuel over zeolite-based adsorbents. Ind Eng Chem Res 2003; 42: 12.

[38] King, L. D., Li, L. Removal of sulfur components from low sulfur gasoline using copper exchanged zeolite Y at ambient temperature. Catal Today 2006; 116: 526-9.

[39] Xue, M., Chitrakar, R., Sakane, K., Hirotsu, T., Ooi, K., Yoshimura, Y., Toba, M., Feng, Q. Preparation of cerium-loaded Y-zeolites for removal of organic sulfur compounds from hydrodesulfurizated gasoline and diesel oil. J Colloid Interface Sci 2006; 298: 535-42.

[40] Herna´Ndez-Maldonado A. J., Yang, R. T. Desulfurization of diesel fuels via π-complexation with Nickel(II)-exchanged X- and Y-zeolites. Ind Eng Chem Res 2004; 43: 9.

[41] Jeevanandam, P., Klabunde, J. K., Tetzler, H. S. Adsorption of thiophenes out of hydrocarbons using metal impregnated nanocrystalline aluminum oxide. Microporous Mesoporous Mater 2005; 79: 101-10.

[42] Herna´Ndez-Maldonado A., Yang R. T. New sorbents for desulfurization of diesel fuels via π-complexation AIChE J 2004; 50: 10.

[43] Phillips starts up new gasoline desulfurization unit. Oil Gas J 2001; 99: 1.

[44] Mesters, M. C. Catalyst particles and its use in desulphurisation. US patent.7297655.

[45] Herna´Ndez-Maldonado, J. A., Gongshin, Q., Yang, T R. Desulfurization of commercial fuels by π-complexation: Monolayer CuCl/g-Al_2O_3. Applied Catalysis B: Environmental 2005; 61: 7.

[46] Gates, C. B., Topsoe, H. Reactivities in deep catalytic hydrodesulfurization: Challenges, opportunities, and the importance of 4-methyldibenzothiophene and 4,6-dimethyldibenzothiophene. Polyhedron 1997; 16: 3213-7.

[47] Ma, X., Sakanishi, K., Isoda, T., Mochida, I. Quantum chemical calculation on the desulfurization reactivities of heterocyclic sulfur compounds. Energy Fuels 1995; 9: 33-7.

[48] Ma, X., Sakanishi, K., Mochida, I. Hydrodesulfurization reactivities of various sulfur compounds in diesel fuel. Ind Eng Chem Res 1994; 33: 218-22.

[49] Kimberlin, N. C., Mason, B. R. Desulfurization of hydrocarbons by adsorption of sulfur compounds by metallic silver. US patent.2791540.

[50] Miller, W. J., Ward, W. J. Catalytic absorbent and a method for its preparation. US patent.4582819.

[51] Klabunde, K., Sanford, R. B., Jeevanandam, P. Method of sorbing sulfur compounds using nanocrystalline mesoporous metal oxides US patent application.20040260139.

[52] Yang, T. R., Hernandez-Maldonado, J. A., Yang, H. F. Desulfurization of transportation fuels with zeolites under ambient conditions. Science 2003; 301: 79-81.

[53] Natal, W. M., Bhasin, M. M., Soo, H., Liu, C. A. Supported silver oxidation catalysts for preparation of alkylene oxides by directly oxidizing alkylenes. WO patent.2007123932.

[54] Verykios, E. X., Stein, P. F., Coughlin, W. R. Oxidation of ethylene over silver: Adsorption, kinetics, catalyst. Catalysis Reviews 1980; 22: 197-234.

[55] Toreis, N., Verykios, E. X. Oxidation of ethylene over silver-based alloy catalysts. J Catal 1987; 108: 161-74.

[56] Minahan, M. D., Hoflund, B. G., Epling, S. W., Schoenfeld, W. D. Study of Cs-promoted, alpha -alumina-supported silver, ethylene epoxidation catalysts. Iii. Characterization of Cs-promoted and nonpromoted catalysts. J Catal 1997; 168: 393-9.

[57] Oliveira, D., Lange, A., Wolf, A., Schüth, F. Highly selective propene epoxidation with hydrogen/oxygen mixtures over titania-supported silver catalysts. Catal Lett 2001; 73: 157-60.

[58] Liu, Q., Cao, Y., Dai, W., Deng, J. The oxidative dehydrogenation of methanol over a novel low loading $Ag/SiO_2–TiO_2$ catalyst. Catal Lett 1998; 55: 87-91.

[59] Lavrenko, A. V., Malyshevskaya, I. A., Kuznetsova, I. L., Litvinenko, F. V., Pavlikov, N. V. Features of high-temperature oxidation in air of silver and alloy Ag-Cu, and adsorption of oxygen on silver. Powder Metallurgy and Metal Ceramics 2006; 45: 476-80.

[60] Satokawa, S., Shimizu, K., Satsuma, A. Adsorptive removal of organic sulfur compounds in city gas at ambient temperature using silver ion-exchanged zeolites. Zeoraito 2007; 24: 60-6.

[61] Salas, V. B., Gonzalez, R. N., Lara, B. A, Beltran, C. M, Muleshkova, V. L. Indoor corrosion of silver components used in electronic industry. International Corrosion Congress: Frontiers in Corrosion Science and Technology, 15th, Granada, Spain, Sept 22-27, 2002 2002: 718/1-/6.

[62] Satokawa, S., Kobayashi, Y., Fujiki, H. Adsorptive removal of dimethylsulfide and t-butylmercaptan from pipeline natural gas fuel on Ag zeolites under ambient conditions. Applied Catalysis B: Environmental 2005; 56: 51-6.

[63] Rovida, G., Pratesi, F. Sulfur chemisorption on the silver (111) and (100) faces. Vide, les Couches Minces 1980; 201: 321-4.

[64] Rovida, G., Pratesi, F. Sulfur overlayers on the low-index faces of silver. Surf Sci 1981; 104: 609-24.

[65] Benard, J., Oudar, J., Carbone-Brouty, F. Reversible chemisorption of sulfur on silver. Surf Sci 1965; 3: 359-72.

[66] Hernandez-Maldonado, J. A., Yang, T. R. Desulfurization of diesel fuels by adsorption via π-complexation with vapor-phase exchanged Cu(I)-Y zeolites. J Am Chem Soc 2004; 126: 992-3.

[67] Song, C., Ma, X. Ultra-deep desulfurization of liquid hydrocarbon fuels: Chemistry and process. International Journal of Green Energy 2004; 1: 167–191

[68] Deka, C. R, Hirao, K. Lewis acidity and basicity of cation-exchanged zeolites: Qm/mm and density functional studies. J Mol Catal A: Chem 2002; 181: 275-82.

[69] Tanabe, K. Solid acid and base catalysts. Catal: Sci Technol 1981; 2: 231-73.

[70] Iengo, P., Serio D., M., Sorrentino, A., Solinas, V., Santacesaria, E. Preparation and properties of new acid catalysts obtained by grafting alkoxides and derivatives on the most common supports note i—grafting aluminium and zirconium alkoxides and related sulphates on silica. Applied Catalysis A, General 1998; 167: 85-101.

[71] Tanabe, K., Sumiyoshi, T., Shibata, K., Kiyoura, T., Kitagawa, J. New hypothesis regarding the surface acidity of binary metal oxides. Bull Chem Soc Jpn 1974; 47: 1064-6.

[72] Nakabayashi, H. Properties of acid sites on titania-silica and titania-alumina mixed oxides measured by infrared spectroscopy. Bull Chem Soc Jpn 1992; 65: 914-16.

[73] Kobayakawa, K., Nakazawa, Y., Ikeda, M., Sato, Y., Fujishima, A. Influence of the density of surface hydroxyl groups on titania photocatalytic activities. Berichte der Bunsen-Gesellschaft 1990; 94: 1439-43.

[74] Boehm, P. H. Chemical identification of surface groups. Advan Catalysis 1966; 16: 179-274.

[75] Contreras M., Lagos G., Escalona N., Soto-Garrido G., Radovic L. R., Garcia R. On the methane adsorption capacity of activated carbons: In search of a correlation with adsorbent properties. Journal of Chemical Technology & Biotechnology 2009; 84: 1736-41.

[76] Fletcher, J. A., Uygur, Y., Thomas, M. K. Role of surface functional groups in the adsorption kinetics of water vapor on microporous activated carbons. The Journal of Physical Chemistry C 2007; 111: 8349-59.

[77] Auroux, A., Gervasini, A. Microcalorimetric study of the acidity and basicity of metal oxide surfaces. The Journal of Physical Chemistry 1990; 94: 6371-9.

[78] Peri, B. J. Infrared study of adsorption of ammonia on dry alumina. The Journal of Physical Chemistry 1965; 69: 231-9.

[79] Herrmann M., Boehm H. P. Über die chemie der oberfläche des titandioxids. Ii. Saure hydroxylgruppen auf der oberfläche. Zeitschrift für anorganische und allgemeine Chemie 1969; 368: 73-86.

[80] Occelli, L. M., Olivier, P. J., Petre, A., Aurouxs, A. Determination of pore size distribution, surface area, and acidity in fluid cracking catalysts (FCCS) from nonlocal density functional theoretical models of adsorption and from microcalorimetry methods. J Phys Chem B 2003; 107: 4128-36.

[81] Benesi, A. H. Acidity of catalyst surfaces. I. Amine titration using Hammett indicators. The Journal of Physical Chemistry 1957; 61: 970-3.

[82] Hammett, P. L, Deyrup, J. A. A series of simple basic indicators. I. The acidity functions of mixtures of sulfuric and perchloric acids with water1. J Am Chem Soc 1932; 54: 2721-39.

[83] Frenkel, M. Surface acidity of montmorillonites. Clays Clay Miner 1974; 22: 435-41.

[84] Johnson, E. C., Lien, P.A., Mccaulay, A. D. Extraction of aromatic hydrocarbons from hydrocarbon mixtures. US patent.2768986.

[85] Benesi, A. H. Determination of proton acidity of solid catalysts by chromatographic adsorption of stearically hindered amines. J Catal 1973; 28: 176-8.

[86] Macht, J., Baertsch, D. C., May-Lozano, M., Soled, L. S., Wang, Y., Iglesia, E. Support effects on brønsted acid site densities and alcohol dehydration turnover rates on tungsten oxide domains. J Catal 2004; 227: 479-91.

[87] Takahashi, A., Yang, H. F., Yang, T. R. New sorbents for desulfurization by π-complexation: Thiophene/ benzene adsorption Ind Eng Chem Res 2001; 41: 10.

[88] Xie, Y., Tang, Y. Spontaneous monolayer dispersion of oxides and salts onto surfaces of supports: Applications to heterogeneous catalysis. Adv Catal 1990; 37: 1-43.

[89] Strohmayer, E. D., Geoffroy, L. G., Vannice, A. M. Measurement of silver surface area by the H_2 titration of chemisorbed oxygen. Applied Catalysis 1983; 7: 189-98.

[90] Czanderna, W. A. The adsorption of oxygen on silver. J Phys Chem 1964; 68: 2765-72.

[91] Yeung, L. K., Gavriilidis, A., Varma, A., Bhasin, M. M. Effects of 1,2 dichloroethane addition on the optimal silver catalyst distribution in pellets for epoxidation of ethylene. J Catal 1998; 174: 1-12.

[92] Verykios, E. X., Stein, P. F., Coughlin, W. R. Influence of metal crystallite size and morphology on selectivity and activity of ethylene oxidation catalyzed by supported silver. J Catal 1980; 66: 368-82.

[93] Smeltzer, W. W., Tollefson, L. E., Cambron, A. Adsorption of oxygen by a silver catalyst. Can J Chem 1956; 34: 1046-60.

[94] Kholyavenko, M. K, Rubanik, Y. M., Chernukhina, A. N. Chemisorption method for the determination of the surface area of Ag on a carrier. Kinet Katal 1964; 5: 505-12.

[95] Luo, M., Yuan, X., Zheng, X. Catalyst characterization and activity of Ag-Mn, Ag-Co and Ag-Ce composite oxides for oxidation of volatile organic compounds. Applied Catalysis A: General 1998; 175: 121-9.

[96] Bogdanchikova, N., Meunier, C. F., Avalos-Borja, M., Breen, P. J., Pestryakov, A. On the nature of the silver phases of Ag/Al_2O_3 catalysts for reactions involving nitric oxide. Applied Catalysis B: Environmental 2002; 36: 287-97.

[97] Tsybulya, V. S., Kryukova, N. G., Goncharova, N. S., Shmakov, N. A., Balzhinimaev, S. B. Study of the real structure of silver supported catalysts of different dispersity. J Catal 1995; 154: 194-200.

[98] Ginosar, M. D., Coates, K., Thompson, N. D. The effects of supercritical propane on the alkylation of toluene with ethylene over usy and sulfated zirconia catalysts. Ind Eng Chem Res 2002; 41: 6537-45.

[99] Seoud E, Ramadan, R. A., Sato, M. B., Pires, R. P. Surface properties of calcinated titanium dioxide probed by solvatochromic indicators: Relevance to catalytic applications. J Phys Chem C; 114: 10436-43.

[100] Sullivan, D., Hooks, P., Mier, M., Hal, W. J., Zhang, X. Effect of support and preparation on silver-based direct propylene epoxidation catalyst. Top Catal 2006; 38: 303-8.

[101] Edwards, T. Liquid fuels and propellants for aerospace propulsion: 1903-2003. J Propul Power 2003; 19: 1089-107.

[102] Okamoto, Y., Arima, Y., Hagio, M., Nakai, K., Umeno, S., Akai, Y., Uchikawa, K., Inamura, K., Ushikubo, T., Katada, N., Hasegawa, S., Yoshida, H., Tanaka, T., Isoda, T., Mochida, I., Segawa, K., Nishijima, A., Yamada, M., Matsumoto, H., Niwa, M., Uchijima, T. A study on the preparation of supported metal oxide catalysts using JRC-reference catalysts. I. Preparation of a molybdena-alumina catalyst. Part 2. Volume of an impregnation solution. Applied Catalysis A: General 1998; 170: 329-42.

[103] Page L., Applied heterogeneous catalysis: Design, manufacture, use of solid catalysts. 1987.

[104] Dorling, A. T., Lynch, J. B., Moss, L. R. Structure and activity of supported metal catalysts. V. Variables in the preparation of platinum/silica catalysts. J Catal 1971; 20: 190-201.

[105] Brunelle, P. J., Sugier, A., Page, L. Active centers of platinum-silica catalysts in hydrogenolysis and isomerization of n-pentane. J Catal 1976; 43: 273-91.

[106] Yates, C. D. Infrared studies of the surface hydroxyl groups on titanium oxide, and of the chemisorption of carbon monoxide and carbon dioxide. The Journal of Physical Chemistry 2002; 65: 746-53.

[107] Pierce, A . J., Spicer, E W. Catalysts. US Patent.2403753.

[108] Sorokin, I. I, Krasii, V. B. Decrepitation of porous solids upon wetting. Chemistry and Technology of Fuels and Oils 1991; 27: 382-7.

[109] Katz, B. S., Burton, J. F., Cullo, A. L. Supported cobalt sulfate desulfurization catalyst. US Patent No 74-483982

[110] Sivaraj, C., Contescu, C., Schwarz, A. J. Effect of calcination temperature of alumina on the adsorption/impregnation of palladium(ii) compounds. J Catal 1991; 132: 422-31.

[111] Keshavaraja, A., She, X., Flytzani-Stephanopoulos, M. Selective catalytic reduction of no with methane over Ag-alumina catalysts. Applied Catalysis B: Environmental 2000; 27: L1-L9.

[112] Shimizu, K., Shibata, J., Yoshida, H., Satsuma, A., Hattori, T. Silver-alumina catalysts for selective reduction of no by higher hydrocarbons: Structure of active sites and reaction mechanism. Applied Catalysis B: Environmental 2001; 30: 151-62.

[113] Bethke, A. K., Kung, H. H. Supported Ag catalysts for the lean reduction of NO with C_3H_6. J Catal 1997; 172: 93-102.

[114] Li, Z., Flytzani-Stephanopoulos, M. On the promotion of Ag-ZSM-5 by cerium for the SCR of no by methane. J Catal 1999; 182: 313-27.

[115] Sato, K., Yoshinari, T., Kintaichi, Y., Haneda, M., Hamada, H. Remarkable promoting effect of rhodium on the catalytic performance of Ag/Al_2O_3 for the selective reduction of no with decane. Applied Catalysis B: Environmental 2003; 44: 67-78.

[116] Primet, M., Pichat, P., Mathieu, V. M. Infrared study of the surface of titanium dioxides. I. Hydroxyl groups. The Journal of Physical Chemistry 2002; 75: 1216-20.

[117] Bacha, J., Barnes, F., Franklin, M., Gibbs, L., Hemighaus, G., Hogue, N., Lesnini, D., Lind, J., Maybury, J., Morris, J. Aviation fuels technical review (FTR-3). Chevron Products Company 2000.

[118] Rajagopal, S., Marzari, A. J., Miranda, R. Silica-alumina-supported mo oxide catalysts: Genesis and demise of brønsted-lewis acidity. J Catal 1995; 151: 192-203.

[119] Du, Y., Deskins, A. N., Zhang, Z., Dohnalek, Z., Dupuis, M., Lyubinetsky, I. Two pathways for water interaction with oxygen adatoms on tio2(110). Phys Rev Lett 2009; 102: 096102/1-/4.

[120] Doolin, K. P., Alerasool, S., Zalewski, J. D., Hoffman, F. J. Acidity studies of titania-silica mixed oxides. Catal Lett 1994; 25: 209-23.

[121] Herna´Ndez-Maldonado, A., Yang, R., Cannella, W. Desulfurization of commercial jet fuels by adsorption via π-complexation with vapor phase ion exchanged Cu(I)-Y zeolites. Ind Eng Chem Res 2004: 8.

[122] Velu, S., Song, C., Engelhard, H. M., Chin, Y. Adsorptive removal of organic sulfur compounds from jet fuel over k-exchanged Ni Y zeolites prepared by impregnation and ion exchange. Ind Eng Chem Res 2005; 44: 10.

[123] Richardson, L. R, Benson, W. S. A study of the surface acidity of cracking catalyst. The Journal of Physical Chemistry 1957; 61: 405-11.

[124] Kulkarni, P. A., Muggli, S. D. The effect of water on the acidity of TiO_2 and sulfated titania. Applied Catalysis A: General 2006; 302: 274-82.

[125] Diran B. The little adsorption book: A practical guide for engineers and scientists. CRC Press; 1997.

[126] El-Sharkawy, A. E., Mostafa, R. M., Youssef, M. A. Changes in surface and catalytic dehydration activities of 2-propanol on alpo-5 induced by silver

impregnation. Colloids and Surfaces A: Physicochemical and Engineering Aspects 1999; 157: 211-8.

[127] Vartuli, C. J., Santiesteban, G. J., Traverso, P., Cardona-Martinez, N., Chang, D. C., Stevenson, A. S. Characterization of the acid properties of tungsten/zirconia catalysts using adsorption microcalorimetry and n-pentane isomerization activity. J Catal 1999; 187: 131-8.

[128] Leuch, L., Bandosz, J. T. The role of water and surface acidity on the reactive adsorption of ammonia on modified activated carbons. Carbon 2007; 45: 568-78.

[129] Gervasini, A., Fenyvesi, J., Auroux, A. Microcalorimetric study of the acidic character of modified metal oxide surfaces. Influence of the loading amount on alumina, magnesia, and silica. Langmuir 1996; 12: 5356-64.

[130] Bandosz, J. T., Jagiello, J., Schwarz, A. J. Comparison of methods to assess surface acidic groups on activated carbons. Anal Chem 1992; 64: 891-5.

[131] Tilocca, A., Selloni, A. Methanol adsorption and reactivity on clean and hydroxylated anatase(101) surfaces. J Phys Chem B 2004; 108: 19314-9.

[132] Scaranto, J., Giorgianni, S. Influence of the OH groups of hydroxylated rutile (110) surface on the lewis acidity: An investigation of CO adsorption by quantum-mechanical simulations. Mol Phys 2008; 106: 2425-30.

[133] Szyja, B., Brodzik, K. Modeling the adsorption of aromatic compounds on the TiO_2/SiO_2 catalyst. Journal of Molecular Modeling 2007; 13: 731-7.

[134] Markovits, A., Ahdjoudj, J., Minot, C. A theoretical analysis of NH_3 adsorption on TiO_2. Surf Sci 1996; 365: 649-61.

[135] Pittman, M. R, Bell, T. A. Raman investigations of NH_3 adsorption on TiO_2, Nb_2O_5, and Nb_2O_5/TiO_2. Catal Lett 1994; 24: 1-13.

[136] Mathieu, V. M., Primet, M., Pichat, P. Infrared study of the surface of titanium dioxides: Acidic and basic properties. The Journal of Physical Chemistry 1971; 75: 1221-6.

[137] Tsyganenko, A. A., Pozdnyakov, V. D., Filimonov, N. V. Infrared study of surface species arising from ammonia adsorption on oxide surfaces. J Mol Struct 1975; 29: 299-318.

[138] Morterra, C., Magnacca, G., Demaestri, P. P. Surface characterization of modified aluminas- Surface-features of PO_4-doped Al_2O_3. J Catal 1995; 152: 384-95.

[139] Weissman, G. J. Niobia-alumina supported hydroprocessing catalysts: Relationship between activity and support surface acidity. Catal Today 1996; 28: 159-66.

[140] Shen, F. Y, Suib, L. S, Deeba, M., Koermer, S. G. Luminescence and IR characterization of acid sites on alumina. J Catal 1994; 146: 483-90.

[141] Kiviat, E. F, Petrakis, L. Surface acidity of transition metal modified aluminas. Infrared and nuclear magnetic resonance investigation of adsorbed pyridine. The Journal of Physical Chemistry 1973; 77: 1232-9.

[142] Yang, T. R, Takahashi, A., Yang, H. F. New sorbents for desulfurization of liquid fuels by π-complexation. Ind Eng Chem Res 2001; 40: 6236-9.

[143] Hernandez-Maldonado, J. A., Yang, T. R. Desulfurization of liquid fuels by adsorption via π complexation with Cu(I)-Y and Ag-Y zeolites. 2003; 42: 123-9.

[144] Auroux, A., Monaci, R., Rombi, E., Solinas, V., Sorrentino, A., Santacesaria, E. Acid sites investigation of simple and mixed oxides by TPD and microcalorimetric techniques. Thermochim Acta 2001; 379: 227-31.

[145] Dines, J. T., Rochester, H. C, Ward, M. A. Infrared and raman study of the adsorption of ammonia, pyridine, nitric oxide and nitrogen dioxide on anatase. J Chem Soc, Faraday Trans 1991; 87: 643-51.

[146] Davydov, A. A, Rochester, H. C. Infrared spectroscopy of adsorbed species on the surface of transition metal oxides. Wiley Chichester; 1990.

[147] Hadjiivanov, K. FTIR study of CO and NH_3 co-adsorption on TiO_2 (rutile). Appl Surf Sci 1998; 135: 331-8.

[148] Armistead, G. C, Hockey, A. J. Reactions of chloromethyl silanes with hydrated aerosil silicas. Transactions of the Faraday Society 1967; 63: 2549-56.

[149] Zhao, S. X, Lu, Q. G. Modification of MCM-41 by surface silylation with trimethylchlorosilane and adsorption study. The Journal of Physical Chemistry B 1998; 102: 1556-61.

[150] Parry, P. E. An infrared study of pyridine adsorbed on acidic solids. Characterization of surface acidity. J Catal 1963; 2: 371-9.

[151] Rochester, H. C, Topham, A. S. Infrared studies of the adsorption of probe molecules onto the surface of hematite. Journal of the Chemical Society, Faraday Transactions 1: Physical Chemistry in Condensed Phases 1979; 75: 1259-67.

[152] Berhault, G., Lacroix, M., Breysse, M., Maugé, F., Lavalley, Jean-Claude, N., Qu, L. Characterization of acidic sites of silica-supported transition metal sulfides by pyridine and 2,6 dimethylpyridine adsorption: Relation to activity in ch3sh condensation. J Catal 1998; 178: 555-65.

[153] Pierre, C. A. Porous sol-gel ceramics. Ceram Int 1997; 23: 229-38.

[154] Walker, S. G., Williams, E., Bhattacharya, K. A. Preparation and characterization of high surface area alumina-titania solid acids. J Mater Sci 1997; 32: 5583-92.

[155] Ma, X., Yang, T. R. Selective adsorption of sulfur compounds: Isotherms, heats, and relationship between adsorption from vapor and liquid solution. Ind Eng Chem Res 2007; 46: 2760-8.

[156] Ng, T., Rahman, A., Ohasi, T., Jiang, M. A study of the adsorption of thiophenic sulfur compounds using flow calorimetry. Appl Catal, B 2005; 56: 127-36.

[157] Jiang, M., Ng, T., Rahman, A., Patel, V. Flow calorimetric and thermal gravimetric study of adsorption of thiophenic sulfur compounds on NaY zeolite. Thermochim Acta 2005; 434: 27-36.

[158] Ma, L., Yang, T. R. Heats of adsorption from liquid solutions and from pure vapor phase:& nbsp; adsorption of thiophenic compounds on nay and 13x zeolites. Ind Eng Chem Res 2007; 46: 4874-82.

[159] Kumar, A., Kumar, S., Kumar, S. Adsorption of resorcinol and catechol on granular activated carbon: Equilibrium and kinetics. Carbon 2003; 41: 3015-25.

[160] Ho, S. Y., Huang, T. C, Huang, W. H. Equilibrium sorption isotherm for metal ions on tree fern. Process Biochem (Oxford, U K) 2002; 37: 1421-30.

[161] Schnoor J. Environmental modeling: Fate and transport of pollutants in water, air, and soil. J. Wiley; 1996.

[162] Fritz, W., Schluender, U. E. Simultaneous adsorption equilibriums of organic solutes in dilute aqueous solutions on activated carbon. Chem Eng Sci 1974; 29: 1279-82.